Gonçalo Abrantes e Figueiró

Licenciado em Bioquímica

Hybrid magnetic systems for the purification of biopharmaceuticals

Dissertação para obtenção do Grau de Mestre em
Biotecnologia

Orientador: Doutora Ana Cecília Afonso Roque, FCT-UNL

Co-orientadores: Doutora Ana Margarida Nunes da Mata Pires de Azevedo, IST

Júri:

Presidente: Prof. Doutor Pedro Miguel Ribeiro Viana Baptista

Arguente: Prof. Doutora Maria Raquel Murias dos Santos Aires Bairros

FACULDADE DE CIÊNCIAS E TECNOLOGIA
UNIVERSIDADE NOVA DE LISBOA

Outubro 2017

Gonçalo Abrantes e Figueiró

Licenciado em Bioquímica

Hybrid magnetic systems for the purification of biopharmaceuticals

Dissertação para obtenção do Grau de Mestre em
Biotecnologia

Orientador: Doutora Ana Cecília Afonso Roque, FCT-UNL

Co-orientadores: Doutora Ana Margarida Nunes da Mata Pires de Azevedo, IST

Júri:

Presidente: Prof. Doutor Pedro Miguel Ribeiro Viana Baptista

Arguente: Prof. Doutora Maria Raquel Murias dos Santos Aires Bairros

Hybrid magnetic systems for the purification of biopharmaceuticals

“If you can dream it, you can do it.”

Walt Disney

Agradecimentos

De forma geral, quero agradecer a todas as pessoas que me ajudaram na conclusão desta etapa da minha vida, a tese de mestrado.

Em primeiro lugar gostaria de agradecer à minha orientadora, professora Ana Cecília Roque, pela oportunidade única que me deu, mas acima de tudo pela forma que me ajudou e orientou nas fases mais difíceis. Obrigado pelas conversas encorajadoras que me permitiram estar sempre de cabeça erguida e nunca desistir.

Também gostaria de agradecer à minha co-orientadora, Doutora Ana Azevedo, por me ter recebido de forma tão acolhedora no IST de Lisboa, e pelas ajudas e explicações dadas às várias dúvidas que me iam surgindo.

Quero agradecer a todos os colegas do laboratório, pelo bom ambiente de trabalho e a espetacular entreajuda que existe dentro do grupo. Susana Palma, obrigado pela ajuda dada nas partículas magnéticas e pelos momentos divertidos passados na caracterização das partículas. Um especial obrigado à Ana Pina, pelos momentos de conversa e de apoio emocional nos momentos de mais stress. Quero, ainda, agradecer à Raquel pelo apoio, pelas conversas e pelas inúmeras perguntas que me ia fazendo, o que me fez estar bem preparado para a tese.

Aos companheiros de laboratório, Gonçalo Teixeira, Marta Banza e Beatriz Mariz quero agradecer vossa companhia e os bons momentos que passamos juntos, quer na centrífuga quer no compartimento do pessoal mais porreiro.

Às amizades que se fizeram, um especial obrigado às Joanas, Joana Valente e Joana Margarida, pela companhia e à grande paciência que tiveram comigo. Quero também agradecer ao Emanuel Capela,à Alexandra Wagner e à Paulinha Amorim por me ajudarem a integrar no grupo de laboratório no IST e pelo apoio dado. Ao José Jurado, Cássia Oliveira e Paula Kaori quero agradecer a vossa companhia e quero dizer que gostei muito de vos ter conhecido e espero que um dia nos voltemos a ver.

Aos meus amigos e colegas de curso, Rita Bernardino, Sara Mateus, Liane Meneses, Gonçalo Teixeira, Eliana Guarda e Juliana Almeida um grande obrigado pelos bons momentos passados todos juntos, pelos jantares e às viagens, que ajudaram animar nos momentos mais difíceis. Bernardo Carvalho, apesar de teres estado na Bélgica, fazes parte também deste pequeno grande grupo.

Um grande obrigado e abraço aos meus amigos Bioqs, Ricardo Santo, Bruna Santos e Adriana Mamede, que apesar de estarem longe terão sempre um lugar no coração e pensamento.

Por fim, quero agradecer de modo especial a toda a minha família por terem acredito em mim e terem investido no meu futuro. Quero agradecer aos meus dois irmãos, Eduardo Abrantes e Duarte Gregório, por fazerem os dias maus, dias mais alegres e animados.

Resumo

Os anticorpos monoclonais são utilizados como agentes terapêuticos em todo o mundo e têm uma grande procura no mercado. No entanto, o processamento de purificação deste biofármaco representa entre 50-80% do custo total de fabricação do produto e, portanto, novos métodos, que sejam menos caros, mas também eficientes, são necessários. O objetivo deste trabalho foi desenvolver um método não cromatográfico para a purificação de anticorpos a partir de sobrenadantes de culturas celulares, combinando dois métodos, nomeadamente a extração em duas fases aquosa (ATPS) e a separação magnética.

O comportamento de um novo ATPS composto por polietilenoglicol (PEG) e poliacrilato de sódio (NaPA) foi investigado variando a concentração de NaCl e o peso molecular do NaPA. Este estudo permitiu selecionar sistemas compostos por 10% de PEG 3.350, 10% de NaPA e 0 mM ou 150 mM de NaCl para estudos posteriores de partição de albumina de soro bovino (BSA), utilizado como contaminante modelo, e imunoglobulina G (IgG).

Simultaneamente, partículas magnéticas (MNPs) com dois revestimentos diferentes foram sintetizadas e avaliados quanto à ligação às proteínas. As MNPs revestidas com dextrano e modificadas com o ligando 22/8 (MNP-DX-22/8) foram selecionados devido à sua fácil síntese e por apresentarem uma grande afinidade e seletividade pela IgG humana (88,0 mg IgG / g suporte, que foi 3,5 vezes maior que a ligação à BSA).

O sistema PEG-NaPA composto por PEG 3,350, NaPA 15,000 e 150 mM de NaCl foi escolhido como o sistema de pesca magnética aquoso de duas fase (MATPFS) mais adequado para recuperar IgG na presença das partículas MNP-DX-22/8. Os estudos de controlo que consistiram na utilização separada de ATPS e pesca magnética para purificar IgG a partir de um sobrenadante de cultura celular apresentaram baixos rendimentos de purificação, 45% e 12%, e baixos graus de pureza, 84% e 76%, respetivamente. A combinação destes dois métodos permitiu uma recuperação de 78% de IgG do sobrenadante da cultura celular com 93% de pureza.

Palavras-chave: Sistema aquoso de duas fases, Partículas magnéticas, Anticorpos, Bioseparação, Processo de purificação

Abstract

Monoclonal antibodies are used as therapeutic agents worldwide and have a great market demand. However, the downstream processing of these biopharmaceuticals represents between 50-80% of the total manufacturing costs and therefore new methods which are less expensive but also efficient are needed. The aim of this work was to develop a non-chromatographic method for the purification of antibodies from cell culture supernatants by process integration of two methods, namely aqueous two-phase extraction (ATPE) and magnetic fishing.

The behavior of a new aqueous two-phase systems (ATPS) composed by polyethylene glycol (PEG) and sodium polyacrylate (NaPA) was investigated by varying the NaCl concentration and the molecular weight of NaPA. From this study, systems composed by 10% of PEG 3,350, 10% NaPA and 0 mM or 150 mM of NaCl were selected to study the partition of bovine serum albumin (BSA) used as a model contaminant and immunoglobulin G (IgG).

Simultaneously, magnetic particles (MNPs) with different coatings were synthesized and assessed for protein binding. Dextran coated MNPs modified with ligand 22/8 (MNP-DX-22/8) were selected due to the easier synthesis and the high affinity and selectivity towards human IgG (88.0 mg IgG/g of support, which was 3.5 higher than the binding to contaminant BSA).

When the MNP-DX-22/8 were applied in the PEG-NaPA systems, the PEG-NaPA 15,000 with 150 mM of NaCl was chosen as the most suitable magnetic aqueous two phase fishing system (MATPFS) to recover IgG. The control studies using separately the ATPE and magnetic fishing to purify IgG from a cell culture supernatant, showed low yields of purification, 45% and 12%, and low purity degree, 84% and 76%, respectively. The combination of these two methods allowed the recovery of 78% of IgG from the cell culture supernatant with 93% of purity.

Keywords: Aqueous two-phase system, Magnetic Particles, Antibodies, Bioseparation, Downstream processing

Contents

Index of Figures

Index of Tables

List of Abbreviations

Abs – Antibodies

APBA - Aminophenylboronic acid hydrochloride

APS - Ammonium persulfate

APTES - (3-aminopropyl)trithoxysilane

ATPE - Aqueous two-phase extraction

ATPS - Aqueous two phase systems

BCA - Bichinchoninic acid

CHO - Chinese hamster ovary

CV – Column volume

DLS – Dynamic light scattering

DMF - N,N-Dimethylformamide

DX – Dextran

Fab - Fragment antigen binding

Fc - Fragment crystallizable

FTIR – Fourier-transform infrared spectroscopy

GA – Gum arabic

GLYMO - (3-Glycidyloxypropyl)trimethoxysilane

Ig – Immunoglobulin

IgG – Immunoglobulin G

mAbs – Monoclonal antibodies

MATPFS - Magnetic aqueous two phase fishing

MNPs – Magnetic nanoparticles

MNP-DX – MNPs coated with dextran

MNP-DX-22/8 - MNPs coated with dextran and functionalized with ligand 22/8

MNP-GA - MNPs coated with gum arabic

MNP-GA-BA - MNPs coated with gum arabic and functionalized with boronic acid

MRI - Magnetic resonance imaging

MW(s) – Molecular weight(s)

NaPA - Sodium polyacrylate

PEG - Polyethylene glycol

scFv - single chain variable fragment

SDS - Sodium dodecyl sulfate

SDS-PAGE - Sodium dodecyl sulfate polyacrylamide gel electrophoresis

TEMED - N,N,N,N – Tetramethylethylenediamine

TEOS - Tetraethyl orthosilicate

UF/DF - ultrafiltration/diafiltration

VH - Variable domains of the heavy chains

VL - Variable domains of the light chains

1. Literature Review

1.1 Antibodies

An immune response is a defense mechanism of the body when fighting a pathogenic organism, for example a bacteria. This defense mechanism involves two systems that complement each other, the humoral and the cellular immune system. The humoral immune system is related to the response at foreign macromolecules found in the body fluids, such as foreign proteins and extracellular viruses. While the cellular immune system is responsible for the destruction of infected cells and also some parasites and foreign tissues.

The humoral immune system is responsible for the antibodies (Abs) or immunoglobulins (Ig) production. Ig or Abs are glycoproteins produced by B cells of immune system in the presence of an antigen molecule, with the aim to neutralize it. When the antibody binds to a specific antigen, macrophages take care of recognizing this complex formed to remove it from the host system. In addition to the ability to identify these foreign molecules, the immune system also has T cells that can be cytotoxic, if they lyse foreign or infected cells, or it can be helper, if they regulate the response of B cells and cytotoxic T cells. The cytotoxic T cells and antibodies can only recognize the antigenic determinant or epitope, which is a specific molecular structure within the antigen.

When different B cell lineages synthesize Abs in response to one antigen, these are designated polyclonal. This production occurs because the B cells population can bind different epitopes within the antigen, and therefore the antigen can be highly recognized by different Abs in different and specific regions. When Abs are produced by a B cell lineage and they are homogeneous and recognize just one epitope, they are designated monoclonal antibodies (mAbs) [1].

1.1.1 Structure

The human Abs can be divided in five classes according to their biological properties and tissue location: IgG, IgM, IgA, IgE, and IgD. These are formed by one or more of a characteristic unit, which has a Y form and two antigen-binding sites. Each unit is formed by four polypeptides, two light chains (L) and two heavy chains (H), that are connected with each other through disulfide bridges and noncovalent bonds. The total molecular weight (MW) of this molecule is 150 kDa, wherein a light chain has around of 25 kDa and a heavy chain around 50 kDa. At the end of these chains, there are variable domains, which contain certain regions that contribute to the selectivity and affinity of the antibodies for antigens. However, what determines the class of antibody is the type of H chain that the antibody has [2].

In the presence of a proteinase, the antibody can be divided structurally into two major fragments, Fab (fragment antigen binding) and Fc (fragment crystallizable). For example, the presence of papain, the immunoglobulin is degraded into two Fab fragments and one Fc fragment, whereas the pepsin can produce one fragment with two Fab fragments (Fab_2), and Fc fragments (pFc') (shown in Figure 1.1) [3], [4].

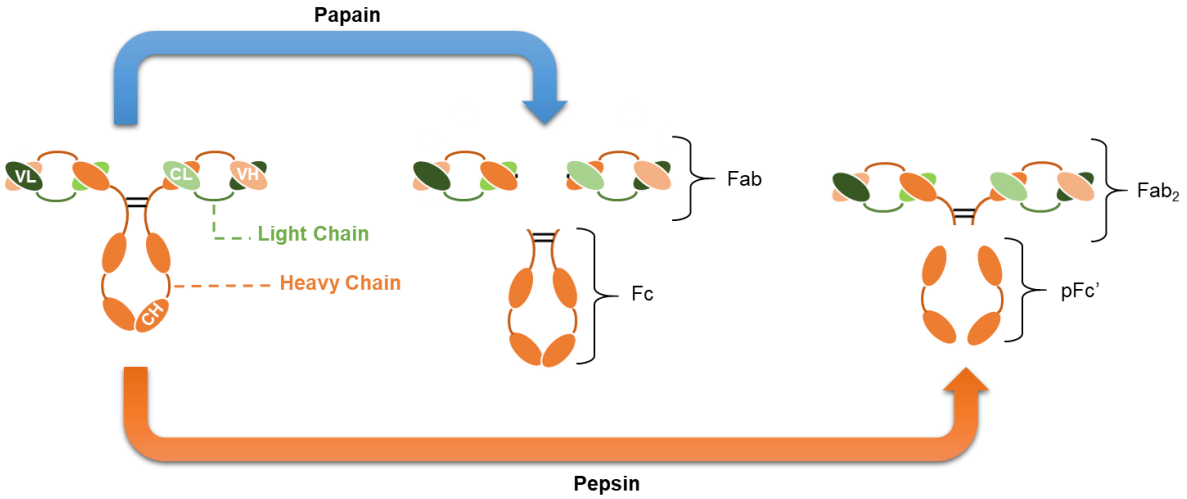

Figure 1.1 – Structure of an IgG antibody and its degradation by proteases like papain and pepsin. An IgG antibody has two heavy chains (orange) and two light chains (green), each one with constant and variable domains. In the heavy chain, there are three constant domains (CH) and one variable (VH), while in the light chain there is only one constant domain (CL) and one variable (VL). The combination between variable chains of heavy and light chains determine the two antigen-binding sites of the antibody. Adapted from [5], [6].

Due to their biological functions and small sizes, these fragments can be used in certain immunochemical techniques and experimental applications with a smaller price when compared with the intact antibody. The Fc fragment is made of the heavy chain constant region of an antibody, acts as a mediator of cellular effector functions. Although this molecule does not have the capability to bind an antigen, because it does not contain binding sites, it can be injected in a host of another specie to produce Anti-Fc Abs. These Abs are very useful since it can help recognize a molecule of antibody, for example in a Western blotting experiment. Another useful use for these fragments is in control of the Fc-binding to Protein A in experiments such as immunoprecipitation [7].

In contrast, the Fab or the Fab_2 fragments have antigen-binding sites. Fab_2 fragments have two antigen-binding Fab portions held together by the hinge region, in which there are disulfide bonds. These fragments have many advantages over an intact antibody, for example allow cheaper antigen-antibody binding studies and because it is easy to them to penetrate tissues sections, they can improve staining in immunohistochemistry (IHC) having lower immunogenicity than an antibody [7].

Others formats derived from antibodies have also been studied, such as the single chain variable fragment (scFv), which consists of the variable domains of the heavy (VH) and light chain (VL) connected by a peptide linker, and camel VH domain (VHH), which is an antigen-binding site formed by variable domains of *Camelidae* only-heavy-chain antibodies. These formats have routinely been used for antibody phage display, where the expression of a peptide with just an antigen-binding domain is convenient. Moreover, they have had a great impact on the pharmaceutical industry, namely in the development of therapeutic proteins [8].

1.1.2 Upstream Processing

The large-scale mAbs production in mammalian cells cultures was caused by their clinical and commercial success alike. The antibody demand led companies to expand the manufacture capacity, to increase the scale of bioreactors and to increase the process efficiency with the concomitant manufacturing cost reduction [9], [10].

The antibodies can be produced by several host systems such as bacteria, plants and even yeast, but the best choice are mammalian cells, since they have the capability to fold, to assembly and to modify the mAbs after translation in the proper way [11].

The Hybridoma technology was the first process introduced for a large-scale antibody production and consists of the fusion of a myeloma cell line with B cells to form hybridoma cells. These cells have characteristics of both fusion cells, can produce antibodies like a B-cell and have longevity and reproductivity of a myeloma cell. Initially, murine cells were used for this purpose, but in a large-scale antibody production, those cells show high sensitivity to environmental changes, to toxic compounds formed during cell growth and to shear and bubble stress in a bioreactor. In order to fulfil these purposes, genetically engineered cell lines were developed, namely Chinese hamster ovary (CHO) cells, NS0 and Sp2/0-Ag 14 [11], [12]. For a large-scale antibody production, a suitable cell line needs to be scalable; to have a high expression of product during long periods of time; to be genetic stable and maintain high viable cell density; to have the proper post-translational modifications; and to be characterize as safe for human applications. Besides these features, the product application has also an important role to the choice of a suitable cell line [13].

In the large-scale cell culture processes, after choosing a suitable cell line and vial thaw, is essential to make the cell line grow through an inoculum flask increase in size and/or volume. After this inoculum expansion, the cell mass is transferred to a series of seed bioreactors until it reaches a proper mass for production of mAbs. Prior to the purification steps in the downstream process, centrifugation and filtration steps are needed to remove cells and cell debris (Figure 1.2) [14].

Another important factor for the antibody production is the cell culture medium, that provides essential nutrients for example amino acids, fatty acids, sugars, vitamins, cofactors, and carbohydrates in order to maintain the proper chemical environment for the cells [15]. In early days, one of the most important components of mammalian cells culture medium was the fetal bovine serum, which contained attachment factors, micronutrients, growth factors, and protective elements (antitoxins, antioxidants, antiproteases), and others components essential for cell growth [15], [16]. The use of serum at large-scale antibody production had many disadvantages such as the high protein content, which can hinder product purification; high cost, representing 85% of all cost of the medium; lot-to-lot variability and specially increased risk of contamination (*e.g* viruses and mycoplasma) [16]. Therefore, many industrial companies have now adopted the use of serum-free medium culture, which could have derived-serum components to fulfil the benefic functions of serum but currently are based on chemically defined media with aim to avoid pathogen contaminations that could be resulted by the presence of animal-derived components [17].

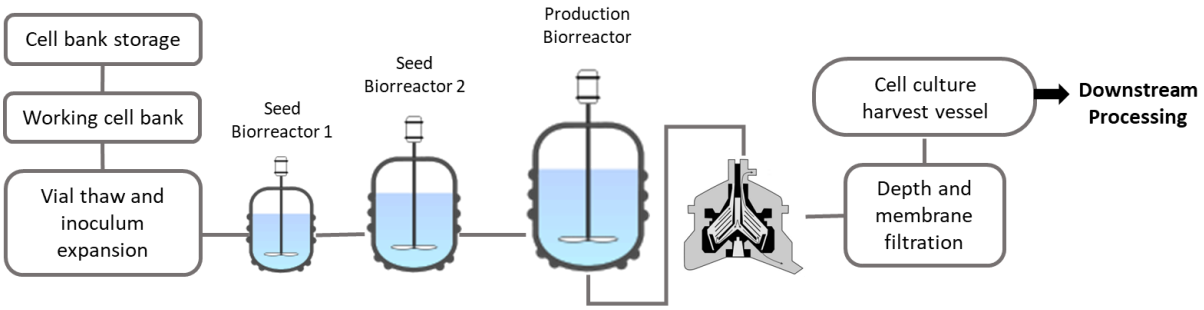

Figure 1.2 – Scheme of the mAbs upstream processing. Adapted from [14]

1.1.3 Downstream Processing

To have a final antibody product without the presence of DNA, virus, pyrogens and/or leachates is very important to design an efficient downstream process to obtain a highest purity product with highest yield. Since the downstream step represents between 50-80% of the total product manufacture cost it is also important to purify at minimum costs possible depending on the final application and percentage of purity required [18].

Since all therapeutic biomolecules and production medium thereof are different, there is not a general purification scheme but common phases instead. A normal antibodies purification process is represented in the Figure 1.3 and there are three main steps: 1) Capture or recovery; 2) Intermediate purification; and 3) Polishing [19], [20]. The first step consists of a fast separation between the interest protein and the cells of the bioreactor with the aim to isolate the protein from proteolytic enzymes and others elements such as growth medium factors. It is possible to reach 95% of purity in this step depending on the specificity of the tools that are used, the most common used on antibody purification is Protein A affinity chromatography [20], [21]. After this, the intermediate purification and the polishing stages are responsible to eliminate host cell proteins, DNA, leached protein A, aggregates and viruses from the product. The difference between these two steps is the fact that the goal of intermediate purification is the elimination of bulk contaminants, including host cell proteins and adventitious viruses, and Protein A affinity chromatography leachates whereas the polishing involves the removal of more specific compounds, such as inactive or unwanted isoforms of the product [20]. Although the purity given by the chromatographic steps, FDA requires the use of two steps for viral removal to assure safety of products produced by mammalian cell culture. These two steps are usually a viral inactivation and a viral filtration, after the Protein A chromatography and after the purification and polishing steps, respectively. The viral inactivation consists of a low pH incubation while, in the viral filtration there is elimination of viruses by inactivation and size [22]. To finish the mAbs downstream processing, normally an ultrafiltration/diafiltration (UF/DF) is performed with the aim of reducing storage volumes and producing the drug substance by putting the product into a desire buffer (Figure 1.3) [14].

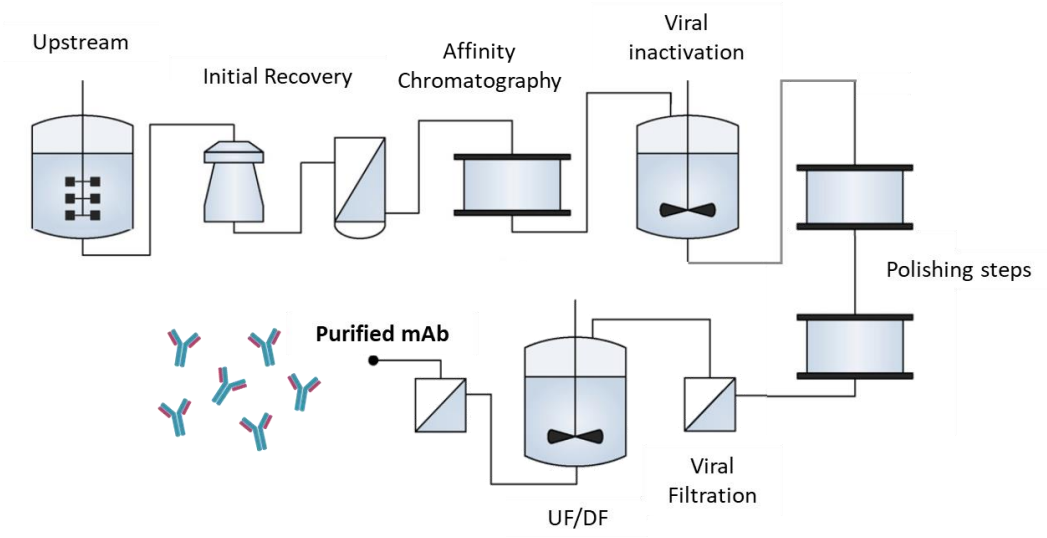

Figure 1.3 – Scheme of mAb purification (UF/DF: ultrafiltration/diafitration). Adapted from [19]

The antibodies upstream processing have been developing new ways to get more product efficiently by developing recombinant technologies, media and strategies to control the process. In 2004, it was normal to obtain antibody concentrations between 3-5 g/L using CHO cells, but, nowadays, companies usually achieve higher concentrations, more than 12 g/L. Moreover, the highest reported IgG production titer was 27 g/L using human embryonic retinal cells [23]. Despite these increased upstream productivity the downstream processing equipment can only work with smaller amounts of antibodies and therefore this manufacturing step can lead to high processing times, to large consumption of material and consequently to high costs [24]. For this main reason there is a great interest on developing alternatives purification technologies that are effective, economical viable and scalable [25]. One of these alternatives is through non-chromatographic approaches such as membrane-based procedures, aqueous two-phase systems (ATPS), precipitation, crystallization or affinity alternatives, for example magnetic particles [26].

1.2 Aqueous Two Phase Systems

1.2.1 Phase Diagram

The aqueous two phase systems (ATPS) is a well established purification process which results through the mixture of two aqueous solutions of hydrophilic polymers, for example polyethylene glycol (PEG) and dextran. This system can also be formed upon mixing one solution of polymer and another of salt such as a potassium phosphate solution [27]. In order to obtain two separated phases in this process the solutions concentration needs to be above a critical concentration, which can be represented by a phase diagram (Figure 1.4).

In the phase diagram, the binodal curve separates one region above the curve, where it is possible to form two immiscible aqueous phases, from another region below the curve, where it is only possible to form homogenous solutions [28]. The line that connects two points in the binodal curve is called tie-line

and any point on this line have the same top and bottom phase equilibrium composition but different volumes of phases. The tie-line length represents the difference between equilibrium phases and therefore if the length decreases the difference decreases as well. In the critical point of the binodal curve (represented by C in Figure 1.4), the equilibrium phases have the same composition and so the length of the tie-line is zero.

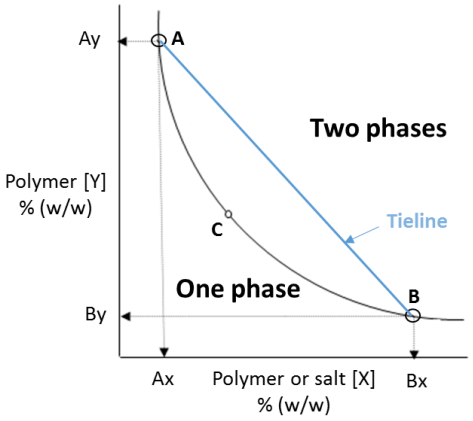

Figure 1.4 – Example of a binodal curve. In the figure, A, B and C are points of the binodal curve, C is the critical point, A and B represent respectively the equilibrium composition of the top phase and the bottom phase for all points on the tie-line represented. Adapted from [28].

Many factors influence this binodal curve such as the polymer molecular weight, temperature and concentration of salt in the system. Due to the formation of a hydration shell, an increase of the polymer molecular weight makes it easier to form two phases. As a result, in the phase diagram is possible to observe an increase on the tie-line slope, indicating a higher difference between the polymer concentrations in the two phases [29]. In contrast, the temperature usually has an opposite effect and therefore an increase of this parameter increase the polymers concentration required to obtain two phases [29].

Regarding the effect of salt type and its concentration, it will depend on the ATPS that is being used. When two non-charged polymers form an ATPS, this factor will not have a great effect on the position of the binodal curve as in a two-polymer system where one or both of the polymers are charged [30]. This last type of system is difficult to form without salt addition, since the phase separation only occur at very high polymer concentration (e.g., 10 wt% of each polymer), and with salt addition the phase separation occurs at lower polymer concentrations (e.g., 3–5 wt% of each polymer) [30].

1.2.2 Bioseperation in Aqueous Two Phase Systems

Due to its advantages, ATPS have been studied as a process to recovery and purify many biological products such as proteins, genetic material, cells and organelles. These advantages include its scale-up potential, its use on a continuous operation, the low toxicity of phase forming chemicals when compared with an organic-aqueous system and its biocompatibility [31].

Partitioning in ATPS is an important tool for separation and purification of many biological products. This technique depends mainly on the interaction between the biological product that it is being studied and the phase components [29]. By manipulating the partition coefficient, it is possible to separate proteins

from one another. This is achieved by altering several intrinsic factors of the system, for example the average molecular weight of the polymers and its concentration, the type of ions in the system, or by adding an additional salt such as NaCl. [31].

The production and purification of proteins with pharmaceutical applications have always an ever-increasing interest in the industry. Some of these therapeutic products have already been successfully recovered by using an ATPS, in Table 1.1 there are some recent examples of these products.

Table 1.1 – Examples of biopharmaceuticals recovered using an ATPS.

Biopharmaceutical	ATPS	Recovery	Additional information	Ref.
Human B19 parvoVLP	PEG 400/Phosphate	63.9%	Combined with precipitation	[32]
Human IgG	PEG 3350/Phosphate	76%	Optimization using experimental design	[33]
Pancreatic trypsin	PEG 3350/NaCitrate	99.7%		[34]
C-phycocyanin	PEG 4000/Phosphate	80%	---	[35]

With the aim of increasing the degree of purification, affinity ligands can also been added to the system as free ligand or attached to a polymer or a support, like magnetic particles [27]. As good example of this effect, there is the partition of Human IgG in the PEG/Dextran systems, which partition suffers a shift to the top phase in the presence of diglutaric acid functionalized PEG. Moreover, it was possible to obtain extraction yields over 90% [36].

Although the ATPS can be used as a downstream processing technique, it also gained a great interest as an analytical tool over the last years [37].

1.3 Magnetic Nanoparticles

Nowadays there is a great interest in finding new and innovative solutions either in the biomedical field or in the biotechnological field. The magnetic nanoparticles (MNPs) have been shown excellent platforms in these fields since they have an inherent superparamagnetic/paramagnetic nature and can be modified with biomolecules or ligands [38].

1.3.1 Properties and applications

In general, MNPs are iron oxide particles, which consist of an inorganic core with a protective shell of polymer. This inorganic core is mainly made up of magnetite (Fe_3O_4) or maghemite ($\gamma - Fe_2O_3$), that have paramagnetic/superparamagnetic properties. Both of these minerals have a similar structure where the oxygen atoms and the iron atoms are coordinating by an octahedral or tetrahedral structure.

The superparamagnetic property consist of an intermediate state between paramagnetic and ferromagnetic and for this reason these particles can be magnetized in the presence of a magnetic field and they can lose it as soon as the magnetic field is removed. Moreover, these materials are biocompatible, easy to synthesize and functionalize, and due to their high surface area to volume ratio, they present high loading capacity [39].

There are many ways to synthesize MNPs depending on the final objective, since each method can obtain iron oxide particles with different characteristics. Co-precipitation, thermal decomposition, microemulsion and hydrothermal synthesis, which are summarized in Table 1.2 are some of the most common methods used to synthesize MNPs. Moreover, these particles can also be synthesized biologically by a microorganism or bacteria, mainly using Magnetotactic bacteria and iron reducing bacteria [40], [41].

The most commonly synthesis method used is the co-precipitation, which consists of a proper mix of iron salts, namely ferric and ferrous ions in a molar ratio of 1:2 (Equation 1.1), under basic conditions and an inert atmosphere at room temperature or at elevated temperature [41].

$$Fe^{2+} + 2Fe^{3+} + 8OH^{-} \rightarrow Fe_3O_4 + 4H_2O \qquad \text{(Eq. 1.1)}$$

Table 1.2 - Comparison between some synthesis methods used to obtain MNPs. (Adapted from [42])

Synthesis Method	Synthesis	Reaction Temperature	Size Distribution	Shape control	Yield
Co-precipitation	Very simple, ambient conditions	20 – 90 °C	Relatively narrow	Not good	High / scalable
Thermal decomposition	Complicated, inert atmosphere	100 – 320 °C	Very narrow	Very good	High / scalable
Microemulsion	Complicated, ambient conditions	20 – 50 °C	Relatively narrow	Good	Low
Hydrothermal Synthesis	Simple, high pressure	220 °C	Very narrow	Very good	Medium

The main challenge of the co-precipitation method is the control of the particle size and the narrow particle size distribution, which can be controlled by adjusting several parameters such as the type of salt used the reaction temperature, the pH value and ionic strength of the media. Even though this difficult control of size, this method can produce great amount of particles [41], [42].

After the synthesis, it is important that MNPs maintain their stability without agglomeration or precipitation. In order to achieve this, a layer can be added, which will act like a protecting shell isolating the core against the environmental threats, such as the oxidation by oxygen, or erosion by acid or base [42]. The MNPs coating can be made by two different types of material: inorganic or organic. One of most inorganic materials used is silica, which can prevent the aggregation of nanoparticles, enhance the nanoparticles chemical stability, and even can provide better protection against toxicity [41]. As organic coating is possible to use for example surfactants or even polymers.

This protective shell not only protects the particles against degradation and aggregation, but also helps further functionalization of MNPs with groups such as $–NH_2$ and –COOH which are the via to put specific compounds on the MNPs surface like enzymes, drugs and chemical ligands [42], [43].

Due to their superparamagnetic properties and depending on the surface components, the MNPs can be applied in different areas. One of those areas is the biomedical area where MNPs are mainly used as magnetic resonance imaging (MRI) contrast agents, as vectors for gene and drug delivery, or as agents for cancer treatment using hyperthermia therapy. Another area is the biotechnological area where the MNPs application goes from bioseparation processes to biocatalysis and bioremediation [44].

1.3.2 Magnetic nanoparticles in Bioseparation

Since the downstream processing is responsible for the majority of the manufacturing costs, an increase of demand for high quality therapeutic proteins at low cost led to the discovery of new and different types of separation techniques.

Nowadays one of the most purification method used is the affinity chromatography, which is a type of liquid chromatography that is based on the selective and reversible binding between a molecule and a ligand and is present in many biological systems, for example the binding of an antibody with an antigen [45]. However, this method has some limitations that must be overcome, such as the limitations by pore diffusion and the column clogging that can be provoked by feed streams containing cells and other colloidal debris [46].

MNP-based separations have appeared as one of the most interesting separation technologies studied since these particles can be used in crude samples with suspended solid material [47]. Moreover, this type of technology present many others advantages such as low-cost, speed, scalability, and can be easily functionalized with affinity ligands towards a specific target [48].

In the literature, there are already many purified biomolecules using magnetic particles, and some of those have biopharmaceutical interest such as influenza virus particles and antibodies. Some of these biomolecules are summarized in the Table 1.3.

Table 1.3 - Summary of some examples of biomolecules purified from crude extracts with magnetic particles. (Adapted from [47]) .

Target	Encapsulation	Ligand	Source	Reference
Trypsin	With polyaniline or none	Azocasein	Crude extract from *Oreochromis niloticus*	[49]
Influenza virus particles	Sulfated cellulose	Sulfated Cellulose	Clarified virus harvest from MDCK cells	[50]
His-tagged β- glucosidase	poly (N, N'-methylenebisacrylamide-co-glycidyl methacrylate)	Iminodiacetic acid and Ni^{2+}	Crude E.coli lysate	[51]
Human IgG	Dextran	22/8	CHO cell culture supernatant	[52]

Magnetic particles can also be applied as the affinity support in other purification techniques such as aqueous two-phase system, which due to their magnetic and affinity properties allow an easier recovery of a certain protein from the crude extract [47].

2. Background and Aim of the work

There is a great interest on developing alternative separation technologies for the purification of human antibodies, and non-chromatographic approaches are appearing as sustainable and profitable solutions. Among these, aqueous two-phase extraction (ATPE) and magnetic fishing are interesting alternatives to conventional chromatographic techniques [26].

The Biomolecular Engineering Group at UCIBIO, REQUIMTE (FCT/UNL) in collaboration with the Institute for Biotechnology and Bioengineering at Instituto Superior Técnico of Lisbon, developed a hybrid process, which combines aqueous two-phase extraction and magnetic fishing for antibody purification. In this developed process, magnetic particles coated with gum arabic and boronic acid were added to a PEG/Dextran ATPSs, obtaining as result a high recovery of IgG with high purity from a crude extract [53]. Despite the success of the method, some issues needed further improvements, such as the use of economically viable alternative solutions for the ATPS polymers, and a better control of the MNPs partitioning in the ATPS to facilitate recovery and increase yield.

In this work, a new magnetic aqueous two-phase fishing technique to purify IgG was developed, by studying a new set of polymers in the presence of different NaCl concentrations in the system, namely 0, 150, 300 and 450 mM. Instead of using the highly expensive dextran, sodium polyacrylate (NaPA) 1,200, 8,000 and 15,000 Da was investigated as a cheaper alternative. Furthermore, magnetic particles previously used by Dr. Vijaykumar Dhadge, namely MNPs coated with dextran and 22/8 ligand, and MNPs coated with gum arabic and boronic acid were also studied to be applied in these new systems.

The research strategy is represented in Figure 2.1. The main goal of this work was to develop a sustainable and profitable solution to protein A chromatography, which is responsible for the majority of the purification costs during IgG manufacturing. Furthermore, at large scale application, the PEG/Dextran ATPS is too expensive mainly due to the high cost of dextran, and NaPA appears as economic solution to this problem.

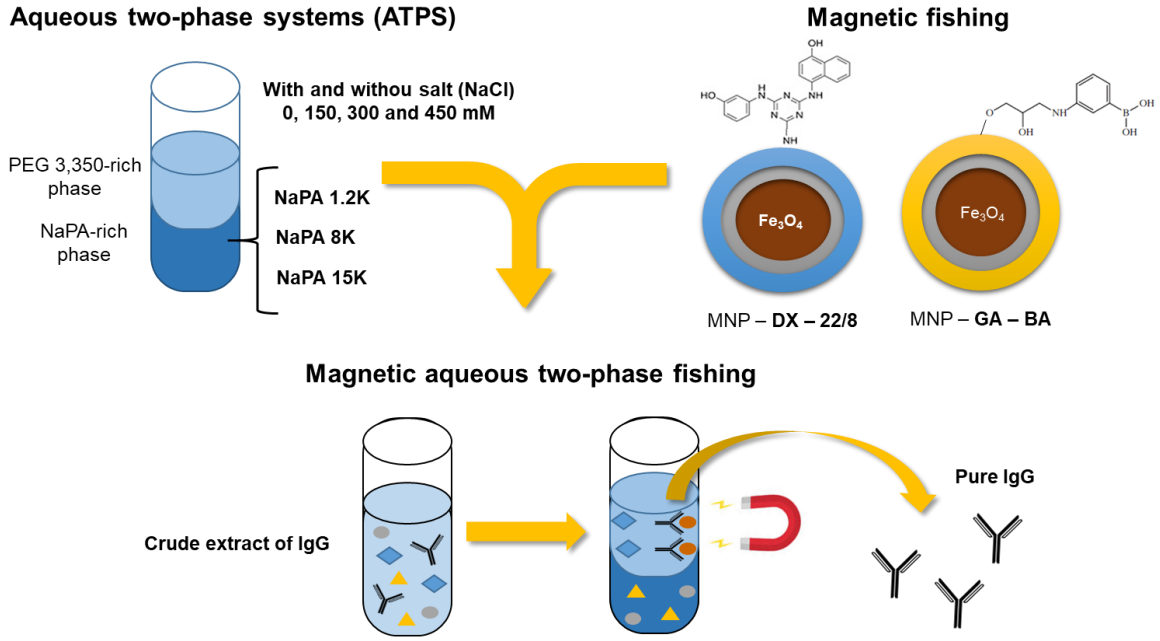

Figure 2.1 - Schematic representation of the research work followed in this work.

3. Materials and Methods

3.1 Materials

3.1.1 Chemicals

The ATPS were made using poly(ethylene glycol) average MW 3,350 (202444), poly(acrylic acid sodium salt) average MW 1,200, 45 wt % (416010), poly(acrylic acid sodium salt) average MW 8,000, 45 wt % (416029) and poly(acrylic acid sodium salt) average MW 15,000, 35 wt % (416037) from Sigma-Aldrich.

For the MNP synthesis was used iron (II) chloride tetrahydrate (44939) and iron (III) chloride hexahydrate (31232) from Sigma-Aldrich and ammonium hydroxide solution 25% (986030501) from Fluka. The MNP surface was modified using Sodium metasilicate pentahydrate (71746), Tetraethyl orthosilicate (TEOS) (131903) from Sigma-Aldrich, ethanol absolute (1210851212) from Panreac, dextran from *Leuconostoc* spp (40000g/mol; 68084) and Gum arabic from acacia tree (G9752) from Sigma-Aldrich. Then for the 22/8 ligand and boronic acid addition was used (3-aminopropyl)trithoxysilane (APTES) (44014-0), 3-aminophenol (100242), 4-amino-1-naphtol hydrochloride (133485), (3-Glycidyloxypropyl)trimethoxysilane (GLYMO) (440167), 3-aminophenylboronic acid hydrochloride (APBA) (410705) from Sigma-Aldrich, acid acetic (XXXXX), N,N-Dimethylformamide (DMF) (23470.293) from VWR and sodium hydroxide from Panreac AppliChem.

The protein recovery studies were performed with using polyclonal human immunoglobulin G (IgG) from Octapharma, which it is known as Gammanorm at a concentration of 165 g/L, and bovine serum albumin (A7906) from Sigma-Aldrich. For protein quantification, it was used either the Bichinchoninic Acid (BCA) kit from Sigma or the protein absorbance at 280 nm.

The IgG crude extract was provided by StabVida and it was produced by myeloma cells, namely Sp2/0 cells. Then, the total protein content was quantified with the Bichinchoninic Acid (BCA) kit from Sigma.

The SDS-PAGE gels were made with 30% acrylamide/Bis Solution 37.5:1 (161-0158) and 10% sodium dodecyl sulfate (SDS) solution (161-0416) from Bio-Rad, and ammonium persulfate (APS) (9592.2) and N,N,N,N – tetramethylethylenediamine (TEMED) (2367.3) from Roth. Moreover, for the loading buffer in the samples preparation, glycerol (G9012) and β-Mercaptoethanol (M6250) from Sigma-Aldrich, bromphenol blue sodium salt (A5212.1) from Roth were used. Either in the gels preparation or samples preparation was used Tris base solutions, which were made with Tris base ultra-pure for molecular biology (MB01601) from NZYTech.

Silver staining of polyacrylamide gels was performed with a Silver Stain Plus Kit (161-0449) from Bio-Rad was used, which includes fixative enhancer concentrate (161-0461), silver complex solution (161-0462), reduction moderator solution (161-0463), image development reagent (161-0464) and development accelerator reagent (161-0448). Furthermore, Methanol ≥ 99 % (8388.5) from Roth and acetic acid glacial (CAS 64-19-7) from Pronalab were also used.

3.1.2 Equipment

All the weights of the ATPSs for the binodal curves construction were obtained by using Mettler AE 100 balance (iBB-IST).

In the MNPs synthesis and chemical functionalization a mechanic stirrer, a water-bath SHC 2000 from Scanvac, a Sonicator SilverCrest, a centrifuge Thermo Scientific Heraeus Multifuge X3R and an Incubator KS4000ic from IKA were used.

The hydrodynamic diameters of MNPs samples with dextran and 22/8 ligand were measured in a Dynamic Light Scattering Zetasizer Nano ZS from Malvern (iBB-IST). For the MNPs samples with gum arabic and boronic acid, the hydrodynamic diameters and zeta potential values were measured with SZ-100 Nanoparticle Analyzer from Horiba (FCT-UNL), and the zeta potential results were acquired also in this equipment.

The Fourier transform infrared (FTIR) spectra for the MNPs samples were acquired on Spectrum Two IR Spectrometer from PerkinElmer.

The incubations for the binding assays and the extract purification were performed in a Bibby Scientific Stuart Rotator Disk.

The BCA reactions were performed in the hybridization oven Boekel Big Shot IIITM from Bockel Scientific. Moreover, all the spectrophotometric measurements, 280 nm and BCA assays, were obtained by using the Microplate Reader – Tecan Infinite F200 from Tecan.

The IgG content in the crude extract was obtained by using a 1 mL HiTrap MabSelect SuRe column in an ÄKTA pure system from GE Healthcare Life Sciences, and the protein was quantified by microBCA.

The Mini-Protean Tetra System from Bio-Rad was used for the electrophoresis SDS-PAGE gels. In addition, the gels photographs were taken with a Gel Doc XR+ System from Bio-Rad.

3.2 Methods

3.2.1 Aqueous two phase systems

3.2.1.1 Characterization – Determination of phase diagrams

The aqueous two phase systems studied were composed by PEG 3,350 and NaPA with different molecular weights (1,200, 8,000 and 15,000) in the presence and absence of NaCl (0, 150, 300 and 450 mM). The binodal curves of these systems were determined by using the turbidometric titration method at 25 ºC (± 1 ºC) and atmospheric pressure [54]. This titration is divided in two methods, direct and indirect, that only differentiate in order at which the polymers are added.

A variety of polymer stock solutions were prepared with different polymers and concentration of salt, as represented in the Table 3.1. In the direct method, 1 g of the stock of PEG was weighted in a glass beaker and a stock solution of NaPA was added dropwise with shaking until a turbid mixture appeared and the final weight was measured. MilliQ water was added dropwise with shaking until the mixture became clear and the final weight was also determined. For the systems with salt, the water added had the same concentration of salt as the polymers in study. This procedure was repeated until the mixture would not become turbid anymore and the polymer concentrations at the binodal curve were calculated using all the weights measured. Since this method can only obtain one part of the binodal curve, an indirect method was applied. This method is the opposite of the direct method and therefore a stock solution of PEG was added dropwise to a stock solution of NaPA, which was weighted previously.

Table 3.1 – Different polymer stock solutions prepared for the determination of each phase diagram, with different concentration of salt.

Solution	Polymers	Concentration % w/w	[NaCl] (mM)
1	PEG 3,350	40%	0, 150, 300 and 450
2	NaPA 1,200	45%	
3	NaPA 8,000	45%	
4	NaPA 15,000	35%	

The binodal curve was adjusted to the Merchuk equation, represented in equation 3.1, using the add-in Solver of the Excel program:

$$[\mathrm{PEG}] = \mathrm{A}e^{[(\mathrm{B}[\mathrm{NaPA}]^{0,5})-(\mathrm{C}[\mathrm{NaPA}]^{3})]} \quad (3.1)$$

[PEG] and [NaPA] represent the mass percentage of polymers, and A, B and C are constants obtained by fitting the binodal curve.

3.2.1.2 BSA and IgG partitioning

In this section, the aqueous two-phase systems were prepared by weighting the stock solutions of different polymers, MilliQ water and protein solution in order to achieve the desired final composition of each system. Moreover, only the NaCl concentrations of 0 and 150 mM were used on these studies. All the systems were prepared in microtubes of 2 mL with a final weight of 1.5 g by adding PEG 3,350 of 40% stock solution (to a final concentration of 10% w/w), NaPA stock solution (to a final concentration of 10% w/w), 300 µL of protein solution at 1 mg/mL (final concentration of 0.02% w/w), MilliQ water and salt if it was necessary. Then the systems were well mixed in a vortex mixer for 15 minutes and the phase separation occurred at room temperature. After forming two phases, the phase volumes were measured and the bottom and top phase were analyzed for protein quantification by using the absorbance at 280 nm.

The calibration samples for this section were prepared by mixing an equal portion of calibration sample of protein and one of the phases, which was collected by making a 20 g system without protein. The calibration samples of protein had a concentration range of 0-0.4 mg/mL.

The partition coefficients (K) of these proteins were calculated based on equation 3.2:

$$\mathrm{K} = \frac{[\mathrm{Protein}]_{\mathrm{PEG}}}{[\mathrm{Protein}]_{\mathrm{NaPA}}} \tag{3.2}$$

Where $[Protein]_{PEG}$ and $[Protein]_{NaPA}$ represent the total concentration of a protein in the PEG rich and NaPA rich phase, respectively.

3.2.2 Magnetic particles

3.2.2.1 Synthesis of MNPs

The bare MNP were synthesized by the chemical co-precipitation method, which is based on the mixture of two different solutions of iron salts. In this protocol, 24.33g of $FeCl_3.H_2O$ are dissolved in 400 mL of water and 10.8 g of $FeCl_2.4H_2O$ are dissolved in 45 mL. After mixing these solutions in a reactor, a mechanical stirrer was used for a short period of time to homogenize the mixture. Then a solution of 75 mL of 25% NH_4OH was added quickly to the reactor and was left reacting for 5 minutes after which the mechanical stirring was stopped. Finally, the particles synthesized were transferred to a proper flask and washed with water by magnetic decantation. The volume of water used in each wash was approximately twice the volume of particles in the flask and these washes were stopped until the supernatant had a neutral pH.

To synthesize silica coated-magnetic particles, a solution of sodium metasilicate pentahydrate was initially prepared, which needs to dissolve overnight, under magnetic stirring and heat was prepared. For 2 g of particles, 2.4 g of silicate were diluted in 84.2 mL 50% (v/v) ethanol/H_2O. Then the particles were resuspended in a certain volume of water to obtain a concentration of 10 mg/mL and were sonicated during 15 minutes. After this, the coating solution was added dropwise to the particles solution

with sonication and was allowed to react during 2 hours in a water bath at 40ºC under mechanical stirring. The MNPs were then washed with 50 % (v/v) ethanol/ H_2O (3x) and distilled water (3x).

For the second silica coating with TEOS, the MNPs were resuspended in 80 mL of 80% (v) ethanol/H_2O to obtain a concentration of 25 mg/mL. This solution was sonicated for 10 minutes and afterwards 3.16 mL of 5 M NH_4OH solution was added. After that, 1.58 mL of TEOS was added dropwise to the solution under sonicating and after was placed in a water bath at 40°C for 2h under mechanical stirring. Finally, the particles were washed by magnetic decantation with 80% ethanol/water (3x) and afterwards with distilled water (3x).

For the last coating with polymer, 2 g of particles were initially resuspended in 175 mL of distilled water and were sonicated for 10 min. A solution of polymer was prepared (2 g of Dextran/Gum arabic in 25 mL of water) and was added dropwise to the particle solution. After this, the solution was placed in a water bath at 60°C for 2h under mechanical stirring, and the particles were washed with distilled water (5x).

3.2.2.2 MNP with Dextran

Amination of MNPs

To aminate the MNPs with Dextran (MNP-DX), 2 g of particles were resuspended in 179 mL 50% ethanol/ H_2O. After sonicating during 5 minutes, 1 mL of acetic acid and 20 mL of APTES (15% V/V) was added to the solution, obtaining a MNPs concentration of 10 mg/mL. The mixture was incubated at 70°C during 1 hour with orbital shaking and subsequently the particles was washed with water.

22/8 ligand synthesis

For the first substitution, the aminated particles were first washed with cold water (2x), then washed with cold 50% acetone/water (2x), and after resuspended in 50% acetone/water, to a final concentration of 5 mg/mL. To this magnetic slurry, a solution of cyanuric chloride (0.116 g/mL) was added, which was dissolved in cold acetone and had 5 excess molar of cyanuric chloride in relation to the amines content. The mixture was incubated at 0°C with orbital shaking (200 rpm) for an hour and a half, and subsequently the particle slurry was washed with acetone (2x), 50% acetone/water (3x) and water (5x).

For the second substitution, the supernatant was removed and a solution of 3-hydroxyalinine in 50% DMF/water was added, in order to obtain a final particle concentration of 5 mg/mL. Afterwards the solution was placed in an orbital shaker at 30°C and 200 rpm during 24 hours. The particles were then washed with water (5x).

To finish the ligand synthesis, the supernatant was again removed and was added a solution of 4-amino-1-naphtol hydrochloride in 50% DMF/water. Since this amine is protected with hydrochloride was necessary to add sodium hydroxide in the correct amount. After the reaction for 48 hours at 80°C and 200 rpm, the particles were washed with 50% DMF/water (3x) and with water (5x).

3.2.2.3 MNP with Gum arabic

Boronic Acid ligand

First, 0.5 mL of GLYMO were added to 25 mL of Gum Arabic coated MNPs (MNP-GA) solution, which had a MNPs concentration of 10 mg/mL. After 3 hours of incubation at room temperature and mechanical stirring, 0.2 g of APBA, which were neutralized with NaOH, were added to the MNP solution and the reaction was allowed to occur overnight. Finally, the solution was washed with distilled water (5x).

3.2.2.4 Affinity Assays towards BSA and IgG

The MNPs were washed with regeneration buffer (0.1M NaOH in 30% (v/v) isopropanol) and then with deionized water to neutralize the pH. After this procedure was repeated two times, the MNPs were equilibrated in binding buffer (50 mM phosphate, pH 8 for MNPs-DX and 22/8 ligand; and 20 mM HEPES, pH 8.5 for the MNP-GA and boronic acid) to a final concentration of 10 mg/mL. Samples with 5 mg of MNPs were prepared and the supernatants were removed. Afterward, 500 µL of IgG or BSA solution in binding buffer (1 mg/mL) were added and the samples were incubated for 30 minutes at room temperature in rotator disk under constant stirring. After incubation the particles were washed five times with binding buffer and elution buffer (50 mM Glycine – NaOH, pH 11 for MNP-DX and 22/8 ligand; and 1 M Tris-HCl Buffer, pH=8,5 for MNP-GA and boronic acid). Each wash was collected and quantified by the BCA assay in the case of MNP-DX-22/8 and by 280 nm in the case of MNP-GA-BA. In this section, the particles with just biopolymer (MNP-DX and MNP-GA) served as a control.

The protein binding (mg of protein/ g of support) of these MNPs was calculated with equation 3.3:

$$\text{Protein binding} = \frac{\text{m(protein bound)}}{\text{m(MNPs)}} \tag{3.3}$$

Where m(protein bound) is the mass of protein that remained bound to the particles after washes and m(MNPs) represents mass of MNPs used in the assay, in this case was 5 mg of particles.

The percentage values of binding, elution and recovery from these assays were calculated using equation 3.4, 3.5 and 3.6, respectively:

$$\text{Binding (\%)} = \frac{\text{m(protein bound)}}{\text{m(protein)}} \times 100\% \tag{3.4}$$

$$\text{Elution (\%)} = \frac{\text{m(protein eluted)}}{\text{m(protein bound)}} \times 100\% \tag{3.5}$$

$$\text{Recovery (\%)} = \frac{\text{m(protein eluted)}}{\text{m(protein)}} \times 100\% \tag{3.6}$$

The m(protein) is the total mass of protein that was used in an assay and the m(protein eluted) represents mass of protein in the elution washes.

3.2.3 Protein A affinity chromatography

Before operation, the ÄKTA system was completely cleaned with degassed MilliQ water and the buffers were put in the correct lines according to the method (A1: binding buffer; B1: elution buffer). The binding buffer used was 20 mM sodium phosphate, 150 mM NaCl, pH 7.2 and the elution buffer was 100 mM sodium citrate, pH 3.0-3.6. After this, the system was purged with all the solutions and conditioned with binding buffer. The 1 mL HiTrap MabSelect SuRe column was placed and conditioned with binding buffer. At this point, the sample of crude extract of IgG was loaded in the sample loop (5 mL). Subsequently, the method was run, which consisted of an equilibration with 5 columns volumes (CVs) of binding buffer, sample load of 10 mL, binding washes with 5 CVs of binding buffer, elution with 5 CVs of elution buffer and, finally, 10 CVs washes of binding buffer. After the chromatographic run, the column was cleaned with a cleaning in place (CIP) solution (250 mM NaOH) with 5 CVs and then was cleaned with MilliQ water until pH 7 was reached. Either the column or the ÄKTA system were left in 20% of ethanol. The column was stored at 4ºC. The samples with the higher values of UV absorbance were collected and analyzed by BCA and by SDS polyacrylamide gel electrophoresis.

3.2.4 Magnetic Aqueous Two Phase Fishing

3.2.4.1 BSA and IgG recovery

These studies were performed with systems similar to the ones in the section 3.2.1.2, but with the addition of an appropriate volume of MNPs. The MNPs concentration used in this studies was 0.02% w/w, (300 µg of MNPs in a final system weight of 1.5 g) and the protein concentration was also 0.02% w/w (300 µL of 1 mg/mL IgG/BSA solution in a final system weight of 1.5 g).. After system mixing and phase separation, the microtubes were put against a magnet and the MNPs were collected along with the top phase. Then the MNPs were washed with binding buffer (x5) and elution buffer (x4) . The binding and elution buffers were the same used in the MNPs affinity assays. The bottom phase of each system was collected from the bottom of the microtubes with the help of a syringe. All the samples collected were analyzed for protein quantification by using the absorbance at 280 nm.

3.2.4.2 Cell culture supernatant purification

The best system to recover IgG determined in the previous sub-section was used was to purify IgG from a crude extract. The procedure was similar to the one described previously but instead of using a pure protein solution, a crude extract solution was used. The final concentration of total protein and MNPs in the system was the same as the previous systems (0.02% w/w). Samples collected were analyzed for protein concentration using the BCA method. To avoid interference from the polymers, an ultrafiltration was performed using Amicon ultra filters with a MWCO of 30 kDa. Moreover, control studies using separately each unit operation, ATPS or magnetic fishing, were also done by replacing the MNPs for water and the polymers for binding buffer, respectively. The yield and purity of the samples were calculated with equations 3.7 and 3.8 using the BCA method and a SDS-PAGE analysis:

$$Y\ (\%) = \frac{m(protein)_R}{m(protein)} \quad (3.7)$$

$$P\ (\%) = \frac{m(protein)_R}{m(total\ protein)} \quad (3.8)$$

Where the m(protein) represents the total mass of a specific protein in the crude extract that was placed into the system; the $m(protein)_R$ is the mass of a specific protein recovered from the crude extract and the m(total proteins) represents the total protein content in a purified sample. The m(protein) and the $m(protein)_R$ extrapolated from the protein bands of SDS-PAGE by densitometry analysis using ImageJ.

3.2.5 Analytical Methods

3.2.5.1 Quantification of amines by Kaiser Test

The Kaiser test is a colorimetric test based on the reaction of ninhydrin with primary amines. In the beginning of each test realized, a 0.01 M glycine stock solution was prepared, to obtain calibration curves in range of 0-5 µmol NH_2/mL. 1mL solutions of aminated particles with different MNPs concentrations were prepared (10 mg/mL, 5mg/mL and 1 mg/mL). For each sample tube 50 µL phenol 80% (v/v) in ethanol, 50 µL 2% 0,001 M KCN in pyridine and 50 µL 5% (v/v) ninhydrin in ethanol were added. Samples were then incubated at 100°C for 5 minutes, and the MNPs samples were centrifuged to recover the supernatant. The amination content was obtained by measuring the absorbance at 560 nm and in this work, this content ranged from 83 µmol NH_2/g support to 103 µmol NH_2/g support depending on the MNP concentration used.

3.2.5.2 Characterization of MNPs

Concentration determination

The concentration of each magnetic particles solution was calculated using dry-weight measurement. This method consist in pippeting 200 µL of solution to a microtube, which was previously weighted, and let it dry overnight. On the next day, the MNP dried mass was weighted and the concentration was calculated by mass difference.

Fourier transform infrared spectroscopy (FTIR)

Fourier transform infrared (FTIR) spectra were acquired using Spectrum Two IR Spectrometer from PerkinElmer. The samples measured were prepared by mixing dry particles and KBr in a concentration of 1% (weight of particles/total weight).

Hydrodynamic Diameter

Hydrodynamic diameter was measured by dynamic light scattering (DLS) and these measurements were performed using the Zetasizer Nano ZS system from Malvern and Horiba SZ-100. For these measurements, samples with a final concentration of 0.05 mg/mL in MilliQ water were prepared.

Zeta Potential

This characterization was performed with a nanoparticle analyzer Horiba SZ-100. The particles were diluted in a 0.01 M KNO_3 solution and using HNO_3 or KOH solutions was possible to adjust the solution pH for different values, ranging from 2.5 to 12.

3.2.5.3 BCA Assay

The colorimetric BCA assay allows the quantification of total protein in a sample. The BCA reagent was prepared by adding 50 parts of reagent A (bicinchoninic acid, sodium carbonate and sodium bicarbonate in 0.1N NaOH pH 11.25) and 1 part of reagent B (4% (w/v) copper(II) sulfate pentahydrate). Then 25 µL of each sample were pipetted to each corresponding well of a transparent 96-well microplate, and 200 µL of BCA reagent were subsequently added. The microplates were incubated at 37°C during 30 min and the absorbance at 560nm was measured. The calibrations curves were obtained by using calibration samples of protein ranging from 0 to 1 mg/mL.

3.2.5.4 SDS-PAGE of protein samples and staining

In this work, 12.5% acrylamide/bisacrylamide SDS-PAGE gels were used and the volumes necessary to prepare this type of gel are presented in Table 3.2. Initially, the solution of running gel was prepared and it was transferred to the glass plates of the casting frame. Then a thin layer of 2-butanol was added on the top of the running gel solution which was allowed to polymerize for 1 hour. After polymerization, the 2-butanol was removed and the 5% acrylamide stacking gel was prepared and added on top of the previous gel. The comb was gently inserted and the gel was left to polymerized for 1 hour. The running buffer (25 mM Tris, 192 mM glycine, 0.1% SDS, pH 8.3) was added to the tank and the final polymerized gel was introduced in the running module. The sample, which were previously prepared, were loaded into each well. The running were set as 30 A for 1 hour.

Table 3.2 - Volumes needed to prepare the polyacrylamide gel for SDS-PAGE.

Stock solutions	Running gel 12.5% Acrylamide	Stacking gel 5% Acrylamide
Solution I (µL) **3M Tris Base, pH 8.8**	750	-
Solution II (µL) **0.5M Tris Base, pH 6.6**	-	450
Solution III (µL) **Acrylamide:Bisacrylamide 30:08**	2080	0.3
SDS 10% (µL)	50	18
Distilled water (µL)	2100	940
APS 10% (µL)	38	13.5
TEMED (µL)	2.5	2.0

Blue-Coomassie staining

After the electrophorese run, the SDS-PAGE gel was stained using a staining solution (1 g Coomassie Blue R-250, 15 mL glacial acetic acid, 90 mL methanol and 95 mL distilled water) during 30 min. The gel was then destained overnight with a destaining solution (75 mL glacial acetic acid, 450 mL methanol and 475 mL distilled water).

Silver Staining

To detect some protein bands, it was necessary to stain the gel with a Silver Stain Coloration kit. Initially, the gel was placed for 20 minutes in 100 mL of Fixative enhancer solution (50% of methanol, 10% of acetic acid, 10% of fixative enhancer concentrate and 30% of distilled water) with gentle agitation. Then the gel was washed twice with 100 mL of distilled water for 10 minutes. A staining solution was prepared with 35 mL of distilled water, 5 mL of silver complex solution, 5 mL of reduction moderator solution, 5 mL of image development reagent and 50 mL development accelerator solution and it was immediately added the gel for 15 minutes. Finally, the gel was placed in a stop solution (5% of acetic acid) and it was after washed with distilled water.

4. PEG and NaPA Aqueous two phase system

4.1 Introduction

The aqueous two-phase systems (ATPSs) have been used to separate biomolecules such as proteins since the 1950s. As it was described previously in the Literature Review, these systems are formed through the mixture of two aqueous solutions of hydrophilic polymers or by mixing one semi-hydrophobic polymer with salt, and since there are many polymers in nature with these characteristics there are many possibilities to form ATPSs [54].

In 2002, Subhash Chand and co-workers reported a new ATPS formed by poly(ethylene glycol) (PEG) and sodium polyacrylate (NaPA) (Figure 4.1) [55]. These polymers are environment-friendly, inexpensive and easy to handle. Besides, the PEG-NaPA ATPSs are quickly formed upon mixing the components, have low viscosity and both polymers can be recycled [56]. All of these properties are of great importance at industrial level, which makes this system a potential technique to study. Some proteins have already been studied for protein partitioning using the PEG-NaPA system, such as example the green fluorescence protein (GFP) [57] and lysozyme [56].

The aim of this chapter was to investigate the effect of NaCl and of different molecular weights of NaPA on the ability of PEG and NaPA to form a two-phase system. The NaCl concentration studied were 0, 150, 300 and 450 mM, whereas the molecular weights of NaPA used were 1,200, 8,000 and 15,000. Furthermore, the partitioning of different proteins were studied in different PEG-NaPA systems, namely BSA and IgG.

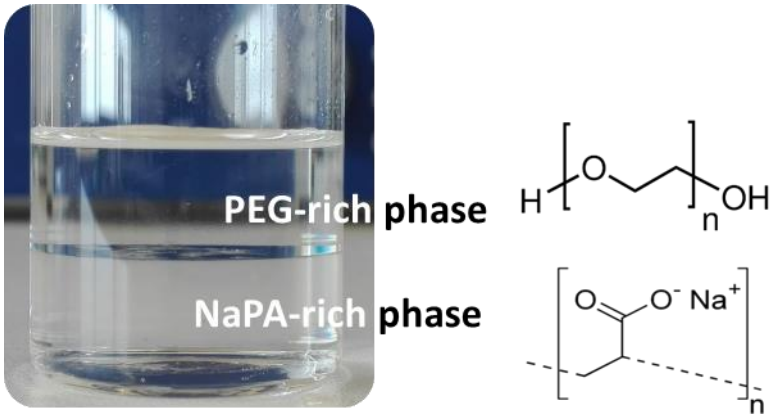

Figure 4.1 – PEG-NaPA system where is represented the polymer-rich phase and their receptively chemical structure. This ATPS was formed by PEG 3,350 (10% w/w) and NaPA 1,200 (10% w/w) without salt adding.

4.2 Binodal curves of PEG/NaPA ATPS

4.2.1 Effect of NaCl concentration

The PEG-NaPA systems are formed by an uncharged polymer (PEG) and a negatively charged polymer (NaPA) (Figure 4.1). In this type of system, salt concentration can have a great influence on the position of the binodal curve, contrary to what happens in ATPSs formed by two uncharged polymers. The effect of NaCl concentration in the binodal curve of PEG-NaPA system with different molecular weights of NaPA is shown in Figure 4.2.

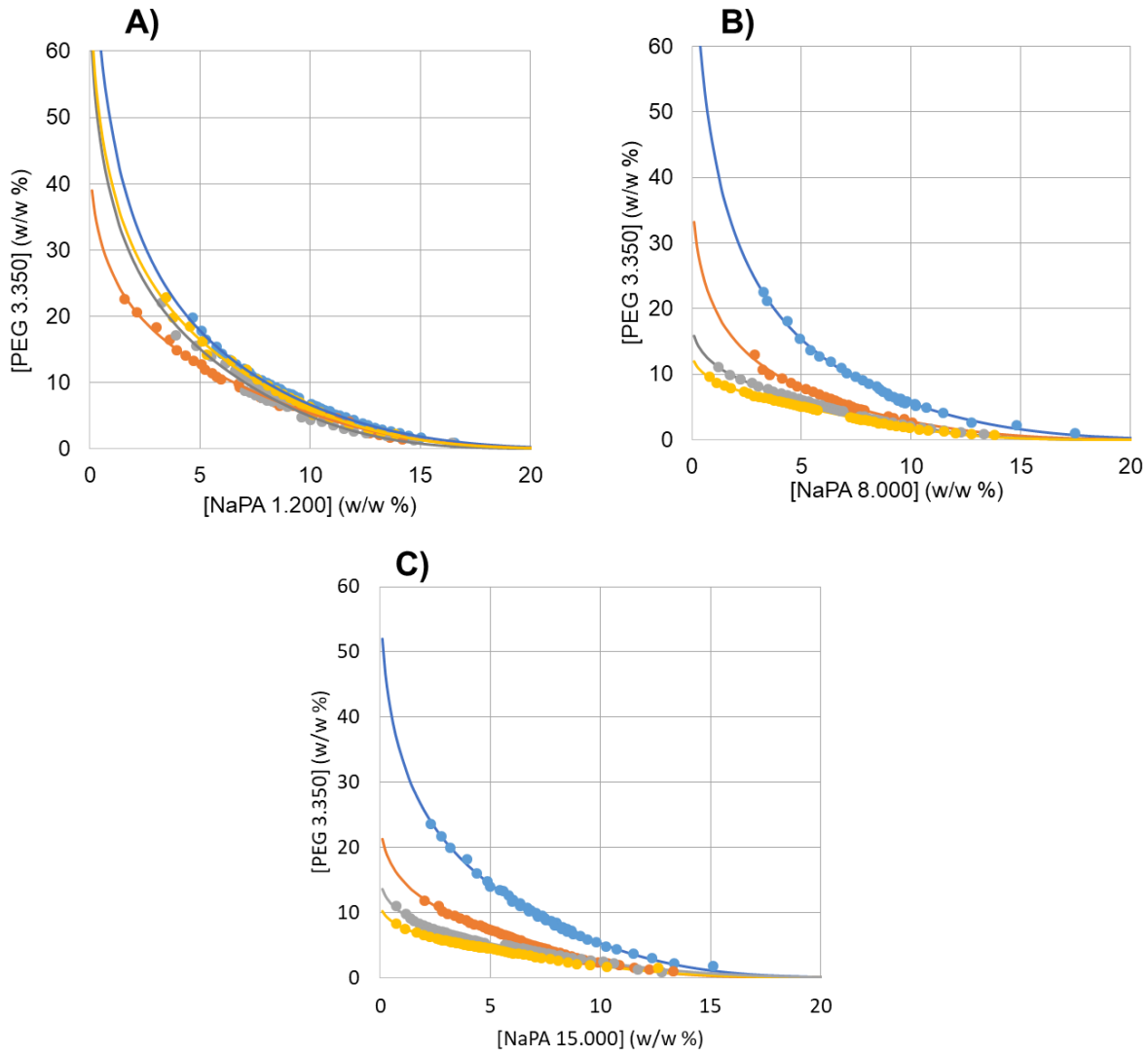

Figure 4.2 - Effect of NaCl concentration in the binodal curve of PEG/NaPA ATPS with different MWs of NaPA. **A)** Binodal curves of PEG/NaPA 1.200 ATPS; **B)** Binodal curves of PEG/NaPA 8.000 ATPS; **C)** Binodal curves of PEG/NaPA 15.000 ATPS. NaCl concentrations: — 0 mM; — 150 mM; — 300 mM; — 450 mM.

In the literature it is reported that to prepare a PEG-NaPA system with a convenient polymer concentration (1–10 wt%), a minimal addition of salt to the system is needed [58]. However, according the results obtained in Figure 4.2, it was possible to prepare two-phase systems within this polymer concentration range without any addition of NaCl. This could have occurred since the pH system was about 8 and NaPA had less negative charges than at pH 11, used in the literature [58]. Moreover, if there is no salt addition to the system, the separation between charged and uncharged polymer is suppressed by the large difference in small ion concentration between the phases, namely of Na^+ [30]. As a result, in this PEG-NaPA ATPS occurred at higher polymer concentration than to the ATPS with salt addition.

With the exception of the ATPS containing NaPA 1,200, when NaCl is added to the PEG-NaPA systems, the binodal curve moves towards the water-rich region of the diagram phase, making these systems easier to form at low polymer concentrations. This change in the binodal curves occurs more strongly effect for the first NaCl concentration (150 mM) being less pronounce upon adding more salt. The salt addition facilitates compartmentalization of the NaPA, making this polymer less charged. When there is a saturation effect, the polyelectrolyte NaPA behaves as an uncharged polymer. Thus adding small ions to the system (Na^+ and Cl^-) makes the influence of the NaPA counter ions (Na^+) less important by decreasing the ion concentration difference between the phases [30].

Regarding the binodal curves of PEG-NaPA 1,200, there is little or none effect of salt adding, being all the binodal curves very similar to each other. Since 1,200 is the smallest MW studied, this polymer is more hydrophilic and has less negative charges. Therefore, the NaPA 1,200 could be behaving as an uncharged polymer, and consequently the salt addition does not have an effect in the binodal curve.

4.2.2 Effect of NaPA molecular weights

In a polymer-polymer ATPSs, the MWs of the polymers has a great influence on the binodal curve of the system. The higher the MW of a polymer, the easier the two phases are obtained, in other words the binodal curve tend to move to the water-rich region with the increase in the polymer MW. Moreover, the larger the difference between the MW of polymers, the higher the asymmetry of the binodal curve [59]. The effect of NaPA MW in the binodal curves of in the binodal curve of PEG-NaPA system with different NaCl concentrations is shown in Figure 4.3.

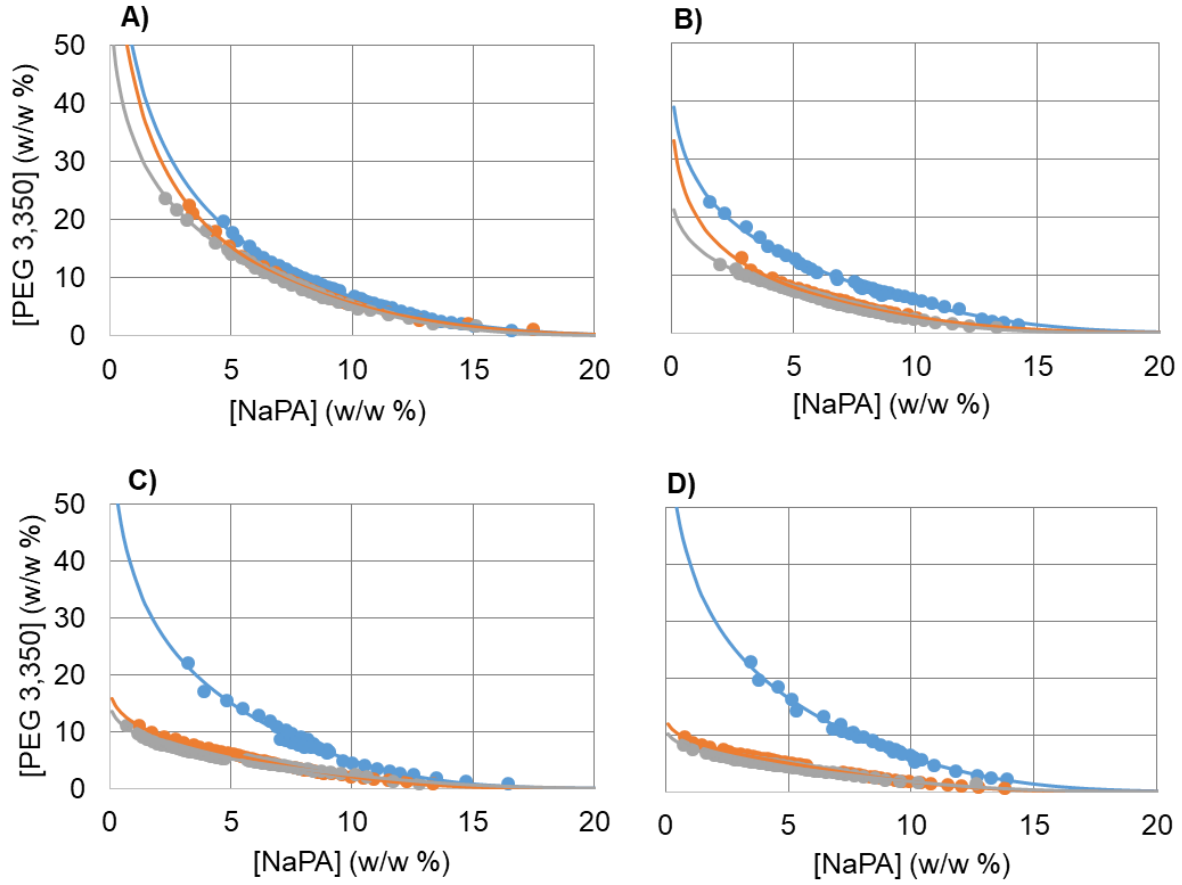

Figure 4.3 - Effect of NaPA MW in the binodal curves of PEG/NaPA ATPS with different NaCl concentrations. . **A)** Binodal curves of PEG/NaPA ATPSs with 0 mM of NaCl; **B)** Binodal curves of PEG/NaPA ATPSs with 150 mM of NaCl; **C)** Binodal curves of PEG/NaPA ATPSs with 300 mM of NaCl; **D)** Binodal curves of PEG/NaPA ATPSs with 450 mM of NaCl. NaPA MWs: — 1.200; — 8.000; — 15.000.

From Figure 4.3, it is possible to observe what was previously described. The binodal curves of ATPSs with NaPA 15,000 are more shifted to the water-rich region than the binodal curves of ATPSs with NaPA 1,200. This may be caused by the increase in the incompatibility between the polymers, since the hydrophobicity of a polymer increases with its molecular weight. However, in the PEG-NaPA systems without salt addition, the shift between binodal curves is less noticeable because the polyacrylate polymers have some negative charges making its hydrophobicity less important. When NaCl is added, the shift between binodal curves increases, namely between PEG-NaPA 1,200 and the others PEG-NaPA systems, because the NaPA 1,200 behaves already as an uncharged polymer at 0 mM of NaCl unlike the others NaPAs, which tend to gain this behavior with the increase of salt addition.

With these results, the PEG-NaPA systems without and with 150 mM of salt addition were chosen to further studies, since at industrial level they are more beneficial. At this level, systems that have high concentration of salt could lead to corrosion of metal pumps, lines and other equipment [60]. Furthermore, a polymer concentration of 10% w/w for each polymer was also chosen for further studies.

4.3 Partitioning of pure proteins in PEG/NaPA ATPSs

As discussed in the introduction of this chapter, PEG-NaPA ATPSs have already been used to study the partitioning of some proteins, such as GFP, hemoglobin and lysozyme. In this chapter, the PEG-NaPA ATPS chosen were used to study the partitioning of BSA and IgG.

4.3.1 BSA

The partitioning of a target biomolecule in an ATPS is often shifted by adding neutral salts to the system, such as NaCl. It is reported that when NaCl is added, the positively charged proteins tend to partition to the top phase (PEG rich) of a ATPS, while negatively charge proteins tend to partition to the bottom phase [33], [61]. The effect of NaCl addition on partition coefficients (K) of BSA in PEG-NaPA systems with different NaPA MWs are shown in Figure 4.4.

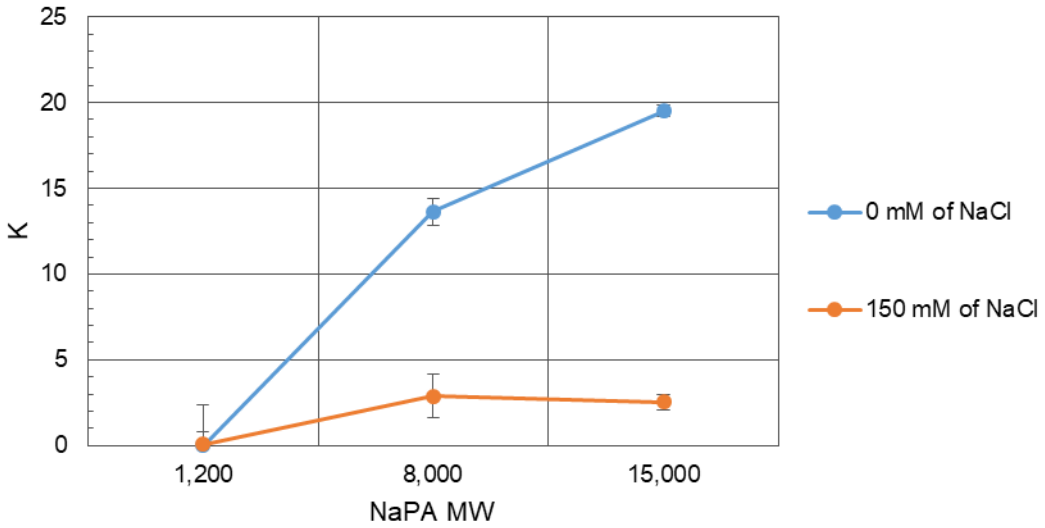

Figure 4.4 - Effect of NaPA MWs (1,200, 8,000 and 15,000) and NaCl concentrations (0 and 150 mM) on the partitioning of BSA in the PEG/NaPA system (n=2).

In Figure 4.4, the expected effect of NaCl is observed, and the partition coefficient of BSA decreases by adding NaCl to the systems with the exception to the PEG-NaPA 1,200, which remained constant. By increasing the NaCl concentration, the partition coefficient in the PEG-NaPA 8,000 and 15,000 decreased, respectively, from 13.62 to 2.89 and from 19.50 to 2.54. Although there was this substantial drop in the partition coefficient, the BSA remained mainly in the top phase in the ATPS with NaCl, about 65% of total BSA. Moreover, the partition coefficient of BSA seemed to increase or maintain with the NaPA MW. These partitioning results could be explain by electrical interaction and repulsion between the charged aqueous two-phase systems and the BSA.

Regarding the results of PEG-NaPA systems without salt, the BSA partitioning could have occurred due to repulsion interactions between the charged NaPAs and this protein, which isoelectric point is 4.6 and thus it was negatively charged [62]. When the MW of NaPA increases, the number its carboxylic groups increases as well, as result the polymer becomes more negatively charged and makes the partition coefficient value higher. In the presence of NaCl, the repulsion between the negatively charged BSA and the NaPA polymer is lessened, and partitioning towards the bottom phase increases.

4.3.2 IgG

The effect of NaCl addition and of NaPA MW on the partitioning of IgG in PEG-NaPA systems are presented in Figure 4.5. From these results and Figure 4.6, it is observed that IgG was precipitating in the interface of these ATPSs, making the calculation of partition coefficient hard to be performed. The amount of precipitated IgG percentage was determined by a balance differences between the total of protein was add to the system and quantified in both phases.

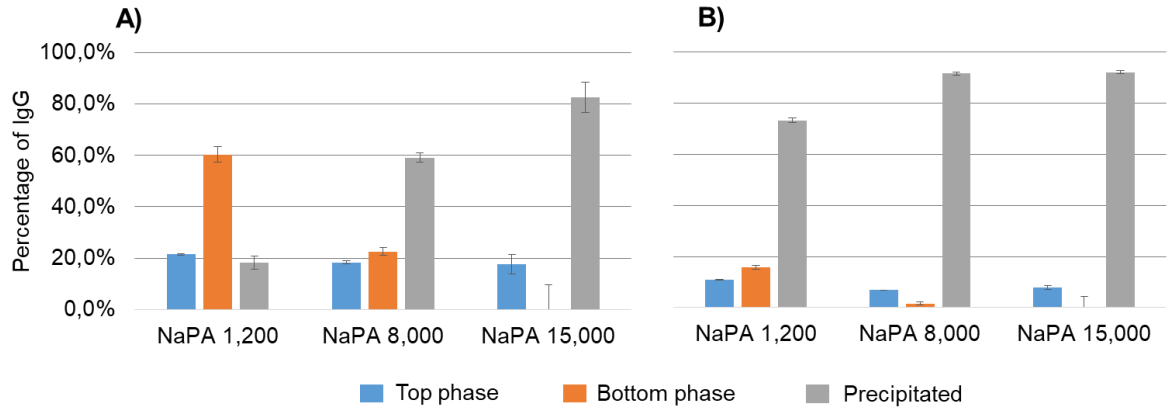

Figure 4.5 –Effect of NaPA MWs (1,200, 8,000 and 15,000) and NaCl concentrations (0 and 150 mM) on the partitioning of IgG in the PEG/NaPA system. **A)** Systems without salt addition; **B)** Systems with 150 mM of NaCl (n=2).

The precipitation of IgG in these ATPSs could be explained by the high polymer concentrations used in these systems. Without salt addition in the system, the precipitation of IgG was dependent of NaPA MW, since an increase of NaPA chain induced an increase of precipitated IgG percentage. When NaCl was added, the ionic strength of the system increased and thus more IgG precipitated. Moreover, it was possible to obtain a percentage maximum of precipitated IgG of 92% using PEG-NaPA 8,000 and 15,000 with salt addition, which were the systems that would be expected to get a higher ionic strength.

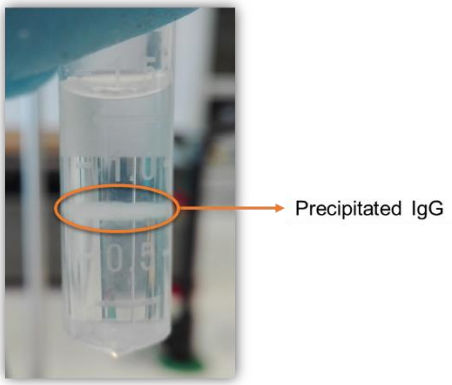

Figure 4.6 - Precipitation of IgG in the PEG-NaPA 1,200 ATPS without salt addition.

4.4 Conclusions

In this chapter, the effect of NaCl and of NaPA MW in the binodal curve of PEG/NaPA ATPS was studied. Both parameters had the same result in the binodal curve, causing a shift towards the water-rich region of the phase diagram. These results were not observe for the PEG-NaPA 1,200, because NaPA 1,200 has less carboxylic groups in its chain than the others NaPAs, and thus it could be behaving as uncharged polymer in absence of salt already.

The PEG-NaPA ATPS without and with 150 mM of NaCl were chosen for the further studies not only to avoid problems that high concentrations of salt could bring at industrial level but also because high concentrations of salt could lead to the precipitation of proteins, by increasing the ionic strength of the system. The concentration of each polymer was also chosen, and ATPSs with 10% (w/w) of each polymer were used the next studies. This concentration is within a convenient polymer concentration (1–10% w/w) to use at industrial level, because lower costs, viscosity and biocompatibility are achieved.

After choosing these ATPSs, the partitioning of BSA and IgG were studied by varying the NaPA MW and the salt concentration. The systems PEG-NaPA 8,000 and 15,000 in presence of salt could have same potential for the purification of an IgG crude extract, since almost all IgG precipitated and some BSA would go to the bottom phase. Although there is no evidence whether the precipitation of IgG in these ATPS could be beneficial to purification of this protein, more studies are needed. Moreover, the addition of other components to the system could stabilize this protein, such as MNPs.

5. Magnetic Fishing

5.1 Introduction

The purification of antibodies has a large impact on the total costs of production of these therapeutic biomolecules mainly due to Protein A chromatography, which represents 70% of the total downstream costs [27]. In order to overcome this problem, several new non-chromatographic techniques have been studied, such as the use of iron oxide magnetic particles, which have many important properties that make them useful for biopurification purposes. There are protein A-coated MNPs available on the market, however over timer there has been development of synthetic affinity ligands that could replace this protein [63].

In 2000, Teng *et al* had designed, synthesized, characterized and immobilized on agarose beads a synthetic affinity ligand (ligand 22/8) that could mimic the natural affinity Protein A to hIgG binding both Fab and Fc fragments of this protein [64]. The ligand 22/8 structure has a triazine scaffold substituted with 3-aminophenol and 4-amino-1- naphthol and has already been studied either on agarose beads [18] or on magnetic particles [48].

Other example of a ligand that has also been studied to purify antibodies is boronic acid. This ligand is less selective than the previous one since it is known to interact with cis-diol containing molecules, such as glycoproteins, carbohydrates and nucleosides. There are boronic acid-coated MNPs commercially available, and although these were able to capture hIgG under mammalian cell culture conditions, their high cost makes them less viable to purify hIgG at industrial level [63]. Taking this into account, Dhadge *et al* developed an easy and scalable procedure to synthesize MNPs with aminophenyl boronic acid with aim to purify hIgG from a crude extract [65].

The goal of this chapter was to synthesize MNPs bearing ligand 22/8 or boronic acid on the surface. Moreover, with aim to verify the synthesis procedure, these MNPs would be characterized by FTIR, zeta potential, hydrodynamic diameter and their affinity towards BSA and IgG. After comparing the results between particles, one would be selected for further partitioning studies in the PEG-NaPA system to purify IgG from a crude extract.

5.2 Production of functionalized magnetic particles

In this work, two different magnetic particles were synthesized and tested. These particles were already used in previous works [52], [53] and their synthesis routes are represented in Figure 5.1 and Figure 5.2.

There are many synthesis methods to produce magnetic particles, but in this work the method applied was the chemical co-precipitation. Although it is difficult to control the size of particles, co-precipitation is a very simple and efficient method that can produce large amounts of iron oxide magnetic particles, namely magnetite (Fe_3O_4). Moreover, this method can be reproducible if the synthesis conditions remain constant [41],[43].

After producing magnetite, the stabilization of these particles is very important since they tend to aggregate in biological medium and in the presence of a magnetic field. This stabilization is achieved by putting a layer on the particle surface that can create an equilibrium between attractive and repulsive forces [40], [41]. Furthermore, this layer can also protect the iron core from environmental threats such as acidic pH [42]. The magnetic particles synthesized in this work were coated with a double layer of silica, the first consist in a thin layer of SiO_3 and the second one in a porous silica coating with TEOS.

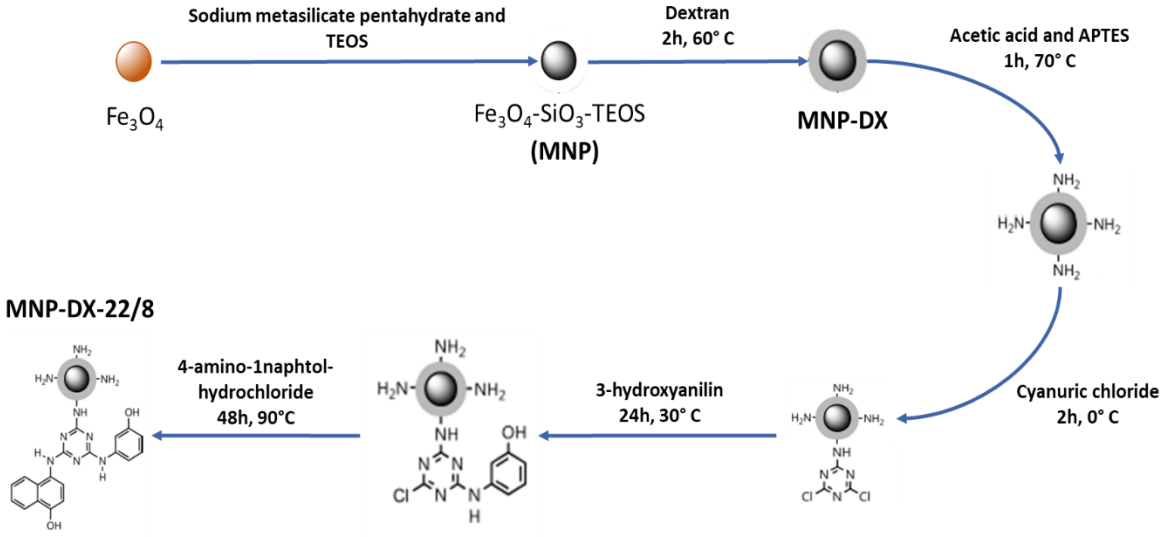

Figure 5.1 – Schematic representation of chemical modifications on iron oxide particles to produce MNP-DX-22/8.

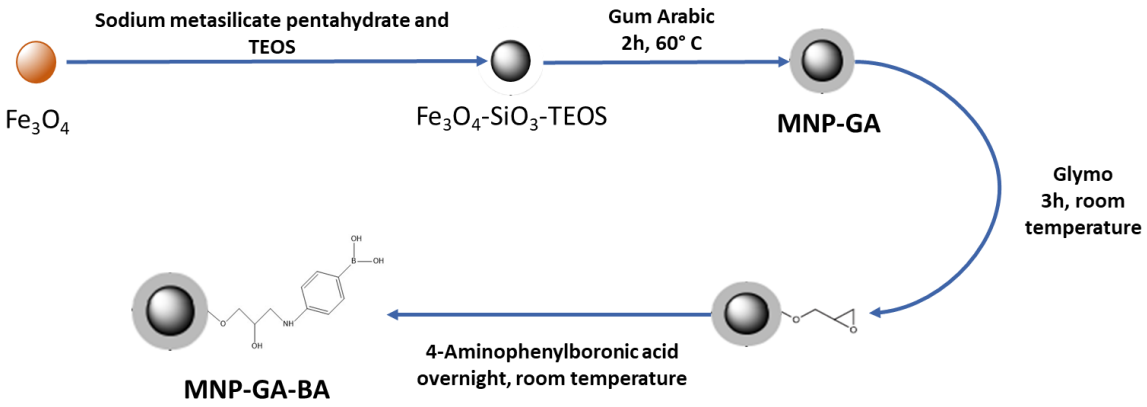

Figure 5.2 - Schematic representation of chemical modifications on iron oxide particles to produce MNP-GA-BA.

Magnetic nanoparticles coated with silica are extremely susceptible to non-specific adsorption and for that reason, there was a need for coating these particles with polymers to avoid undesirable protein adsorption. In this case, coatings of Dextran 500,000 and Gum Arabic 250,000 from acacia tree were used.

Dextran is a polysaccharide which has mainly α-D(1-6) linkages between anhydroglucoses, and rarely it has α-D(1→3) glycosidic bonds at branching points (Figure 5.3) [66]. This polymer is one of the most common coating for MNPs, already existing some MNPs coated with dextran (MNP-DX) available in the market for biomedical purposes, such as Ferumoxytol (Advanced Magnetics) for MRI applications [44]. MNP-DX have already been applied in others research fields like bioseparation, for example to separate proteins, cells or organelles [52], and biosensing, for example to monitor the kinetics of proteins interactions [67].

Gum arabic (GA) is a complex polysaccharide, which has three main components: (i) a β-(1→3) galactose backbone with linked branches of arabinose and rhamnose with glucuronic acid at the end, this backbone represents almost 90% of the total weight (wt); (ii) a high-protein content arabinogalactan rich in hydroxyprolines, prolines and serines, representing about 10 % (wt); (iii) less than 1% (wt) is a high-protein content of glycoproteins [44]. This polymer is widely used in many fields, for instance it is used as stabilizer in the food and pharmaceutical industry because it is a natural, nontoxic, biocompatible, and environment friendly polymer. In the field of nanomaterials, namely biomedicine and bioseparation, GA have been studied as coating since it can improve colloidal stability and it has lots of carboxylic groups which can allow further functionalization with other biomolecules [48], [68].

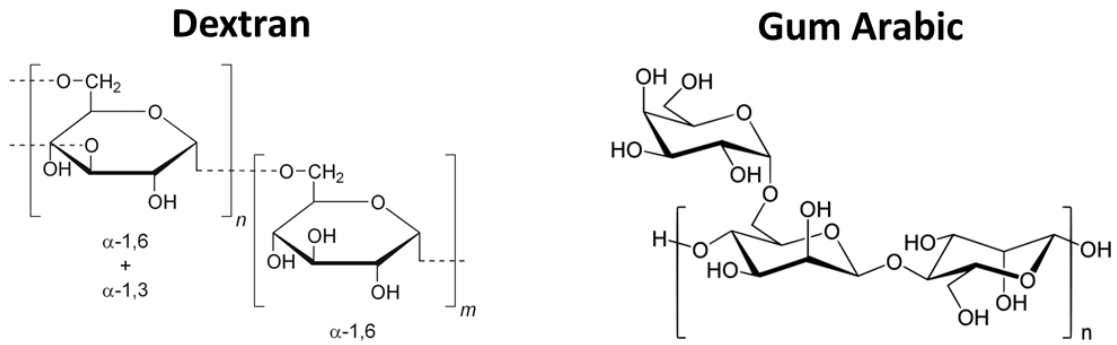

Figure 5.3 – Chemical structure of Dextran and Gum arabic.

The ligands on the particles surface are important for the MNPs specificity and therefore to add them, the surface needs to have functional groups such as amine groups ($–NH_2$), which are able to react chemically and synthesize the desirable ligand. In this work, the MNP-DX were functionalized with ($–NH_2$) and the MNP-GA were functionalized with GLYMO.

The amination of MNP-DX was done by using APTES (Figure 5.4). This procedure has two steps, the first consists in the hydrolysis and condensation of APTES molecules at low pH and the second one in the formation of covalent bonds with OH groups which are present on the dextran structure [69]. To progress in the 22/8 ligand synthesis, the amine content was quantified by Kaiser test and three different MNP concentrations, 10 mg/mL, 5 mg/mL and 1 mg/mL were used. For the sample at 10 mg/mL the

concentration of amines was 82 µmol of amines/ g of particles, for the sample at 5 mg/mL was 103 µmol/g and for the sample at 1 mg/mL no amines concentration was obtained because the values of absorbance were too low. Comparing these results, it becomes evident that would more beneficial to work with a MNP concentration of 5 mg/mL in the next steps of ligand synthesis, since there are more amine groups available. The ligand 22/8 is a triazine-based ligand, which was synthesized as described previously [52], in three steps: (i) reaction with cyanuric chloride; (ii) first nucleophilic substitution with 3-hydroxyalinine; (iii) second nucleophilic substitution with 4-amino-1-naphtol hydrochloride.

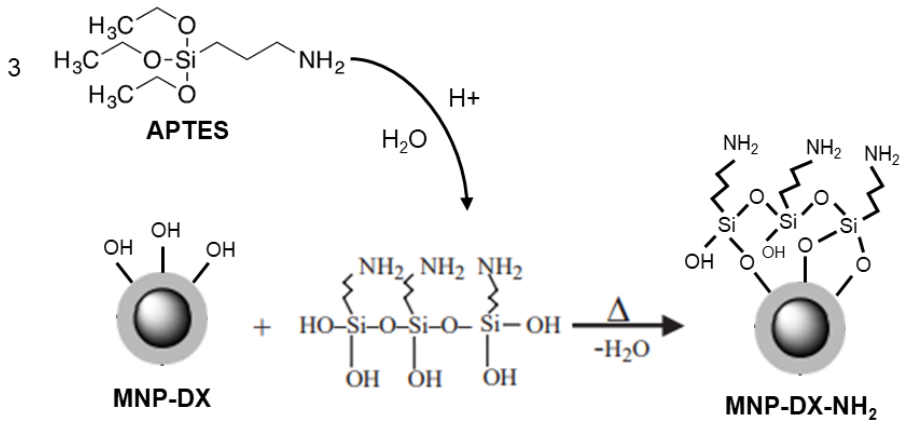

Figure 5.4 – Schematic representation of the reaction of APTES with hydroxyl groups presents on the MNP surface. Adapted from [69].

The boronic acid ligand on the gum arabic coated MNPs was synthesized as a previous work [65], although it was not reported how much GLYMO was used to functionalize the MNPs. To get around this difficult situation, it was used the same volume as APTES, which was also used in that previous work. GLYMO is an organofunctional alkoxysilane that has epoxide groups, which are very reactive and will allow further reaction with the free amine of aminophenylboronic acid (APBA).

5.3 Magnetic Particles Characterization

With the aim to check if the MNPs were well synthesized and functionalized, they were characterized by FTIR, zeta potential, hydrodynamic diameter and their affinity towards IgG and BSA.

5.3.1 Fourier transform infrared spectroscopy

The Fourier Transform Infrared Spectroscopy (FTIR) is a technique that uses infrared radiation and the Fourier Transform to obtain a molecular 'fingerprint' spectrum, allowing for that reason to distinguish different samples [70]. The FTIR spectra of the particles that were synthesized are represented in Figure 5.5.

In the Fe_3O_4 spectrum (Figure 5.5 – a)), it is possible to confirm the presence of Fe_3O_4 nanoparticles due to the absorption peak at 590 cm^{-1}, which is attributed to the Fe-O bond. The others peaks at about 3431.1 cm^{-1}, 1635.3 cm^{-1} and 1384.3 cm^{-1} are, respectively, ascribed to the O-H stretching, bending and deforming vibrations of water molecules that are usually absorbed to the sample [71].

The presence of the double layer of silica was confirmed by FTIR because a new peak around 1100 cm^{-1} appeared which represents the asymmetry stretching vibration of Si-O-Si. This peak appeared with lower intensity in the Fe_3O_4-SiO_3 spectrum since the MNPs in this stage just have a thin layer of silica. In the literature, other peaks have been described for the presence of silica such as peaks at 3470-3450 cm^{-1} and around 955 cm^{-1}, that belong to the Si-OH bond [71], [72]. The first peak did not appear in the spectra since it can be easily overlapped by others bands such as the O-H stretching of water molecules. The peak at 955 cm^{-1} could be seen in the Fe_3O_4-SiO_3 spectrum whereas in the Fe_3O_4-SiO_3-TEOS spectrum the Si-O-Si peak overlapped it.

Both the MNP-DX spectrum and the MNP-GA spectrum show the same peak at about 2925 cm^{-1} that belongs to the stretching vibration of $–CH_2$ groups from the polymeric structure of dextran and gum arabic. The C-OH bound is easily found in these polysaccharide structures whereby the stretching vibration peak of this bound should have appeared around at 1011 and 1111-1157 cm^{-1}, however, the asymmetry stretching vibration of Si-O-Si peak overlapped these peaks [48],[73]. These results showed that dextran and gum arabic were successfully coated on the magnetic particles surface.

Regarding the MNP-DX-22/8 spectrum, it is possible to observe that there was an increase of peak intensity around at 1600 cm^{-1}, which was caused by the aromatic ring stretching of C=C-C bound [74]. There is also a slight increase around at 1300 cm^{-1} that can be an indicative of the presence of triazine rings and therefore this ligand was doubtless well synthesized on the MNP particles surface [75].

Finally, in the MNP-GA-BA spectrum, it was not possible to observe any new peak. The peaks for C=C-C aromatic ring stretching, C-B stretching vibration and B-O bending vibration should have appeared, respectively, around at 1600 cm^{-1}, 1089 cm^{-1} and 1025 cm^{-1} [74], [76]. For this reason, other peaks like the O-H bending from water molecules and the Si-O-Si asymmetry stretching vibration could have overlapped these peaks. Moreover, this may also suggest that APBA surface modification did not occur or APBA modification occurred in very low amounts. Nevertheless, more experiments are needed.

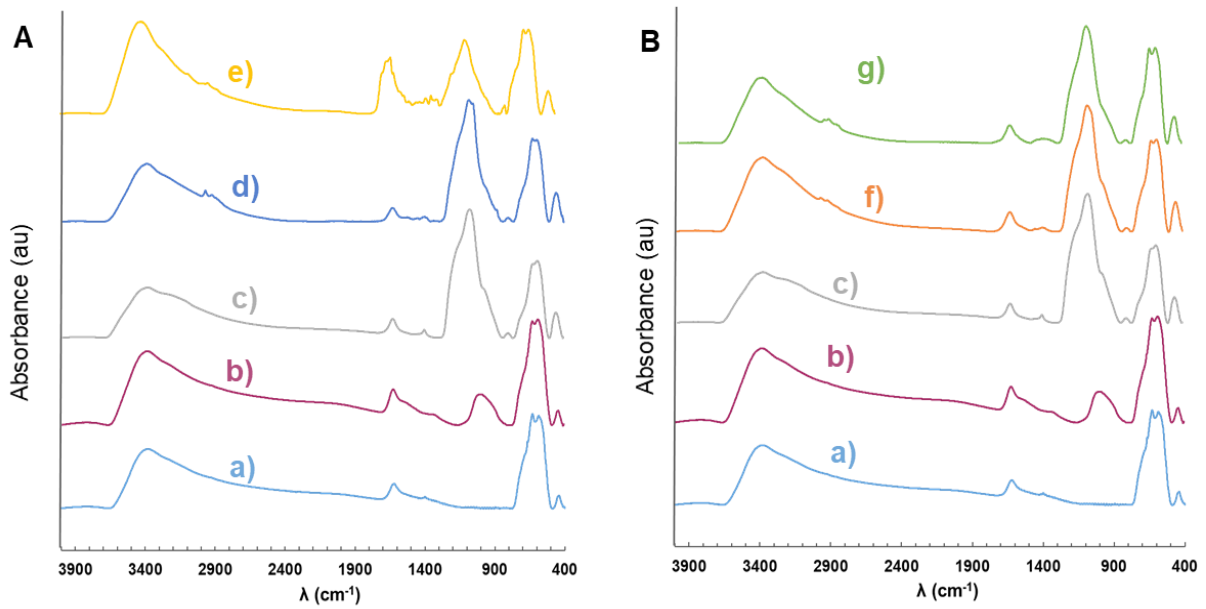

Figure 5.5 – FTIR spectra for MNPs coated with dextran (A) and MNPs coated with gum arabic (B). a) Fe_3O_4; b)Fe_3O_4-SiO_3, c) Fe_3O_4-SiO_3-TEOS, d) MNP-DX, e) MNP-DX-22/8, f) MNP-GA, g) MNP-GA-BA.

5.3.2 Hydrodynamic diameter

The MNPs hydrodynamic diameters were obtained by dynamic light scattering (DLS), which is a technique that measures the particles Brownian motion by light scattering and relates it to their size. This technique is extremely sensitive to the presence of larger particles in the sample, which can be very useful to confirm the homogeneity of a sample [77]. This technique measures an intensity autocorrelation function from the scattered light, which is then fit by using two main fitting algorithms: cumulants and distribution analysis. These analysis produce different terms that can be compare, while the cumulants analysis produce a mean value for the size (Z-average), the distribution analysis produces peaks that can be defined with a statistical mean and standard deviation. In a monodisperse sample, the values of Z-average and mean of the peak (one and only – for this case) should be the similar. The opposite happens for a polydisperse sample, where these values are not the same [78]. The hydrodynamic diameter results for the MNPs are summarized in Figure 5.6 and Figure 5.7.

Although in both figures the hydrodynamic diameter of Fe_3O_4 seem to be in range of 200 nm or more [40]. This happens, because the MNPs cores tend to aggregate due to their small size and large surface area when they are synthesized [79]. Moreover, the values for Z-average and mean of intensity peaks are very different, which corroborates with the possibility of having polydispersity in this sample.

Regarding the hydrodynamic diameter results for Fe_3O_4-SiO_3-TEOS, the values for Z-average and mean of intensity peaks are very similar, which indicates that the double layer of silica helped to produce a monodisperse sample with a hydrodynamic diameter around of 200 nm. Therefore, it was able to provide a proper surface coating that could stabilize the MNPs.

After coating the MNPs with dextran (Figure 5.6), the hydrodynamic diameter increased as it as expectable from previous works [52], the main reason for this to occur are the noncovalent interactions

that can form between the dextran and the particles around it, creating larger agglomerates. Furthermore, the difference between the Z-average value and the mean of intensity peak indicates that there is some polydispersity but not some much as Fe_3O_4 results. When these MNPs-DX were functionalized with ligand 22/8, the hydrodynamic diameter of the agglomerates decreases, as a result of creating steric restrictions, surface charge or hydrophobicity changes [48], obtaining MNPs with around 380 nm.

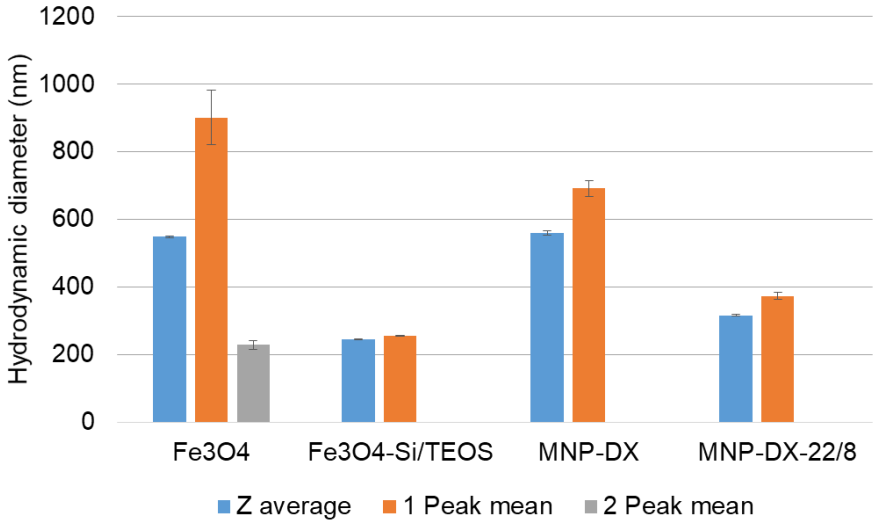

Figure 5.6 – Hydrodynamic diameter for the magnetic particles using the Zetasizer Nano ZS system (n=3).

Upon coating the MNPs with gum arabic (Figure 5.7) it would be expectable to MNPs increase their size, since gum arabic also have the ability to form noncovalent interaction with the particles as it was observed in other previous works [48], but instead of increasing, the hydrodynamic diameter remained constant. After functionalizing the MNPs-GA with boronic acid, the sample became more polydisperse and MNPs with a larger diameter were obtained. As previously to functionalize the MNPs surface with boronic acid, these were first reacted with GLYMO, which would act as bridge. This molecule is very reactive due to its epoxy group that can quickly react with different nucleophilic groups such as amines and hydroxyl groups [80]. When this group reacts with the 3-aminophenylboronic acid (APBA) a secondary hydroxyl group is formed, which can react subsequently with other epoxy group forming other secondary hydroxyl group and so on. Therefore, due to the GLYMO ability of crosslinking the MNPs could have increased their size heterogeneously.

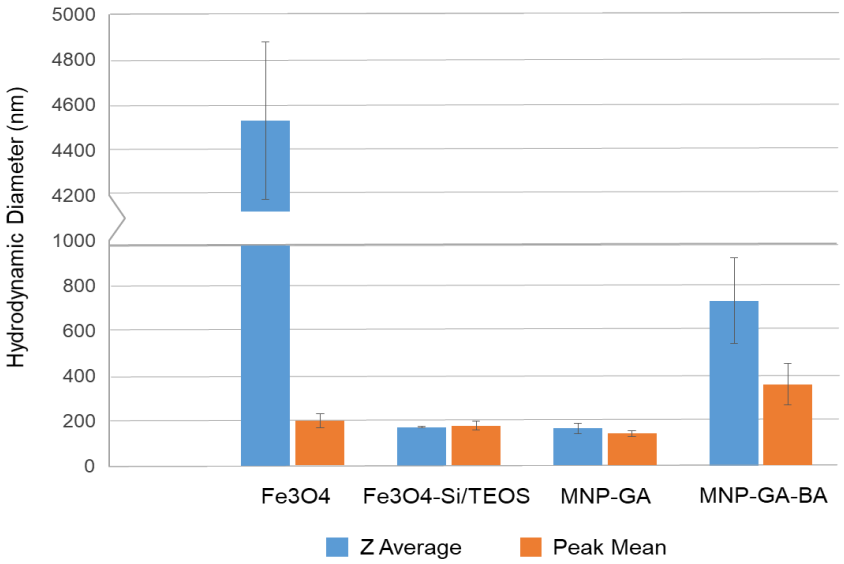

Figure 5.7 – Hydrodynamic diameter for the magnetic particles using the Horiba SZ-100 (n=3).

5.3.3 Zeta potential

Zeta potential (ζ-potential) is a physical property that any particles in suspension has and its magnitude provides information about the potential stability of a colloidal system. In other words, if the particles in suspensions have a low zeta potential, there will be aggregation of these particles and therefore they will be consider as unstable. On the other hand, if the particles have a large negative or positive zeta potential, there will be forces to avoid this aggregation to occur and the particles will be stable in suspensions. The ζ-potential range to consider particles as unstable in suspensions is between +30 mV and -30 mV, if the zeta potential value goes above or below these values, respectively, the particle is considered as stable. [81]

The MNPs coated with polymers and the MNPs with ligand were characterized by zeta potential at different pHs, ranging from 2.5 to 12 (Figure 5.8). All the particles were considered as unstable for this pH range, since their zeta potential values are between +30 mV and -30 mV.

The dextran is a neutral polysaccharide so it would be expectable to obtain values of zeta potential closer to 0 mV. However, the zeta potential values for MNP-DX remained negative in the pH range studied, being less negative for acidic pHs. In terms of stability, both cases are the same, being the particles considered as unstable in suspension. For the MNP-DX-22/8 the results can be corroborated with the value obtained by Santana [52]. Although the zeta potential variations for the MNP-DX and MNP-22/8 were similar, there is difference between the values of zeta potential, which can indicate the presence of ligand on the surface of MNP-DX-22/8.

For the MNP-GA, the zeta potential values obtained were negative mainly because of carboxylic groups that there are in gum arabic structure. The zeta value at pH 7 was very similar to the value obtained by Batalha and for that reason it was possible to conclude that these particles were well coated with gum arabic [48]. Regarding the zeta potential variation for MNP-GA-BA, it would be expectable to observe a considerable drop in the zeta potential value between pH 8 and 9, which would be related to the pKa of boronic acids where a structural change from a trigonal to a tetrahedral structure occurs. The pKa of phenylboronic acid free and immobilized is, respectively, 8.4 and 9.2 [65]. Although there is not any drop in the zeta potential value, this decreases from -25 mV (at pH 7) to -29 mV (at pH 9.2), which can indicate that there is a slight quantity of ligand on the particles surface.

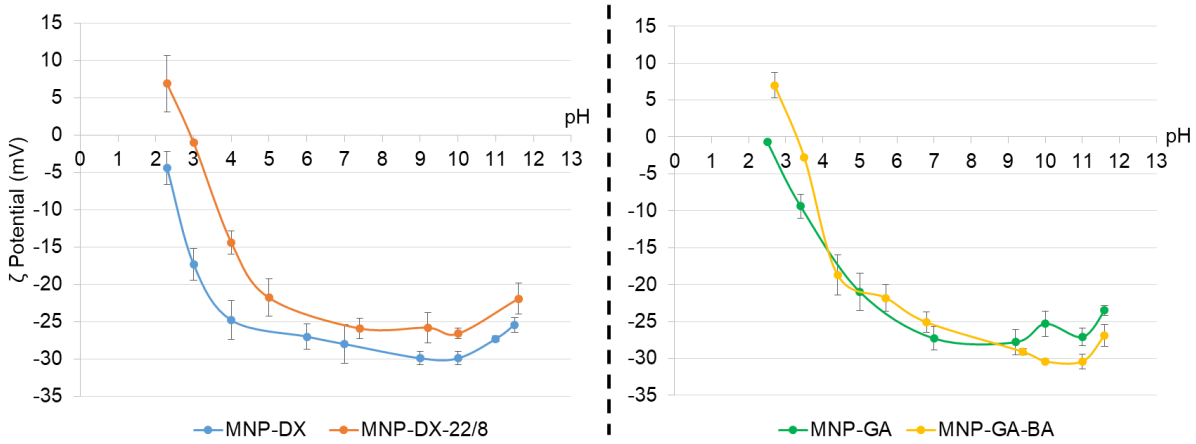

Figure 5.8 – Variation of zeta potential with pH for the MNPs coated with polymer and with ligand (n=3).

5.3.4 Affinity Assays

Once functionalized and characterized, the prepared magnetic particles were tested for binding to pure solutions of Bovine Serum Albumin (BSA) and IgG, with the MNPs coated just with biopolymer used as control. BSA was used in these studies because it is a model impurity protein in a crude extract, which the MNPs should not bind. These assays were done with the aim to select the MNPs most suitable to apply in the ATPS that would be studied to purify IgG from a crude extract. The buffer condition for each ligand was chosen based on previous works, where for MNP-DX-22/8, 50 mM phosphate, pH 8 and 50 mM glycine–NaOH, pH 11 were used as binding and elution buffer, respectively; and for MNP-GA-BA, 20 mM HEPES, pH 8.5 and 1 M Tris-HCl, pH 8.5, were respectively used as binding and elution buffer [52], [65].

5.3.4.1 Protein Binding to MNP-DX-22/8

Regarding the ligand 22/8, the 50 mM phosphate, pH 8 used as binding buffer was found suitable for the purification of IgG because the neutral pH and high salt concentration promote hydrophobic interactions between the IgG and the ligand [82]. As showed by molecular docking approach allied to molecular dynamics simulations showed, this ligand binds mainly to the Fc fragment of IgG, interacting in a similar way as the protein A. Moreover this ligand can also bind to the Fab fragment of IgG but with less affinity [83]. These interactions established between these fragments and the ligand are extremely

affected by the change of pH to extreme values like pH 3 and 11 [64]. However, in an application where MNPs are used to purify a protein, elution conditions at acidic pH could lead to leaching problems from the iron oxide MNPs. For this reason, 50 mM glycine–NaOH, pH 11 was found as a suitable buffer to elute IgG [48]. The results of affinity assays for MNP-DX and MNP-DX-22/8 are presented in Figure 5.9 and were obtained by quantifying the binding and elution washes with the BCA assay.

The objective of coating the MNPs with dextran was to minimize the nonspecific interactions between the MNPs and proteins. The results show a higher tendency of MNPs-DX to bind IgG than BSA, with protein binding (mg of protein/ g of support) of 7.70 mg/g for BSA and 36.7 mg/g for IgG. Although the affinity binding value towards IgG was high, these results showed that nonspecific interactions were minimized towards BSA. Moreover, the total recovery of these proteins in percentage using MNP-DX was less than 5%. After functionalizing the MNPs with the ligand 22/8, the MNPs affinity increased for both proteins, and were able to recover about 61% of IgG but only 13% of BSA. This increase shows that the MNPs were well functionalized with the ligand and they are promising supports to be used to purify IgG from a crude extract.

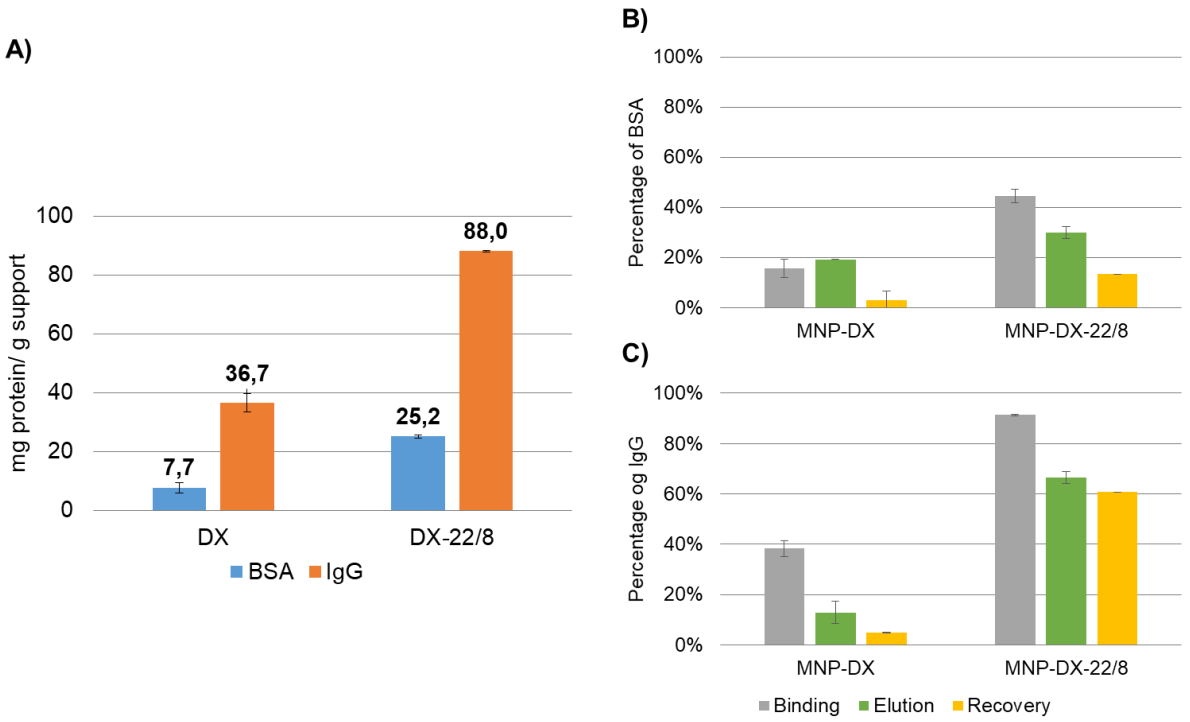

Figure 5.9 – Affinity assays results for MNP-DX-22/8, where: **A)** is the affinity binding of BSA and IgG to MNP-DX and MNP-DX-22/8, this result is normalized per gram of particles used in each assay; **B)** and **C)** are the percentage results of binding, elution and recovery of BSA and IgG, respectively (n=2).

5.3.4.2 Protein Binding to MNP-GA-BA

The antibodies are glycoproteins, having a carbohydrate chain in the CH2 domain of Fc portion. The sugars present on this chain include fucose, galactose and mannose, which have 1,2-cis-diol groups. The boronic acid interacts reversibly with this kind of groups by establishing covalent ester bounds [84]. As result of this, it was important to use a binding buffer that favors these interactions and therefore 20 mM HEPES, pH 8.5 was used. HEPES is not a cis-diol competitor and improves the affinity of compounds with cis-diol groups to boronic acid-modified supports. Moreover, alkaline pH values such

as 8.5, enhance this affinity [84],[85]. These cis-diol and boronic acid interactions can be affected by decreasing the pH or increasing the concentration of a diol competitor. However, regarding the elution of antibodies, the decrease of pH did not show to be efficient to break these interactions [84]. For this reason, 1 M Tris-HCl, pH 8.5 was found as a suitable buffer to elute IgG from MNPs [85]. The results of affinity assays for MNP-GA-BA are presented in Figure 5.10 and were obtained by quantifying the binding and elution washes using the absorbance at 280 nm.

The gum arabic coated MNPs should also show low affinity as the MNPs-DX, but according to the results obtained there was a great interaction between these particles with IgG, achieving a binding of 101.6 mg of IgG per g of support. This interaction can be due to ionic contributions, at pH 8.5 these particles are negatively charged and IgG, which is mainly composed by IgG1, is either neutral or positively charged [86]. To back even more this idea, when elution buffer was applied on these MNPs, it was only possible to elute about 36% of IgG bound, since there was no changes in the pH buffer. Regarding the albumin protein, at pH 8.5 this protein is negatively charged and therefore electrostatic interactions with the MNPs do not occur. As a result, the MNPs affinity towards BSA was low, 8.6 mg of BSA per g of

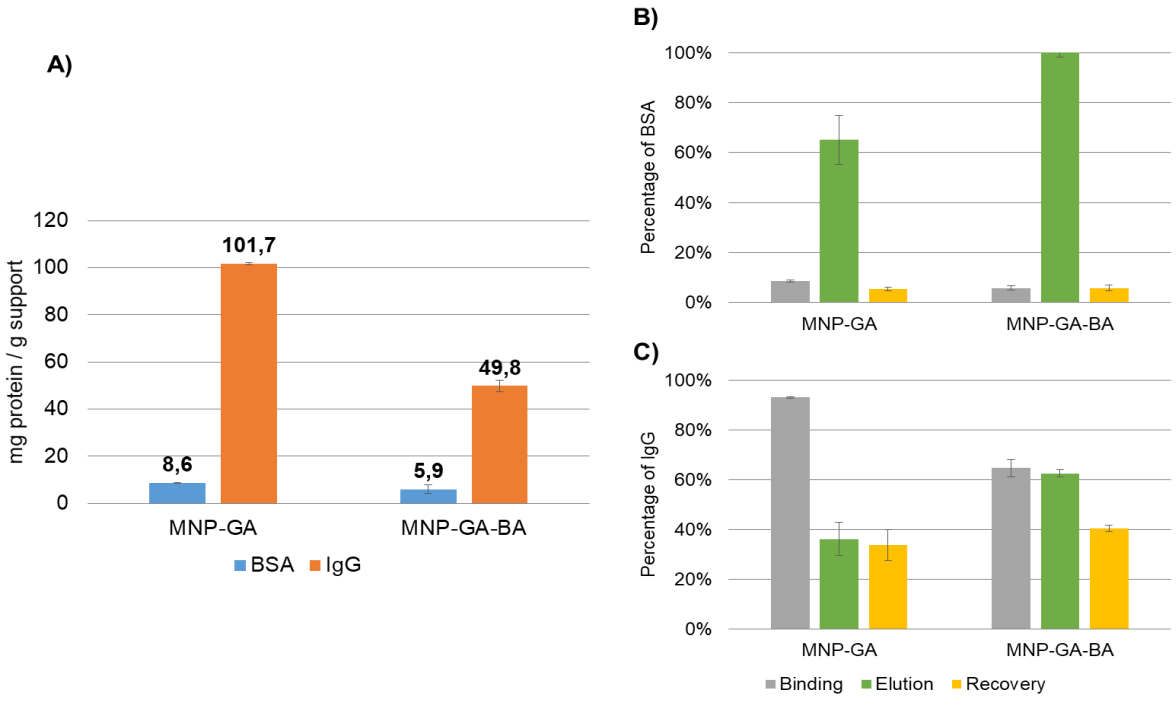

Figure 5.10 - Affinity assays results for MNP-GA-BA, where: **A)** is the affinity binding of BSA and IgG to MNP-GA and MNP-GA-BA, this result is normalized per gram of particles used in each assay; **B)** and **C)** are the percentage results of binding, elution and recovery of BSA and IgG, respectively (n=2).

support.

When MNPs-GA were functionalized with phenylboronic acid, their affinity for IgG decreased from 101.6 mg/g to 49.78 mg/g, whereas for BSA their affinity maintained almost the same. Moreover, both protein recovery were similar to the recovery with MNPs-GA. These results suggest that the MNPs functionalization with phenylboronic acid was not successful and could have occurred crosslinking between MNPs, as previously discussed.

5.4 Conclusions

Iron oxide nanoparticles were synthesized by the co-precipitation method and coated with different layers, namely a double layer of silica and biopolymers (dextran and gum arabic). After MNPs coating, these proceeded to the ligand synthesis on the MNP surface. The dextran coated MNPs were functionalized with ligand 22/8 whereas the gum arabic MNPs were functionalized with phenylboronic acid. These particles have already been used in others previous works with aim to purify IgG, moreover the MNP-GA-BA have also been used as ligand support in a PEG-Dextran ATPS to purify IgG from a crude extract [53].

The FTIR characterization of these particles allowed to follow the MNPs synthesis procedure. Although in the FTIR spectrum of MNP-GA-BA there was no evidence that these would have boronic acid on the surface, the other spectra showed the MNPs were well synthesized and coated. Through the particles characterization by DLS and zeta potential, their hydrodynamic diameter and surface charge were followed. Moreover these last characterization results and the affinity assays allowed to conclude that the MNP-GA were not well functionalized with phenylboronic acid, perhaps due to crosslinking between MNPs.

Finally, after gathering all the characterization results, the MNP-DX-22/8 were chosen to be applied in the PEG-NaPA systems, with an affinity towards IgG of 88.02 mg of protein per g of support. Although the MNP-GA were not chosen, these particles showed some specificity to IgG and thus it would also be interesting to find another elution buffer that could elute all IgG bound.

6. Magnetic aqueous two phase fishing

6.1 Introduction

Aqueous two-phase systems are usually considered as a downstream processing approach for recovery and partial purification of biomolecules. However, this technique is sometimes unviable due to high cost of polymers and lack of understanding about the physical principles underlying the partitioning behavior of a protein. To promote the partitioning of a target protein, an emergent ATPS-based purification strategy was developed, the affinity-enhanced ATPS. The objective of these type of ATPS is to enhance the extraction of the target biomolecule by partitioning it into one of the two phases, which can be achieved by modifying chemically one phase-forming polymer or introducing affinity ligands in the system [87]. Recently a new system to introduce affinity ligands in ATPS was developed. In this system, affinity ligands are immobilized onto MNPs, which are then added to the ATPS. This new method combines thus two different techniques, magnetic separations and ATPS.

The combination of ATPS with magnetic particles has a great potential at industrial level not only because both methods are simple, rapid and easily scalable and but also because it allows a dual-step purification after applying a magnetic field [60]. The first successful magnetic aqueous two phase fishing was achieved by Suzuki *et al* in 1995 [88], who reported the purification of protein A by adding IgG-bound MNPs in a PEG-phosphate system. In other more recent study reported by Dhadge *et al* [53], it was possible to short the phase separation time of ATPS by the addition of the magnetic particles and to obtain high values of yield and purity of IgG from a cell culture supernatant.

The first goal of this chapter was to study the recovery of pure BSA and IgG by applying the modified MNPs synthesized in PEG-NaPA systems. Once the best magnetic aqueous two phase fishing system was chosen, it was used to purify IgG from a cell culture supernatant (Figure 6.1).

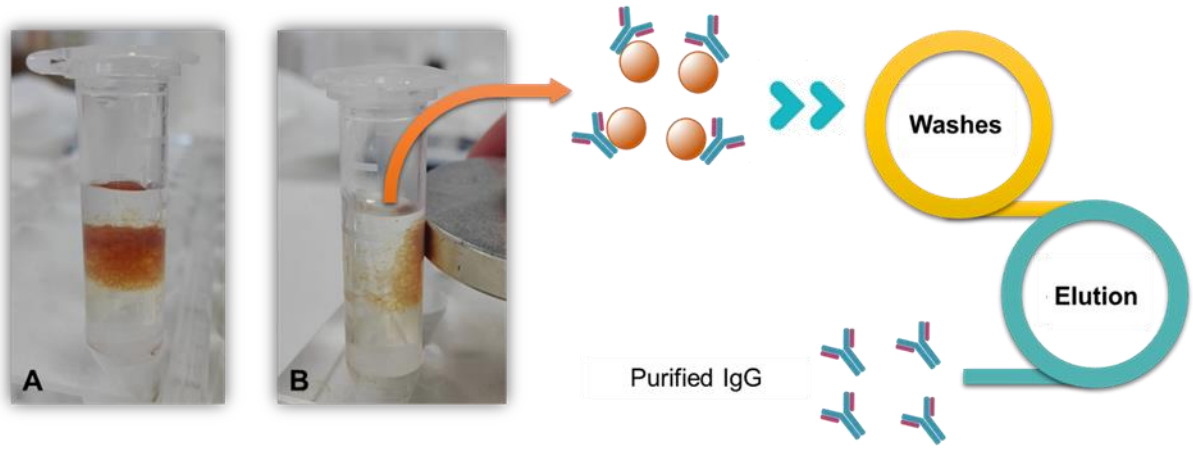

Figure 6.1 – Schematic representation of the magnetic aqueous two phase fishing system (MATPFS). In **A** is represented a PEG-NaPA system with MNP-DX-22/8; in **B** is represented the response of MNPs upon application magnetic field. After the MNPs capturing these will be washed to remove non-specifically adsorbed proteins, and then elution conditions are applied to recover the protein bound to the MNPs, in order to obtain purified IgG.

6.2 MNPs partitioning

Magnetic particles partition in ATPSs. For example, in the Dhadge *et al* report, the MNPs were usually partitioned to the bottom phase of a PEG-Dextran system. Therefore, the partition of MNP-DX and MNP-DX-22/8 in the PEG-NaPA system was studied.

Figure 6.2 shows the results of partitioning of dextran coated MNPs in every PEG-NaPA system with and without salt addition. From these results, the MNPs positioning either in the top phase or in the bottom phase was independent of salt addition, although there was an exception namely for the PEG-NaPA 1,200 with MNP-DX. Here, the addition of salt made the MNPs-DX move to the bottom phase.

The presence of the ligand 22/8 on the MNPs-DX surface appears to have an effect on their partition, since the MNP-DX-22/8 were in the top phase whereas MNP-DX were mainly in the bottom phase. This could be explained by the ligand 22/8 structure, which has aromatic rings groups. These groups would prefer to interact with the hydrophobic chain of PEG than the carboxylic groups of NaPA structure, which are hydrophilic. This explanation could also be applied to the MNPs-DX, which would prefer to interact with the NaPA structure due to the hydrophilic nature of dextran carbohydrate chain.

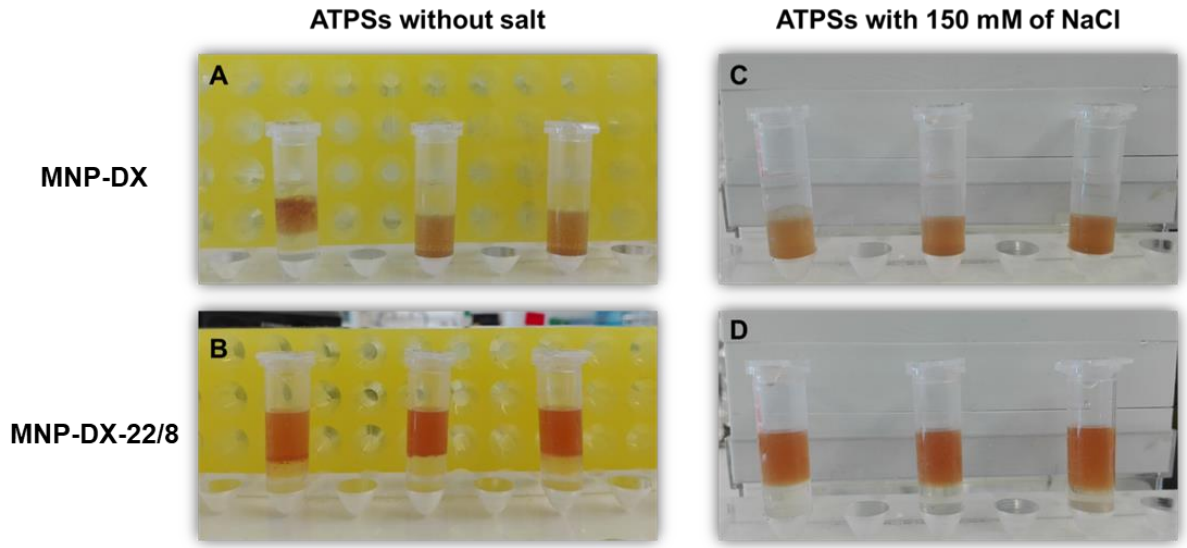

Figure 6.2 - PEG-NaPA systems with MNP-DX (A and C) and MNP-DX-22/8 (B and D). In each figure, from left to right: PEG-NaPA 1,200, PEG-NaPA 8,000 and PEG-NaPA 15,000.

6.3 Protein Recovery

In order to choose the most suitable magnetic aqueous two phase fishing system (MATPFS) to purify IgG from a cell culture supernatant, a study about the recovery of BSA and IgG using these systems was required. These studies were performed by making systems composed by 10% (w/w) of each polymer, 0.02% w/w of MNPs and 0.02% w/w of protein.

6.3.1 BSA recovery from MATPFS

In Figure 6.3 are represented the results of BSA distribution in the MATPFSs components, namely in the top phase, the bottom phase and the magnetic particles. The effects of salt and molecular weight of NaPA on the partitioning of BSA in these systems were similar to the ones observed in Partitioning of pure proteins in PEG/NaPA ATPSs study.

From Figure 6.3, BSA tend to partition to the particles in the presence of larger NaPA molecular weights, and therefore in the PEG-NaPA 15,000 systems the percentage of BSA bound to the particles were higher, more than 20% for MNP-DX-22/8. As it was also observed in the study of BSA Partitioning of pure proteins in PEG/NaPA ATPSs, there was a change in the BSA partitioning from the bottom to the top phase when the molecular weight of NaPA increased from 1,200 to 8,000.

Upon adding NaCl to the system, the percentage of BSA bound to the particles increased, although it remained low, and was less perceptible to the PEG-NaPA 15,000, wherein the percentage value suffered just a slight increase. The concentration of salt could promote hydrophobic interactions between BSA and ligand, as for IgG. Furthermore, in the systems with NaPA 8,000 and 15,000 there was an increase and a decrease of the quantity of BSA in the bottom and top phase, respectively. Whereas in the PEG-NaPA 1,200 the values of BSA percentage in both phases maintained more or less constant. These behaviors were already discussed in a previous chapter (4.3.1).

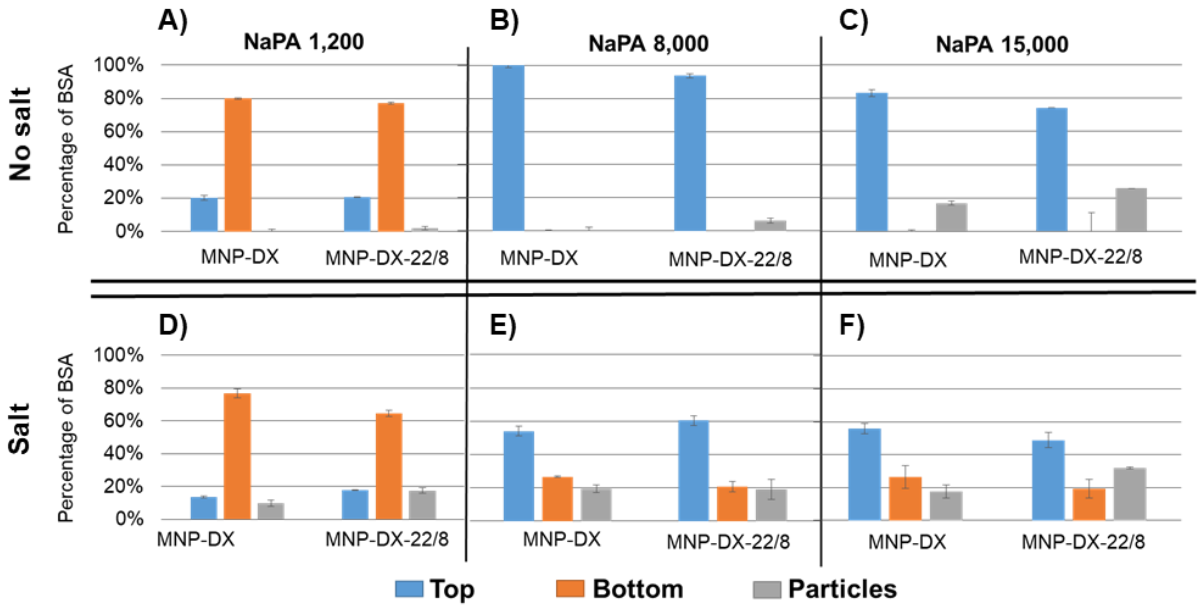

Figure 6.3 – Distribution of BSA in the PEG-NaPA systems in the presence of MNPs without (**A)**, **B)**, **C)**) or with (**D)**, **E)**, **F)**) salt addition. **A)** and **D)** represent the results to the PEG-NaPA 1,200 system; **B)** and **E)** represent the results to the PEG-NaPA 8,000 system; and **C)** and **F)** represent the results to the PEG-NaPA 15,000 system (n=2).

After the system mixing and phase separation, MNPs were magnetically collected along with the top phase. Then the MNPs were washed with binding buffer (50 mM phosphate, pH 8) and elution buffer (50 mM glycine–NaOH, pH 11) (Figure 6.4). In the binding chart (Figure 6.4 - A), the BSA percentage values represent the quantity of BSA that remained in the particles after washing. In the elution chart (Figure 6.4 - B), the BSA percentage values represent the quantity of BSA that eluted from the particles.

In the binding chart, a decrease in BSA binding percentage is observed, which means that the majority of BSA was washed out from the particles. The only exception to this was the MNP-DX-22/8 that were used in the PEG-NaPA 15,000 without NaCl addition. When these particles were resuspended in the with elution buffer, almost all bound BSA was eluted, obtaining, thus, 100% of elution. Once all the BSA from the washes and elutions was quantified, the BSA recovery was calculated. It was possible to obtain a maximum recovery of BSA of about 11.2%, when the MNP-DX-22/8 were applied in a PEG-NaPA 1,200 system with 150mM of NaCl. This clearly shows that BSA has very low affinity for the MNP-DX-22/8 particles.

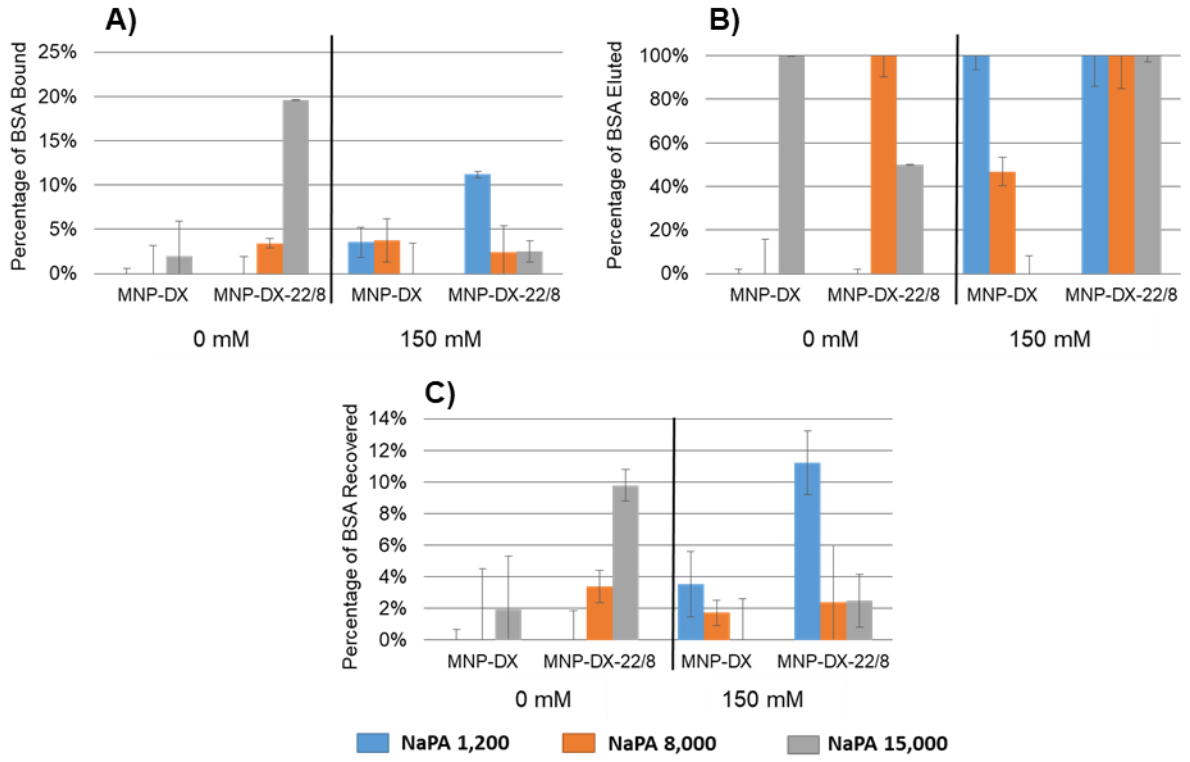

Figure 6.4 –Binding and recovery of BSA from the MATPFS: **A)** Binding chart - Percentage of BSA bound to the MNPs after washing with binding washes; **B)** Elution chart - percentage of BSA eluted from them after washing with elution buffer; **C)** Recovery chart **-** percentage of BSA that was able to recover from a BSA pure solution, after all washes (n=2).

6.3.2 IgG recovery from MATPFS

In Figure 6.5 the results of IgG distribution in the MATPFSs, namely in the top phase, bottom phase and magnetic particles, are represented. In this section, the effects of salt and MW of NaPA in the partitioning of IgG in these systems were also similar to the ones observed in the studies of Partitioning of pure proteins in PEG/NaPA ATPSs. However, instead of precipitating, the IgG remained bound to the particles. The maximum amount of IgG bound to the MNP-DX-22/8 was 98.2%, when they were applied in a PEG-NaPA 15,000 system without NaCl addition.

For higher molecular weight of NaPA, the particles seemed to bind more IgG, with the exception of PEG-NaPA 15,000 with 150 mM of NaCl. However, this binding between IgG and the particles appears to be non-specific since there is no difference between the particles with the ligand and without the ligand.

Supplementing the system with 150mM of NaCl seemed to favor the IgG partition towards the particles, although in the PEG-NaPA 15,000 system the amount of IgG bound to the particles suffered a small decrease. As described previously, adding salt to the system increases the ionic strength, which can make the IgG structure more unstable. Its stabilization could involve the MNPs binding, instead of precipitating as it occurred in the partitioning studies.

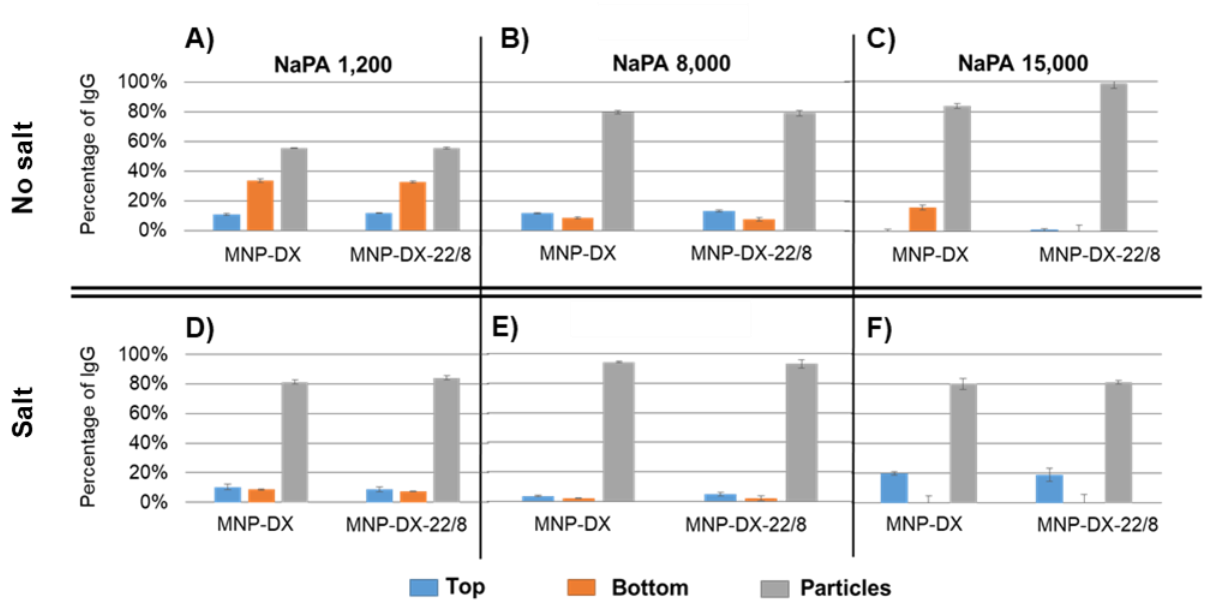

Figure 6.5 - Distribution of IgG in the PEG-NaPA systems in the presence of MNPs without (**A)**, **B)**, **C)**) or with (**D)**, **E)**, **F)**) salt addition. **A)** and **D)** represent the results to the PEG-NaPA 1,200 system; **B)** and **E)** represent the results to the PEG-NaPA 8,000 system; and **C)** and **F)** represent the results to the PEG-NaPA 15,000 system (n=2).

MNPs were magnetically collected after mixing the system and they were also washed with the same buffers as in the previous section. The results for the binding, elution and recovery of IgG are shown in Figure 6.6.

The binding of IgG decreased considerably after washing the MNPs with binding buffer, showing that IgG bound to MNPs in a non-specific way or that some protein precipitated at the MNPs surface. For instance, for the MNPs that were applied in the PEG-NaPA 15,000 system without NaCl addition, the amount of IgG bound to MNPs decreased from 98.2% to 20.5% after washing.

After elution of bound IgG, the three best systems to recover IgG were obtained: i) the PEG-NaPA 1,200 with 150 mM of NaCl and ii) PEG-NaPA 15,000 with 150 mM of NaCl and iii) PEG-NaPA 15,000 without salt. However, comparing the recovery results for both proteins it was possible to choose the PEG-NaPA 15,000 with 150 mM of NaCl as the most suitable platform to purify IgG from cell culture supernatant, since in the other two systems there was an higher BSA recovery.

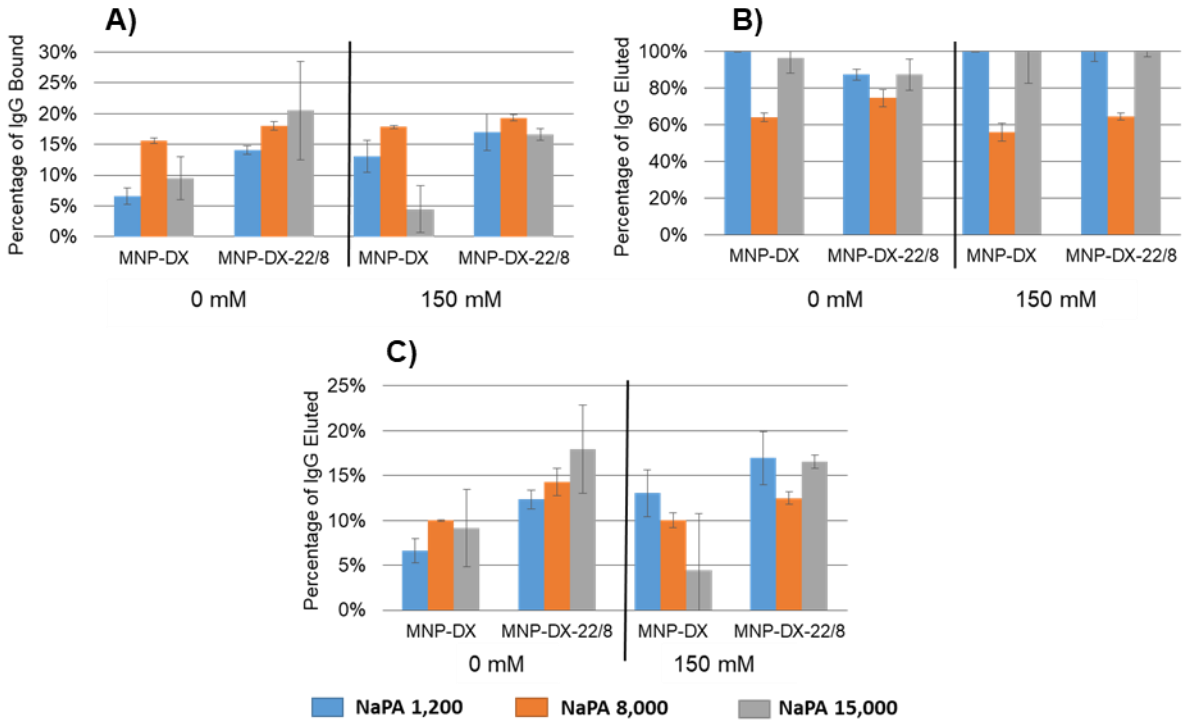

Figure 6.6 - Binding and recovery of IgG from the MATPFS: **A)** Binding chart - Percentage of IgG bound to the MNPs after washing with binding washes; **B)** Elution chart - percentage of IgG eluted from them after washing with elution buffer; **C)** Recovery chart **-** percentage of IgG that was able to recover from a IgG pure solution, after all washes (n=2).

6.4 Cell culture supernatant purification

6.4.1 Protein A Affinity Chromatography

The IgG crude extract was provided by StabVida and it was produced by myeloma cells. The IgG content in this extract was unknown and therefore it was essential to quantify it before applying the crude extract into the most suitable MATPFS to purify IgG. The quantification was indirectly done by purifying 5 mL of crude extract by a protein A Affinity Chromatography and determining the IgG concentration in the elution pool by BCA method.

Initially, a SDS-PAGE gel was done to verify whether the IgG content in the extract was high or low (Figure 6.7). From this electrophoresis, it was verified that there was a very small quantity of IgG in the crude extract provided by the presence of the band at 50 kDa, which represents the heavy chains of IgG, and of the band at 25 kDa, which represents the light chains of IgG. Moreover, it also confirmed a high content of others proteins by the presence of a blur band.

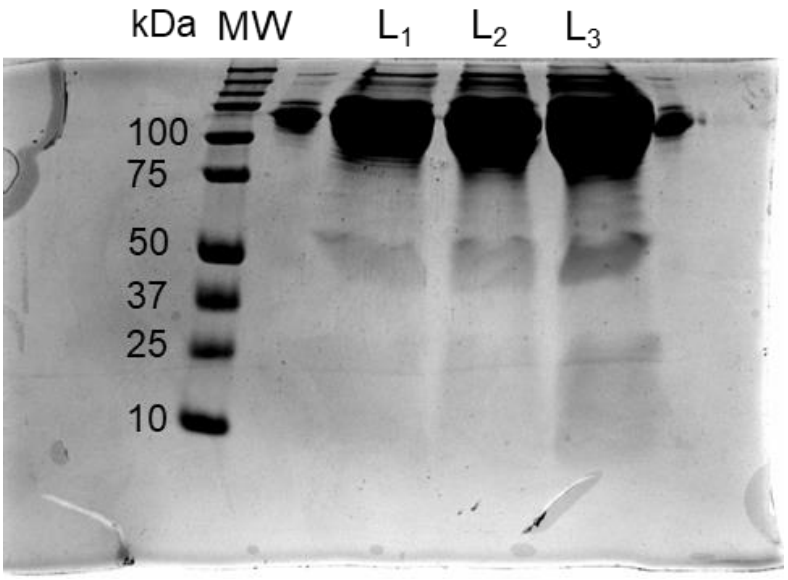

Figure 6.7 - SDS-PAGE analysis of the crude extract composition. MW - Molecular Weight Marker, L1- loading sample (sample of crude extract) diluted 1:4 with the loading buffer, L2 - loading sample diluted 1:3 with the loading buffer, L3 - loading sample diluted 1:2 with the loading buffer.

Once the IgG content was confirmed by SDS-PAGE, a purification of 5 mL of cell supernatant crude extract using a protein A Affinity Chromatography column was performed. Fractions of 2 mL were collected during the experiment and by measuring their absorbance at 280 nm, it was possible to gather the fractions with protein in pools. Those pools were the flow-through, the binding washes and elution washes. These pools were then analyzed by SDS-PAGE (Figure 6.8) and the protein content was quantified using microBCA assay (Table 6.1).

The bands related to IgG, namely at 50 kDa and 25 kDa, were not observed in the SDS-PAGE (Figure 6.8) after Coomassie staining, and thus a silver staining was needed to detect this protein. When the gel was stained, a band at 50 kDa in the elution washes lane appeared, indicating that the IgG was

purified from the crude extract. This band did not appear in the loading lanes, showing that the concentration of IgG in the crude extract could be too low, which was confirmed by quantifying the pools microBSA assay. This assay showed a total protein concentration in the crude extract of 7.23 mg/mL, and a concentration IgG of 0.396 µg/mL, assuming that the yield of this purification was 100% because it was not possible to calculated. Although it is an unreal condition, the HiTrap MabSelect SuRe column, that it was used, present usually high values of IgG purification yields [89].

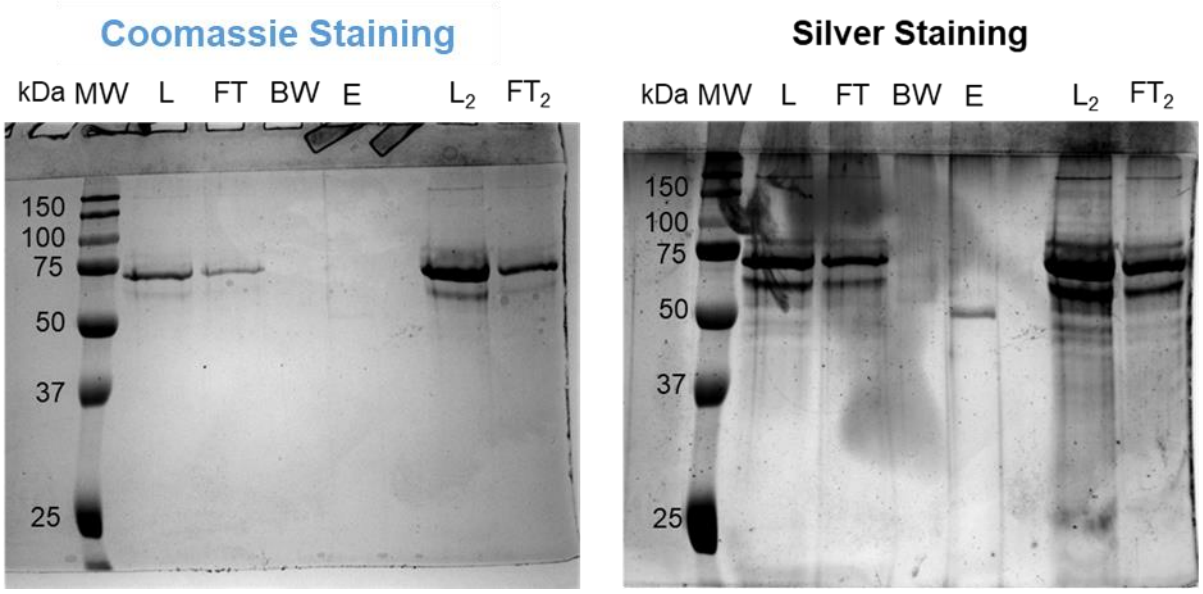

Figure 6.8 - SDS-PAGE analysis of crude extract purification using protein A affinity chromatography, the gel was stained by Coomassie (left) and by silver staining (right). MW - Molecular Weight Marker, L- loading sample diluted 1:100 with the loading buffer, FT – flow-through diluted 1:100 with the loading buffer, BW – binding washes pool diluted 10:1 with the loading buffer , E – elution washes pool diluted 10:1 with the loading buffer, L2 - loading sample diluted 1:50 with the loading buffer, FT2 - flow-through diluted 1:50 with the loading buffer.

Table 6.1 – Results of IgG purification using protein A chromatography

[Total Protein]	[IgG]	Purity of the crude extract (%)	Final purity (%)
7.23 mg/mL	0.396 µg/mL	0.005	98

Since the total protein concentration and the IgG concentration in the crude extract were, respectively, high and low, a dilution and a supplementation were needed before applying it in the MATPFS. These procedures were done in order to obtain a final crude extract with a total protein concentration of 0.7 mg/mL and an IgG concentration of 0.3 mg/mL.

6.4.2 Aqueous two phase system

In order to verify the performance of combined method for IgG purification from a crude extract, studies using the methods separately were needed as a control.

Regarding the ATPS, the PEG-NaPA 15,000 systems with 150mM of NaCl were composed by 10% w/w of each polymer and about 0.43 mL of crude extract. As in the studies of Partitioning of pure proteins in PEG/NaPA ATPSs, a precipitate was formed upon mixing the system. After mixing, the top and bottom phases were collected as well as the precipitate formed at the interface. These were quantified by BCA assay and analyzed by SDS-PAGE (Figure 6.9 and Figure 6.10).

From the SDS-PAGE analyses, it was observed that no protein of the crude extract partitioned to the bottom phase and almost all IgG precipitated. Moreover, there was a small amount of IgG in the top phase, which was only observed when the gel was silver stained and a slight band at 50 kDa appeared. Consequently, the values of yield recovery and purity of IgG in the top phase were too low, respectively, 2.0% and 7.8% (Figure 6.11).

The collection of precipitate was done in order to avoid contamination by the top and the bottom phase, and resuspended in phosphate buffer (50 mM phosphate, pH 8). Although this procedure only allowed to recover about 45% of IgG from the crude extract, the IgG was 84% pure. The IgG purity could have been obtained due to the precipitation of other proteins that were not studied. The yield of extraction could have been low due to a bad precipitate collection. Since in the SDS-PAGE there is a BSA band at 66 kDa, and from the Partitioning of pure proteins in PEG/NaPA ATPSs there should be no protein precipitation under these conditions. Moreover, the addition of MNPs to the system could facilitate the IgG collection due to their magnetic properties.

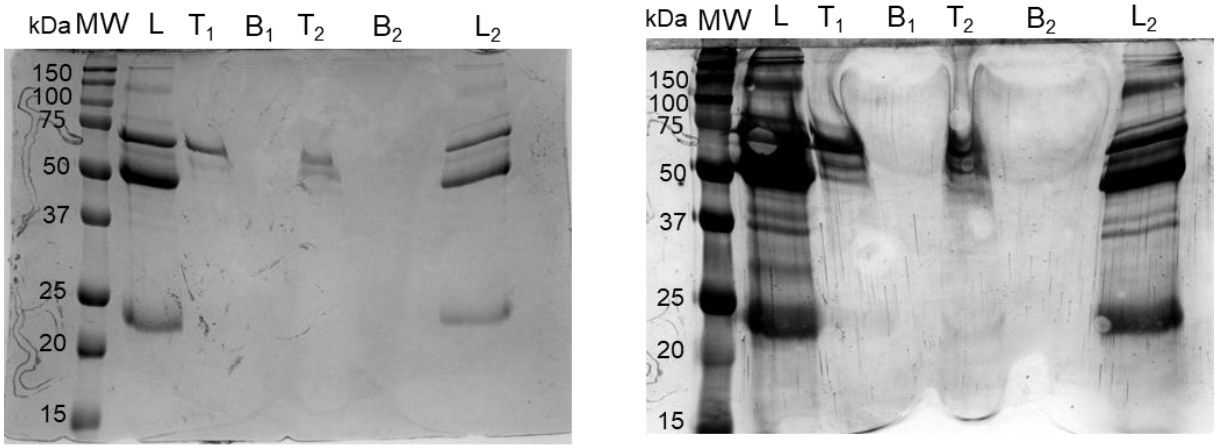

Figure 6.9 - SDS-PAGE analysis of crude extract partitioning using the PEG-NaPA 15,000 ATPS with 150 mM of NaCl, the gel was stained by by Coomassie (left) and by silver staining (right). MW - Molecular Weight Marker; L- loading sample diluted 1:2 with the loading buffer; $T_{1/2}$ – Top phase of PEG-NaPA 15,000 diluted 1:2 with the loading buffer (sample 1 and 2); $B_{1/2}$ – Bottom phase of PEG-NaPA 15,000 diluted 1:2 with the loading buffer (sample 1 and 2) ;L_2- loading sample diluted 1:3 with the loading buffer.

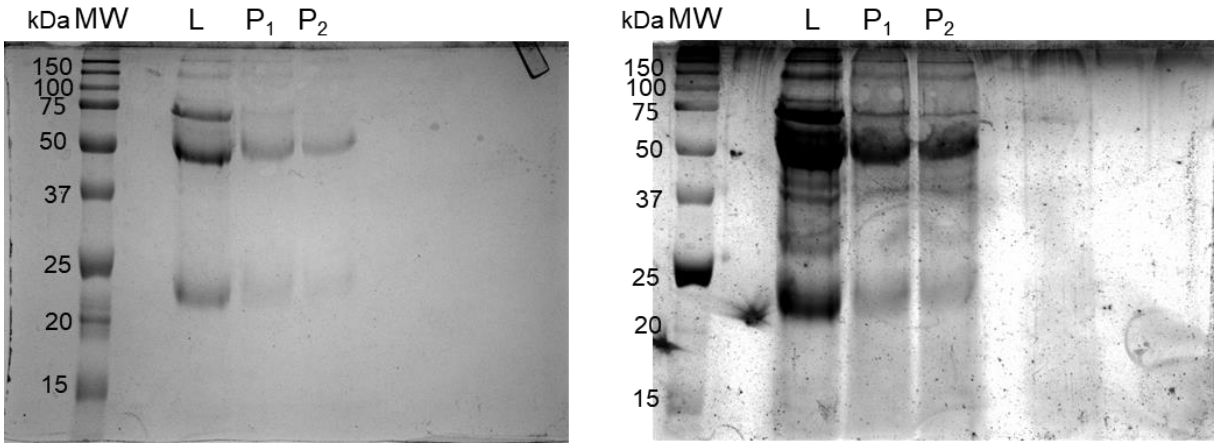

Figure 6.10 - SDS-PAGE analysis of precipitate recovered in the PEG-NaPA 15,000 ATPS with 150 mM of NaCl, the gel was stained by silver staining (image to the right). MW - Molecular Weight Marker, L- loading sample diluted 1:2 with the loading buffer; $P_{1/2}$ – Precipitate formed in the ATPS 1 and 2.

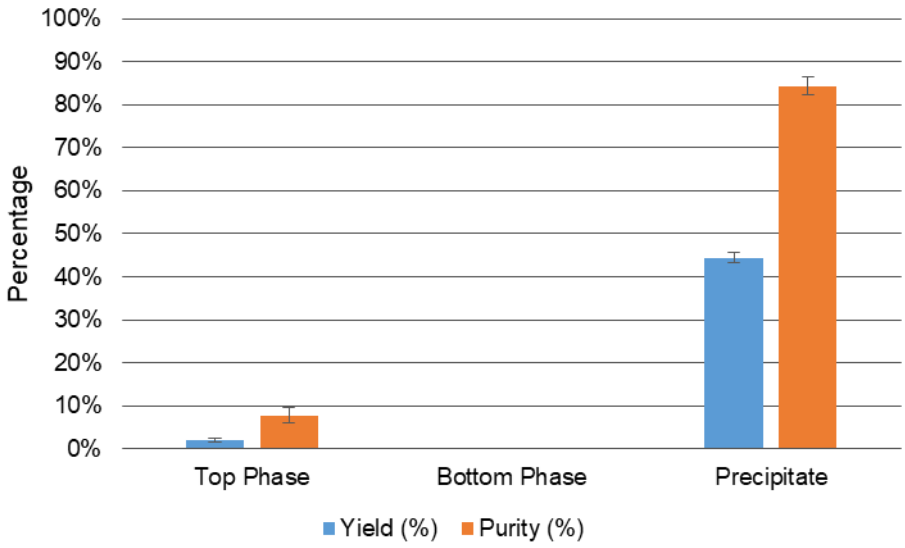

Figure 6.11 – Results of IgG purification using PEG-NaPA 15,000 with 150 mM of NaCl (n=2).

6.4.3 Magnetic Fishing

In order to do an IgG purification control study using magnetic particles, systems similar to the ones used in the MATPFS were prepared, with binding buffer (50 mM phosphate, pH 8). After an incubation of 15 minutes, the MNPs were magnetically collected and washed with binding and elution buffer. The amount of protein in these samples was then quantified by BCA assay, which gives the total protein content, and analyzed by SDS-PAGE (Figure 6.12), thus allowing to calculate the affinity binding of MNPs towards all proteins and specifically IgG (Figure 6.13).

From the SDS-PAGE analysis (Figure 6.12), it was observed that after incubation the majority of IgG would bind neither to the MNP-DX nor to MNP-DX-22/8, by the presence of its band in the flow-through lane. Moreover, when the particles were washed with binding buffer more IgG was washed away from

the particles, as a result the purification yield and purity were only of 12% and 76%, respectively (Figure 6.14). These unexpected results could have been obtained due to a low incubation time (15 minutes) or even to a low concentration of MNPs used. In the Affinity Assays studies (5.3.4), a MNPs concentration of 10 mg/mL and a protein concentration of 1 mg/mL were used, whereas in this section, the MNPs concentration and the protein concentration were the same, around 0.2 mg/mL. Moreover, MNPs present affinity towards proteins other than IgG, since the values of affinity binding towards IgG were lower than the affinity towards all the proteins (Figure 6.13). The MNP-DX presented an affinity binding of 88 mg of IgG/g of support and 119 mg of proteins/g of support, whereas the MNP-DX-22/8 showed higher values of affinity binding, 129 mg of IgG/g of support and 171 mg of proteins/g of support.

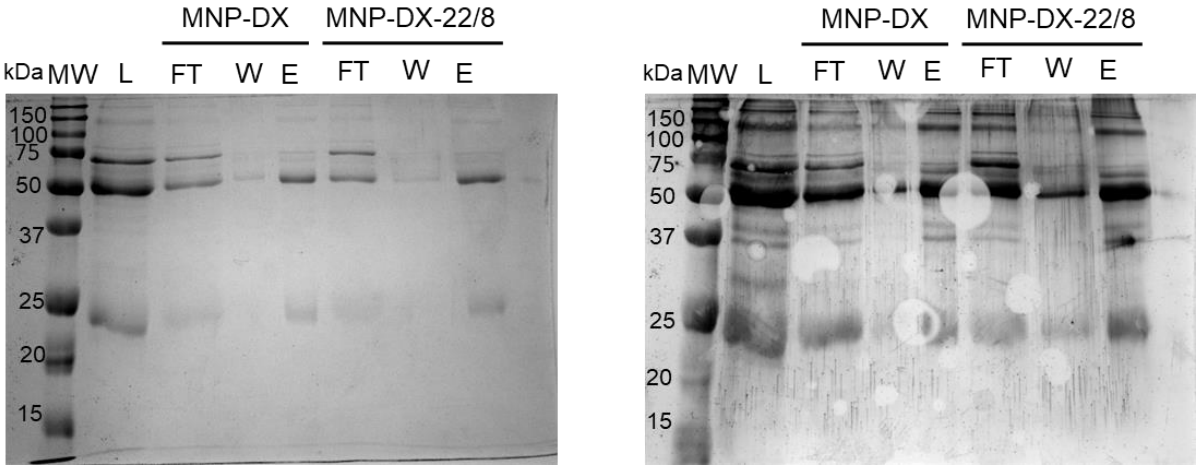

Figure 6.12 - SDS-PAGE analysis of crude extract purification using the MNP-DX and MNP-DX-22/8, the gel was stained by Coomassie staning (left) and silver staining (right). MW - Molecular Weight Marker; L- loading sample diluted 1:2 with the loading buffer; FT – Flow-through diluted 1:2 with the loading buffer; B – First binding wash diluted 1:2 with the loading buffer; E- First elution wash diluted 1:2 with the loading buffer.

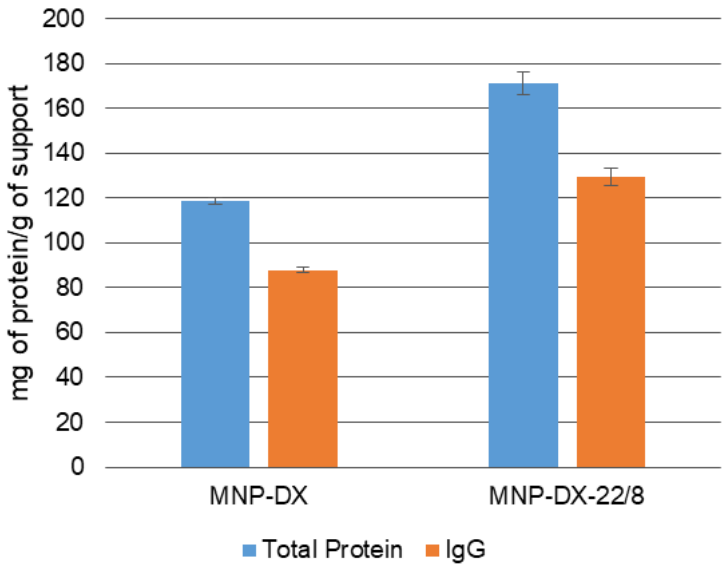

Figure 6.13 – Affinity binding of MNP towards all the proteins and IgG (n=2).

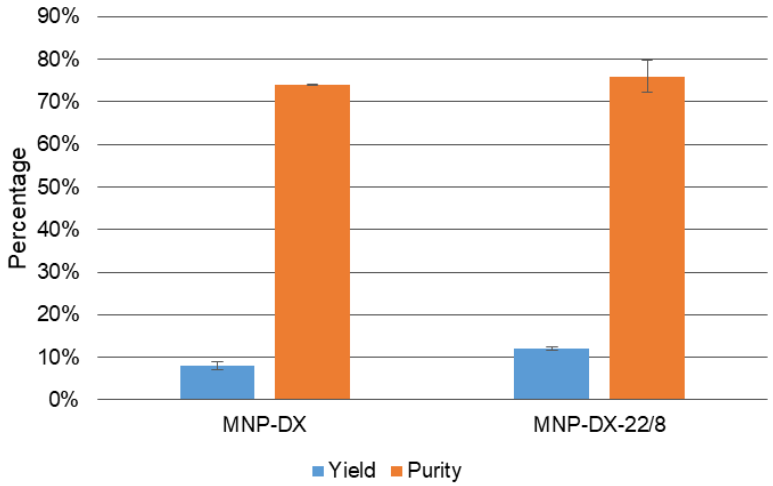

Figure 6.14 - Results of IgG purification using MNP-DX and MNP-DX-22/8 (n=2).

6.4.4 Magnetic Aqueous Two Phase Fishing

When the control studies of IgG purification from a crude extract using separately the methods of ATPS and magnetic fishing were finished, the combination of these two techniques was applied, namely the PEG-NaPA 15,000 with 150 mM of NaCl with MNP-DX-22/8 or with MNP-DX, for control purposes. After mixing the systems and waiting for the phase separation, MNPs were magnetically collected along with the top phase. Then MNPs were washed with binding buffer (50 mM phosphate, pH 8) and then elution buffer (50 mM glycine–NaOH, pH 11). The samples were quantified by BCA assay to calculate the total protein and analyzed by SDS-PAGE to verify the purity (Figure 6.15 and Figure 6.16).

The SDS-PAGE top and bottom phases collected (Figure 6.15) indicated a high quantity of BSA in the top phase, and almost all IgG bound the MNPs, since there is no visible band at 50 kDa or at 25 kDa. As expected from the control IgG purification study using ATPS, no band appeared in the bottom phase.

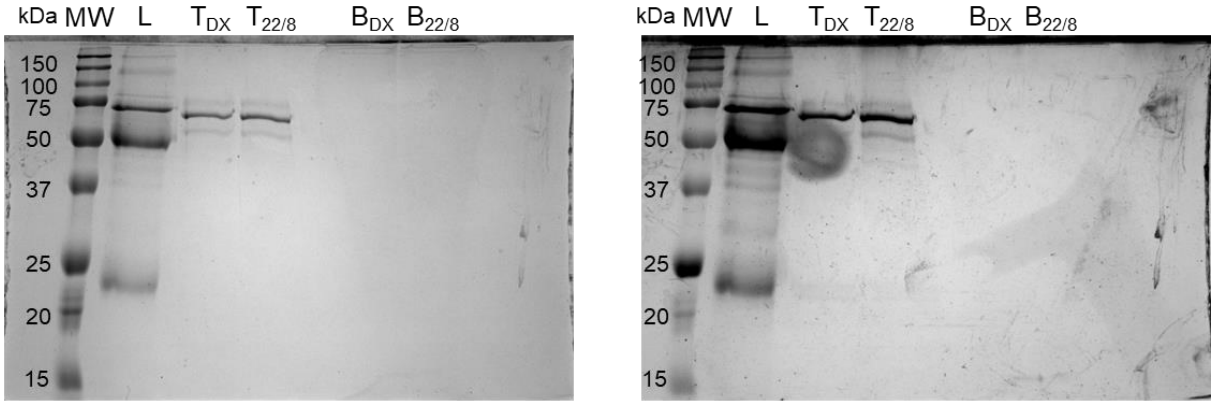

Figure 6.15 - SDS-PAGE analysis of top and bottom phases collected from the PEG-NaPA 15,000 ATPS with 150 mM of NaCl using MNP-DX and MNP.22/8, the gel was stained by Coomassie staning (left) and silver staining (right). MW - Molecular Weight Marker; L- loading sample diluted 1:2 with the loading buffer; T– Top phase of MATPFS diluted 1:2 with the loading buffer; B – Bottom phase of MATPFS diluted 1:2 with the loading buffer (Subscript DX – system where was used MNP-DX; subscript 22/8 – system where was used MNP-DX-22/8).

Although the MNP-DX-22/8 seemed to have bound IgG, this binding did not occur as expected by hydrophobic interactions between the IgG and the ligand 22/8, since both MNP-DX and MNP-DX-22/8 had similar results after its washes with binding buffer and elution buffer (Figure 6.16 and Figure 6.17). This IgG purification process allowed to obtain only a yield of purification of 6.4%, which could been explained by the great loss of IgG in the first binding buffer wash due to the non-specific interactions between the IgG and the MNPs or to protein precipitation around the particles. Moreover, it was possible to achieve purity degree of 91.8%.

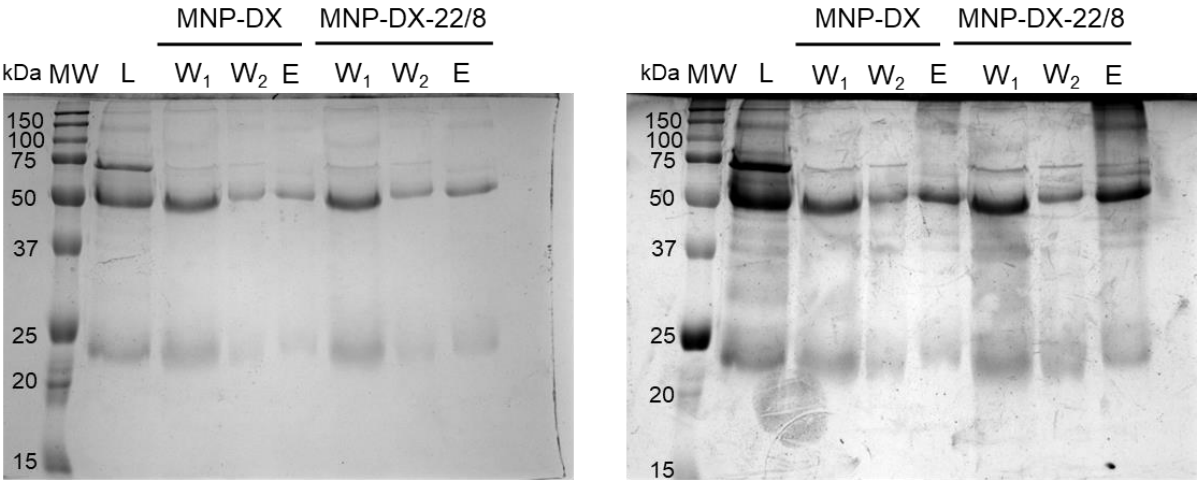

Figure 6.16 - SDS-PAGE analysis of MNP-DX and MNP-DX-22/8 binding and elution washes, the gel was stained by stained by Coomassie staning (left) and silver staining (right). MW - Molecular Weight Marker; L- loading sample diluted 1:2 with the loading buffer; $W_{1/2}$ – First and second binding washes of MNP-DX and MNP-DX-22/8 (W_1 was diluted 1:2 with the loading buffer and W_2 was diluted 1:5 with loading buffer); E –Elution wash of MNP-DX and MNP-DX-22/8 diluted 1:5 with the loading buffer.

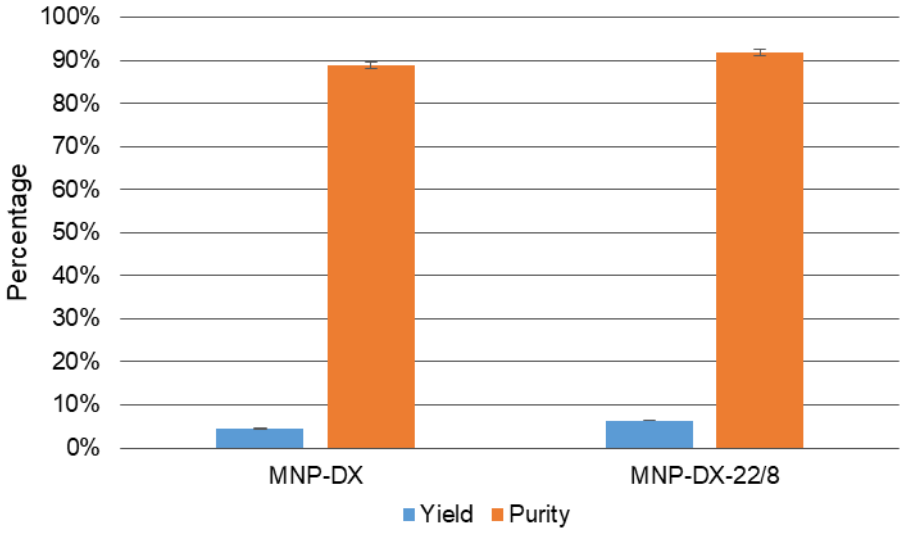

Figure 6.17 - Results of IgG purification using MNP-DX and MNP-DX-22/8 in the PEG-NaPA 15,000 with 150 mM NaCl (n=2).

Since there was a great loss of IgG in the first binding wash, if this were assumed as the final product for this purification process, it would be possible to obtain a purification yield of 78% and 93% of purity using MNP-DX-22/8 (Figure 6.18). A higher value of yield was obtained when MNP-DX were washed,

because these are not specific towards IgG and thus when they were washed more protein was lost. Either way, it was possible to enhance the purification of IgG from a crude extract by combining two different techniques (Table 6.2), which separately obtained lower values of yield and purity.

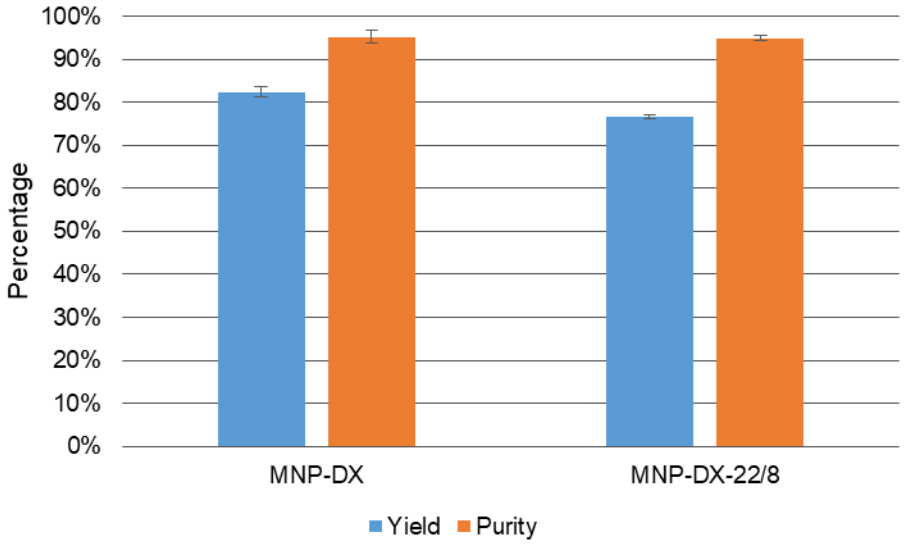

Figure 6.18 - Results of IgG purification using MNP-DX and MNP-DX-22/8 in the PEG-NaPA 15,000 with 150 mM NaCl and assuming the first binding wash as final product (n=2).

Table 6.2 – Comparison of the MATFS used in this work with the control methods, Magnetic Fishing and ATPS, and the Protein A chromatography.

	IgG	
Purification Method	Yield (%)	Purity (%)
Protein A chromatography	---	98
Direct magnetic Fishing	12	76
ATPS alone (Precipitate)	45	84
MATPFS (assuming the first elution wash as final product)	6	92
MATPFS (assuming the first binding wash as final product)	78	93

6.5 Conclusions

This chapter started with study of the partitioning of MNPs-DX and MNPs-DX-22/8 in PEG-NaPA systems with different MWs of NaPA (1,200, 8,000 and 15,000) and with 150 mM or 0 mM of NaCl. From this study, it was observed that the presence of the ligand 22/8 on the MNPs-DX surface has an effect in their partitioning behavior, since the MNP-DX-22/8 would go to the top phase whereas MNP-DX would go mainly to the bottom phase.

Regarding the recovery study of BSA and IgG, the PEG-NaPA 15,000 with 150 mM of NaCl was chosen as the most suitable magnetic aqueous two phase fishing system to purify IgG from a cell culture supernatant. This system was more selective towards IgG, when compared with the other systems studied.

A Protein A Affinity Chromatography was performed in order to quantify the amount of IgG in the crude extract provided by StabVida. The pools collected were quantified and an IgG concentration of 0.4 µg/mL in the crude extract was obtained. Moreover, the total protein concentration in crude extract was 7.23 mg/mL, showing that this sample needed to be diluted and supplemented with pure IgG before applying it in the MATPFS.

The control studies for the MATPFS, which consisted of using the ATPS and magnetic fishing separately to purify IgG from the crude extract, showed low yields of purification, 45% using ATPS (but with protein precipitated) and 12% using magnetic fishing. When these two methods were combined, and the MNPs were washed with binding and elution buffer, only 6% of total IgG was purified with 92% of purity. However, if the first binding wash were assumed as the final product of this all process, it would be possible to obtain higher values of yield and purity (78% and 93%). Furthermore, if the MNPs had not been washed with binding buffer, the yield of purification would have been higher but the IgG purity would had been similar or lower.

7. Concluding Remarks

In this work, a new combination of two different purification methods, namely aqueous two phase system (ATPS) and magnetic fishing, was investigated as an integrated process for the purification of IgG from a cell culture supernatant.

In the initial chapter, a new ATPS was stablished. The behavior of the binodal curve of ATPS, composed by poly(ethylene glycol) 3,350 (PEG) and sodium polyacrylate (NaPA), in the presence of different NaCl concentrations and different molecular weights of NaPA was studied. It was observed that the increase of both parameters NaCl and NaPA MW helped to form systems with lower polymer content, which is of interest in an industrial environment due to the lower cost, viscosity and biocompatibility associated with it. However, at this level, systems with high concentration of salt could lead to corrosion problems and therefore the systems with 0 mM and 150 mM of NaCl were selected to further studies. Furthermore, in the future these systems could be further characterized for example by changing the pH or the temperature and determining the concentration of each polymer in both phases in order to determine the tie-lines.

Using the ATPSs previously chosen, the partitioning of two pure proteins, BSA and IgG, were investigated. These two proteins had different partitioning behaviors, since IgG had the tendency to precipitate whereas the BSA partitioned mainly to the top phase. It was also observed that the NaPA MW have a higher effect in the partitioning behavior when there is no NaCl. These difference of behaviors could be beneficial for the purification of IgG from the crude extract as long as it is possible to provide structural stabilization and keep its biological function.

Regarding the magnetic fishing chapter, different magnetic particles were produced and modified with aim to investigate the most suitable affinity support for the purification of IgG. Initially, the magnetic particles were synthesized by the most commonly used method, co-precipitation, and then were coated with a double layer of silica. These MNPs were then coated with different biopolymers, dextran or gum arabic, and were functionalized with different ligands, the ligand 22/8 or the phenylboronic acid, respectively.

The synthesized particles were characterized by different methods, namely FTIR, zeta potential, DLS From this characterization, it was verified that the MNP-DX-22/8 were well synthesized, having a hydrodynamic diameter about 380 nm and instability in suspension, this is because MNPs tend to aggregate. Moreover, the affinity assays for these MNPs showed a higher affinity binding towards IgG (88.0 mg of protein/g of support) than BSA (25.2 mg/g), being corroborated with previous works results [52]. Regarding the MNP-GA-BA characterization results, the FTIR spectra did not allowed to confirm the presence of phenylboronic acid on the MNPs surface. Furthermore, these MNPs were neither monodisperse, having a Z-average value of 733 nm and a mean peak value of 363 nm, nor had a drop in their zeta potential variation between pH 8 and 9, which is a feature of boronic acid modified supports. These results seem to suggest that the MNPs had suffered crosslinking during their functionalization with GLYMO, which was confirmed by the affinity assays where low affinity binding were obtained, 49.8 mg/g to the IgG and 5.9 mg/g to the BSA. As a result, the MNP-DX-22/8 were chosen for further studies. In future studies would be interesting to synthesize the MNP-GA-BA correctly and apply them to the

PEG-NaPA system, and although the MNP-GA were not chosen, their study would also be appealing since they showed specificity towards IgG.

In the last chapter, the MNPs were applied in the PEG-NaPA systems to study their partitioning behavior and their potential to recover BSA and IgG, with aim to find a suitable magnetic aqueous two phase fishing system (MATPFS) to purify IgG from a cell culture supernatant. From the MNPs partitioning study, the ligand 22/8 had an important role in their partitioning, since the MNP-DX would go mainly to the bottom phase and MNP-DX-22/8 would go to the top. These results showed an improvement in the MNPs partitioning from the Dhadge *et al* report, where the MNPs partitioned to the bottom phase of a PEG-Dextran system. Moreover, from the recovery study of BSA and IgG, the PEG-NaPA 15,000 with 150 mM of NaCl was chosen for further IgG purification studies from a cell culture supernatant, wherein the IgG concentration was unknown. Using a protein A affinity chromatography, the IgG concentration in the cell culture supernatant was determined (0.4 µg/mL) as well as the total protein concentration (7.23 mg/mL), which led to its dilution and supplementation with IgG.

The individual performance of ATPS and magnetic fishing, showed that separately both unit operations were inefficient to purify IgG from the crude extract, since yields of purification obtained were low, 45% to the ATPS and 12% to the magnetic fishing, and the purity was not the desired. In the ATPS, IgG precipitated and therefore its recovery was difficult to perform. Moreover, the unexpected results from magnetic fishing could have been obtained due to a low incubation time (15 minutes) and a low concentration of MNPs used. The combination of these two methods allowed to recover just 6% of total IgG with 92% of purity, when the experimental design was followed. However, regarding the MNP-DX-22/8, the first binding wash presented 78% of the total IgG and 93% of purity, which confirmed that the binding between the MNPs and IgG was by non-specific interactions or occurred protein precipitation around the particles. Furthermore, if these MNPs had been firstly washed with elution buffer, the yield of purification would have been higher.

The PEG-NaPA system may have prevented the success of MATPFS to purify IgG from a crude extract by promoting protein precipitation, however for other proteins or biologic systems this MATPFS could have worked. The PEG-NaPA systems have been recently reported and although they have already been studied in several applications, this study was one of the first that combined this type of ATPS with magnetic particles for the purification of IgG from a cell culture supernatant, and therefore more studies are needed to optimize this purification platform.

8. Bibliographic References

[1] D. Lane, *Antibodies - A laboratory manual*, First Edit. 1988.

[2] J. N. Arnold, M. R. Wormald, R. B. Sim, P. M. Rudd, and R. a Dwek, “The impact of glycosylation on the biological function and structure of human immunoglobulins.,” *Annu. Rev. Immunol.*, vol. 25, pp. 21–50, 2007.

[3] J. W. Goding, “Monoclonal Antibodies: Principles and Practice.” p. 492, 1996.

[4] M. Adamczyk, J. C. Gebler, and J. Wu, “Papain digestion of different mouse IgG subclasses as studied by electrospray mass spectrometry,” *J. Immunol. Methods*, vol. 237, no. 1–2, pp. 95–104, 2000.

[5] P. Vanlandschoot, C. Stortelers, E. Beirnaert, L. I. Ibañez, B. Schepens, E. Depla, and X. Saelens, “Nanobodies: New ammunition to battle viruses,” *Antiviral Res.*, vol. 92, pp. 389–407, 2011.

[6] L. K. Roskos, C. G. Davis, and G. M. Schwab, “The clinical pharmacology of therapeutic monoclonal antibodies,” *Drug Dev. Res.*, vol. 61, no. 3, pp. 108–120, 2004.

[7] S. Antibodies and C. A. Specificities, “Choosing a secondary antibody : A guide to fragment specificity,” *Meridian*, vol. 747, no. 815, pp. 0–3.

[8] S. Dübel and J. M. Reichert, *Handbook of Therapeutic Antibodies*, Second Edi., vol. 1–4. 2014.

[9] J. R. Birch and A. J. Racher, “Antibody production,” *Adv. Drug Deliv. Rev.*, vol. 58, no. 5–6, pp. 671–685, 2006.

[10] F. Li, N. Vijayasankaran, A. Shen, R. Kiss, and A. Amanullah, “Cell culture processes for monoclonal antibody production,” *MAbs*, vol. 2, no. 5, pp. 466–479, 2010.

[11] E. Jain and A. Kumar, “Upstream processes in antibody production: Evaluation of critical parameters,” *Biotechnol. Adv.*, vol. 26, no. 1, pp. 46–72, 2008.

[12] A. C. A. Roque, C. R. Lowe, and M. Â. Taipa, “Antibodies and genetically engineered related molecules: Production and purification,” *Biotechnol. Prog.*, vol. 20, no. 3, pp. 639–654, 2004.

[13] A. Rita Costa, M. Elisa Rodrigues, M. Henriques, J. Azeredo, and R. Oliveira, “Guidelines to cell engineering for monoclonal antibody production,” *Eur. J. Pharm. Biopharm.*, vol. 74, no. 2, pp. 127–138, 2010.

[14] A. A. Shukla and J. Thömmes, “Recent advances in large-scale production of monoclonal antibodies and related proteins,” *Trends Biotechnol.*, vol. 28, no. 5, pp. 253–261, 2010.

[15] M. Arora, “Cell Culture Media: A Review,” *MATER METHODS*, no. 175, p. 3, 2013.

[16] S. S. Ozturk and W.-S. Hu, *Cell Culture Technology for Pharmaceutical and Cell-Based Therapies*. 2006.

[17] P. Gronemeyer, R. Ditz, and J. Strube, “Trends in Upstream and Downstream Process Development for Antibody Manufacturing,” *Bioengineering*, vol. 1, no. 4, pp. 188–212, 2014.

[18] A. C. A. Roque, C. S. O. Silva, and M. Â. Taipa, “Affinity-based methodologies and ligands for antibody purification: Advances and perspectives,” *J. Chromatogr. A*, vol. 1160, no. 1–2, pp. 44–55, 2007.

[19] P. A. J. Rosa, I. F. Ferreira, A. M. Azevedo, and M. R. Aires-Barros, “Aqueous two-phase systems: A viable platform in the manufacturing of biopharmaceuticals,” *J. Chromatogr. A*, vol. 1217, no. 16, pp. 2296–2305, 2010.

[20] M. Ottens, J. A. Wesselingh, and L. A. M. van der Wielen, “Introduction to Biomanufacturing: Downstream Processing,” *Basic Biotechnol.*, pp. 220–249, 2006.

[21] P. A. Marichal-Gallardo and M. M. Álvarez, “State-of-the-art in downstream processing of monoclonal antibodies: Process trends in design and validation,” *Biotechnol. Prog.*, vol. 28, no. 4, pp. 899–916, 2012.

[22] A. A. Shukla, B. Hubbard, T. Tressel, S. Guhan, and D. Low, “Downstream processing of monoclonal antibodies-Application of platform approaches,” *J. Chromatogr. B Anal. Technol. Biomed. Life Sci.*, vol. 848, no. 1, pp. 28–39, 2007.

[23] A. Frenzel, M. Hust, and T. Schirrmann, “Expression of recombinant antibodies,” *Front.*

Immunol., vol. 4, no. JUL, pp. 1–20, 2013.

[24] Suzanne S. Farid, “Economic Drivers and Trade-Offs in Antibody Purification Processes,” *BioPharm Int. Suppl.*, pp. S38–S42, 2009.

[25] N. Singh, A. Arunkumar, S. Chollangi, Z. G. Tan, M. Borys, and Z. J. Li, “Clarification technologies for monoclonal antibody manufacturing processes: Current state and future perspectives,” *Biotechnol. Bioeng.*, vol. 113, no. 4, pp. 698–716, 2016.

[26] D. Low, R. O. Leary, and N. S. Pujar, “Future of antibody purification,” vol. 848, pp. 48–63, 2007.

[27] A. M. Azevedo, P. A. J. Rosa, I. F. Ferreira, and M. R. Aires-Barros, “Chromatography-free recovery of biopharmaceuticals through aqueous two-phase processing,” *Trends Biotechnol.*, vol. 27, no. 4, pp. 240–247, 2009.

[28] S. Raja, V. R. Murty, V. Thivaharan, V. Rajasekar, and V. Ramesh, “Aqueous Two Phase Systems for the Recovery of Biomolecules – A Review,” *Sci. Technol.*, vol. 1, no. 1, pp. 7–16, 2012.

[29] B. Y. Zaslavsky, *Aqueous Two-Phase Partitioning: Physical Chemistry and Bioanalytical Applications*. New York: Marcel Dekker, Inc., 1995.

[30] H.-O. Johansson, E. Feitosa, and A. P. Junior, “Phase Diagrams of the Aqueous Two-Phase Systems of Poly(ethylene glycol)/Sodium Polyacrylate/Salts,” *Polymers (Basel).*, vol. 3, no. 1, pp. 587–601, 2011.

[31] J. A. Asenjo and B. A. Andrews, “Aqueous two-phase systems for protein separation: A perspective,” *J. Chromatogr. A*, vol. 1218, no. 49, pp. 8826–8835, 2011.

[32] C. Ladd Effio, L. Wenger, O. Ötes, S. A. Oelmeier, R. Kneusel, and J. Hubbuch, “Downstream processing of virus-like particles: Single-stage and multi-stage aqueous two-phase extraction,” *J. Chromatogr. A*, vol. 1383, pp. 35–46, 2015.

[33] P. A. J. Rosa, A. M. Azevedo, and M. R. Aires-Barros, “Application of central composite design to the optimisation of aqueous two-phase extraction of human antibodies,” *J. Chromatogr. A*, vol. 1141, no. 1, pp. 50–60, 2007.

[34] R. L. Pérez, D. B. Loureiro, B. B. Nerli, and G. Tubio, “Optimization of pancreatic trypsin extraction in PEG/citrate aqueous two-phase systems,” *Protein Expr. Purif.*, vol. 106, pp. 66–71, 2015.

[35] S. Chethana, C. A. Nayak, M. C. Madhusudhan, and K. S. M. S. Raghavarao, “Single step aqueous two-phase extraction for downstream processing of C-phycocyanin from Spirulina platensis,” *J. Food Sci. Technol.*, vol. 52, no. 4, pp. 2415–2421, 2015.

[36] P. A. J. Rosa, A. M. Azevedo, I. F. Ferreira, J. De Vries, R. Korporaal, H. J. Verhoef, T. J. Visser, and M. R. Aires-barros, “Affinity partitioning of human antibodies in aqueous two-phase systems,” vol. 1162, pp. 103–113, 2007.

[37] A. L. Grilo, M. R. Aires-Barros, and A. M. Azevedo, “Separation & Purification Reviews Partitioning in Aqueous Two-Phase Systems: Fundamentals, Applications and Trends Partitioning in Aqueous Two-Phase Systems: Fundamentals, Applications and Trends,” *Sep. Purif. Rev.*, vol. 45, no. 45, pp. 68–80, 2016.

[38] K. Hola, Z. Markova, G. Zoppellaro, J. Tucek, and R. Zboril, “Tailored functionalization of iron oxide nanoparticles for MRI, drug delivery, magnetic separation and immobilization of biosubstances,” *Biotechnol. Adv.*, vol. 33, no. 6, pp. 1162–1176, 2015.

[39] F. Assa, H. Jafarizadeh-Malmiri, H. Ajamein, N. Anarjan, H. Vaghari, Z. Sayyar, and A. Berenjian, “A biotechnological perspective on the application of iron oxide nanoparticles,” *Nano Res.*, vol. 9, no. 8, pp. 2203–2225, 2016.

[40] W. Wu, Q. He, and C. Jiang, “Magnetic iron oxide nanoparticles: Synthesis and surface functionalization strategies,” *Nanoscale Res. Lett.*, vol. 3, no. 11, pp. 397–415, 2008.

[41] S. Laurent, D. Forge, M. Port, A. Roch, C. Robic, L. Vander Elst, and R. N. Muller, “Magnetic iron oxide nanoparticles: Synthesis, stabilization, vectorization, physicochemical characterizations and biological applications,” *Chem. Rev.*, vol. 108, no. 6, pp. 2064–2110, 2008.

[42] A. H. Lu, E. L. Salabas, and F. Schüth, “Magnetic nanoparticles: Synthesis, protection, functionalization, and application,” *Angew. Chemie - Int. Ed.*, vol. 46, no. 8, pp. 1222–1244, 2007.

[43] J. He, M. Huang, D. Wang, Z. Zhang, and G. Li, “Magnetic separation techniques in sample preparation for biological analysis: A review,” *J. Pharm. Biomed. Anal.*, vol. 101, pp. 84–101, 2014.

[44] A. C. A. R. A.M.G.C. Dias, A. Hussain, A.S. Marcos, “A biotechnological perspective on the application of iron oxide magnetic colloids modified with polysaccharides,” *Biotechnol. Adv.*, vol. 29, no. 1, pp. 142–155, 2011.

[45] David S. Hage, *Handbook of Affinity Chromatography: 1) An Introduction to Affinity Chromatography*. Taylor & Francis Group, 2006.

[46] A. Ditsch, J. Yin, P. E. Laibinis, D. I. Wang, and T. A. Hatton, “Ion-exchange purification of proteins using magnetic nanoclusters,” *Biotechnol Prog*, vol. 22, no. 4, pp. 1153–1162, 2006.

[47] L. Borlido, A. M. Azevedo, A. C. A. Roque, and M. R. Aires-Barros, “Magnetic separations in biotechnology,” *Biotechnol. Adv.*, vol. 31, no. 8, pp. 1374–1385, 2013.

[48] I. L. Batalha, A. Hussain, and A. C. A. Roque, “Gum arabic coated magnetic nanoparticles with affinity ligands specific for antibodies,” *J. Mol. Recognit.*, vol. 23, no. 5, pp. 462–471, 2010.

[49] M. Helena, M. Estevam, G. Ayres, M. Paola, S. Isabel, C. Nobre, J. António, L. Bezerra, and D. C. Júnior, “Trypsin purification using magnetic particles of azocasein-iron composite,” *Food Chem.*, vol. 226, pp. 75–78, 2017.

[50] A. Serve, M. M. Pieler, D. Benndorf, E. Rapp, M. W. Wolff, and U. Reichl, “Comparison of Influenza Virus Particle Purification Using Magnetic Sulfated Cellulose Particles with an Established Centrifugation Method for Analytics,” *Anal. Chem.*, vol. 87, no. 21, pp. 10708–10711, 2015.

[51] Y. Zhou, S. Yuan, Q. Liu, D. Yan, Y. Wang, L. Gao, J. Han, and H. Shi, “Synchronized purification and immobilization of his-tagged β-glucosidase via Fe3O4/PMG core/shell magnetic nanoparticles,” *Sci. Rep.*, vol. 7, no. December 2016, p. 41741, 2017.

[52] S. D. F. Santana, V. L. Dhadge, and A. C. A. Roque, “Dextran-Coated Magnetic Supports Modified with a Biomimetic Ligand for IgG Purification,” *ACS Apllied Mater. Interfacesaterials Interfaces*, no. 4, pp. 5907–5914, 2012.

[53] V. L. Dhadge, S. A. S. L. Rosa, A. Azevedo, R. Aires-Barros, and A. C. A. Roque, “Magnetic aqueous two phase fishing: A hybrid process technology for antibody purification,” *J. Chromatogr. A*, vol. 1339, pp. 59–64, 2014.

[54] P.-Å. Albertsson and F. Tjerneld, “Phase Diagrams,” in *Aqueous Two-Phase Systems*, 1st ed., J. N. Abelson, M. I. Simon, H. Walter, and G. Johansson, Eds. Methods in Enzymology 228 in Elsevier, Academic Pres, 1994, pp. 3–13.

[55] V. Gupta, S. Nath, and S. Chand, “Role of water structure on phase separation in polyelectrolyte-polyethyleneglycol based aqueous two-phase systems,” *Polymer (Guildf).*, vol. 43, no. 11, pp. 3387–3390, 2002.

[56] H. O. Johansson, F. M. Magaldi, E. Feitosa, and A. Pessoa, “Protein partitioning in poly(ethylene glycol)/sodium polyacrylate aqueous two-phase systems,” *J. Chromatogr. A*, vol. 1178, no. 1–2, pp. 145–153, 2008.

[57] H. O. Johansson, M. Ishii, M. Minaguti, E. Feitosa, T. C. V. Penna, and A. Pessoa, “Separation and partitioning of Green Fluorescent Protein from Escherichia coli homogenate in poly(ethylene glycol)/sodium-poly(acrylate) aqueous two-phase systems,” *Sep. Purif. Technol.*, vol. 62, no. 1, pp. 166–174, 2008.

[58] L. A. Pereira Alcântara, K. S. Do Nascimento, C. A. Mour??o, V. P. R. Minim, and L. A. Minim, “Aqueous two-phase poly(ethylene glycol)-sodium polyacrylate system for amyloglucosidase purification: Equilibrium diagrams and partitioning studies,” *Sep. Purif. Technol.*, vol. 118, no. August, pp. 888–894, 2013.

[59] M. Iqbal, Y. Tao, S. Xie, Y. Zhu, D. Chen, X. Wang, L. Huang, D. Peng, A. Sattar, M. A. B. Shabbir, H. I. Hussain, S. Ahmed, and Z. Yuan, “Aqueous two-phase system (ATPS): an overview and advances in its applications,” *Biol. Proced. Online*, vol. 18, no. 1, p. 18, 2016.

[60] R. R. G. Soares, A. M. Azevedo, J. M. Van Alstine, and M. Raquel Aires-Barros, “Partitioning in aqueous two-phase systems: Analysis of strengths, weaknesses, opportunities and threats,” *Biotechnol. J.*, vol. 10, no. 8, pp. 1158–1169, 2015.

[61] J. Huddleston, A. Veide, K. Köhler, J. Flanagan, S. O. Enfors, and A. Lyddiatt, “The molecular basis of partitioning in aqueous two-phase systems,” *Trends Biotechnol.*, vol. 9, no. 11, pp. 381–8, 1991.

[62] L. A. Sarubbo, L. A. De Oliveira, A. L. Figueiredo Porto, G. M. De Campos-Takaki, and E. B. Tambourgi, “Partition of proteins in aqueous two-phase systems based on cashew-nut tree gum and poly(ethylene glycol),” *Brazilian Arch. Biol. Technol.*, vol. 47, no. 5, pp. 685–691, 2004.

[63] L. Borlido, A. M. Azevedo, A. C. A. Roque, and M. R. Aires-Barros, “Potential of boronic acid functionalized magnetic particles in the adsorption of human antibodies under mammalian cell culture conditions,” *J. Chromatogr. A*, vol. 1218, no. 43, pp. 7821–7827, 2011.

[64] S. F. Teng, K. Sproule, A. Husain, and C. R. Lowe, “Affinity chromatography on immobilized ‘biomimetic’ ligands,” *J. Chromatogr. B Biomed. Sci. Appl.*, vol. 740, no. 1, pp. 1–15, 2000.

[65] V. L. Dhadge, A. Hussain, A. M. Azevedo, R. Aires-Barros, and A. C. A. Roque, “Boronic acid-modified magnetic materials for antibody purification.,” *J. R. Soc. Interface*, vol. 11, no. 91, p. 20130875, 2014.

[66] M. Carmen Bautista, O. Bomati-Miguel, M. Del Puerto Morales, C. J. Serna, and S. Veintemillas-Verdaguer, “Surface characterisation of dextran-coated iron oxide nanoparticles prepared by laser pyrolysis and coprecipitation,” *J. Magn. Magn. Mater.*, vol. 293, no. 1, pp. 20–27, 2005.

[67] R. S. Gaster, L. Xu, S.-J. Han, R. J. Wilson, D. A. Hall, S. J. Osterfeld, H. Yu, and S. X. Wang, “Quantification of protein interactions and solution transport using high-density GMR sensor arrays.,” *Nat. Nanotechnol.*, vol. 6, no. 5, pp. 314–320, 2011.

[68] L. Zhang, F. Yu, A. J. Cole, B. Chertok, A. E. David, J. Wang, and V. C. Yang, “Gum arabic-coated magnetic nanoparticles for potential application in simultaneous magnetic targeting and tumor imaging,” *Aaps J*, vol. 11, no. 4, pp. 693–699, 2009.

[69] M. Yamaura, R. L. Camilo, L. C. Sampaio, M. A. Macêdo, M. Nakamura, and H. E. Toma, “Preparation and characterization of (3-aminopropyl)triethoxysilane-coated magnetite nanoparticles,” *J. Magn. Magn. Mater.*, vol. 279, no. 2–3, pp. 210–217, 2004.

[70] ThermoNicolet, “Introduction to Fourier Transform Infrared Spectrometry,” 2001. .

[71] C. Ma, C. Li, N. He, F. Wang, N. Ma, L. Zhang, Z. Lu, Z. Ali, Z. Xi, X. Li, G. Liang, H. Liu, Y. Deng, L. Xu, and Z. Wang, “Preparation and Characterization of Monodisperse Core–Shell Fe3O4 @SiO2 Microspheres and Its Application for Magnetic Separation of Nucleic Acids from E. coli BL21,” *J. Biomed. Nanotechnol.*, vol. 8, no. 6, pp. 1000–1005, 2012.

[72] S. Rezaei, I. Manoucheri, R. Moradian, and B. Pourabbas, “One-step chemical vapor deposition and modification of silica nanoparticles at the lowest possible temperature and superhydrophobic surface fabrication,” *Chem. Eng. J.*, vol. 252, pp. 11–16, 2014.

[73] R. Y. Hong, B. Feng, L. L. Chen, G. H. Liu, H. Z. Li, Y. Zheng, and D. G. Wei, “Synthesis, characterization and MRI application of dextran-coated Fe3O4 magnetic nanoparticles,” *Biochem. Eng. J.*, vol. 42, no. 3, pp. 290–300, 2008.

[74] J. Coates, “Interpretation of Infrared Spectra, A Practical Approach,” *Encycl. Anal. Chem.*, pp. 10815–10837, 2000.

[75] P. Kuhn, M. Antonietti, and A. Thomas, “Porous, covalent triazine-based frameworks prepared by ionothermal synthesis,” *Angew. Chemie - Int. Ed.*, vol. 47, no. 18, pp. 3450–3453, 2008.

[76] J. A. Faniran and H. F. Shurvell, “Infrared spectra of phenylboronic acid (normal and deuterated) and diphenyl phenylboronate,” *Can. J. Chem.*, vol. 46, no. 12, pp. 2089–2095, 1968.

[77] Malvern Instruments, “Dynamic Light Scattering : An Introduction in 30 Minutes,” *Zetasizer Nano Serles Tech. Note.*, pp. 1–13, 2014.

[78] Malvern Instruments, “Dynamic Light Scattering: Common Terms Defined,” *Malvern Guid. - Inf. White Pap.*, pp. 1–6, 2011.

[79] M. Baalousha, “Aggregation and disaggregation of iron oxide nanoparticles: Influence of particle concentration, pH and natural organic matter,” *Sci. Total Environ.*, vol. 407, no. 6, pp. 2093–2101, 2009.

[80] G. Nikolic, S. Zlatkovic, M. Cakic, S. Cakic, C. Lacnjevac, and Z. Rajic, “Fast fourier transform IR characterization of epoxy GY systems crosslinked with aliphatic and cycloaliphatic EH polyamine adducts,” *Sensors*, vol. 10, no. 1, pp. 684–696, 2010.

[81] Malvern Instruments, “Zeta potential: An Introduction in 30 minutes,” *Zetasizer Nano Serles Tech. Note. MRK654-01*, pp. 1–14, 2015.

[82] R. Li, V. Dowd, D. J. Stewart, S. J. Burton, and C. R. Lowe, “Design, synthesis, and application of a protein A mimetic.,” *Nat. Biotechnol.*, vol. 16, no. March, pp. 190–195, 1998.

[83] R. J. F. Branco, A. M. G. C. Dias, and A. C. A. Roque, “Understanding the molecular recognition between antibody fragments and protein A biomimetic ligand,” *J. Chromatogr. A*, vol. 1244, pp. 106–115, 2012.

[84] A. M. Azevedo, A. G. Gomes, L. Borlido, I. F. S. Santos, D. M. F. Prazeres, and M. R. Aires-Barros, “Capture of human monoclonal antibodies from a clarified cell culture supernatant by phenyl boronate chromatography,” *J. Mol. Recognit.*, vol. 23, no. 6, pp. 569–576, 2010.

[85] L. Borlido, A. M. Azevedo, A. G. Sousa, P. H. Oliveira, A. C. A. Roque, and M. R. Aires-Barros, “Fishing human monoclonal antibodies from a CHO cell supernatant with boronic acid magnetic particles,” *J. Chromatogr. B Anal. Technol. Biomed. Life Sci.*, vol. 903, pp. 163–170, 2012.

[86] Octapharm, “Product Information - Gammanorm,” pp. 1–8, 2013.

[87] I. Fischer, C.-C. Hsu, M. Gärtner, C. Müller, T. W. Overton, O. R. T. T. Thomas, and M. Franzreb, “Continuous protein purification using functionalized magnetic nanoparticles in aqueous micellar two-phase systems.,” *J. Chromatogr. A*, vol. 1305, pp. 7–16, 2013.

[88] M. Suzuki, M. Kamihira, T. Shiraishi, H. Takeuchi, and T. Kobayashi, “Affinity partitioning of protein a using a magnetic aqueous two-phase system,” *J. Ferment. Bioeng.*, vol. 80, no. 1, pp. 78–84, 1995.

[89] GE Healthcare, “HiTrap MabSelect SuRe - Data File,” pp. 1–20, 2014.